GEOTECHNICAL CENTRIFUGE INSTRUMENTATION AND MODELLING

FINAL YEAR PROJECT UG 2015

By

NUST BE-CE-15-137380   Hamza Nadeem
NUST BE-CE-15-145966   Kaynat Akmal
NUST BE-CE-15-135466   Faran Asif
NUST BE-CE-15-120719   Muhammad Salman

NUST Institute of Civil Engineering
School of Civil and Environmental Engineering
National University of Sciences and Technology, Islamabad, Pakistan

2019

This is to certify that the

Final Year Project Titled

GEOTECHNICAL CENTRIFUGE INSTRUMENTATION AND MODELLING

Submitted by

NUST BE-CE-15-137380	Hamza Nadeem
NUST BE-CE-15-145966	Kaynat Akmal
NUST BE-CE-15-135466	Faran Asif
NUST BE-CE-15-120719	Muhammad Salman

has been accepted towards the requirements
for the undergraduate degree

in

CIVIL ENGINEERING

_____
Dr. S. Muhammad Jamil- Dean SCEE
Designation (Professor)
NUST Institute of Civil Engineering
School of Civil and Environmental Engineering
National University of Sciences and Technology, Islamabad, Pakistan

GEOTECHNICAL CENTRIFUGE INSTRUMENTATION AND MODELLING

ABSTRACT

Centrifuge machines are being used widely worldwide for different purposes including geotechnical testing, Earthquake simulation and testing, Soil Structure Interaction etc. While in our country there isn't much work being done on the concept of centrifuge machine and there existed a research gap in the working in our country as compared to other countries. To fill this void, we had undertaken this project to develop a custom centrifuge and use it for the geotechnical testing of soil samples. Our project is divided into two phases. First one is the machine development and modelling is mainly the mechanical and electrical component of the project and doesn't have much to do with the soil testing. While the second phase is related to the soil testing part where we had tested the soil samples to obtain the geotechnical properties of respective soils and have also validated our results and the developed centrifuge by the comparison of results obtained from this centrifuge with those obtained from already existing Triaxial and Direct Shear Testing Machine.

In the first phase we have designed our machine and validated it on a software called Solid works and we have also carried out a detailed stability study of our machine, its constituent parts and its foundation to check foe any necessity of a damping system. We have also worked on providing the maximum possible Stability in our apparatus in terms of Vibration control so that our results don't get affected by these factors.

In the second phase we have carried out the soil testing on our centrifuge and we have carried out the testing in three stages i.e. Densification, Saturation, Shearing. At the same time, we have also performed the Triaxial and Direct Shear Test on the same soil samples and at the end we have compared the results from all these three testing machines to validate and verify our machine's credibility.

Identifying the differences in the results obtained from our machine with those obtained from the already existing procedures of Triaxial and Direct Shear Test we have proposed a future working on the machine and certain correction factors related to the machine to achieve maximum accuracy in the results.

GEOTECHNICAL CENTRIFUGE
INSTRUMENTATION AND MODELLING

GEOTECHNICAL CENTRIFUGE
INSTRUMENTATION AND MODELLING

DEDICATION

We dedicate our work to our beloved parents and teachers who enabled us to achieve education and meet our objectives with such dignity and respect.

GEOTECHNICAL CENTRIFUGE
INSTRUMENTATION AND MODELLING

ACKNOWLEDMENT

TABLE OF CONTENTS

LIST OF FIGURES

LIST OF TABLES

CHAPTER 1

INTRODUCTION

The civil engineering structures like building, bridge, highway, tunnel, dam, tower, etc. are founded below or on the surface of the earth. For their stability, suitable foundation soil is required. To check the suitability of soil to be used as foundation or as construction materials, its properties are required to be assessed. As per different researchers, assessment of geotechnical properties of subsoil at project site is necessary for generating relevant input data for design and construction of foundations for the proposed structures. Researchers have stated that proper design and construction of civil engineering structures prevent an adverse environmental impact or structural failure or post construction problems.

Information about the surface and sub-surface features is essential for the design of structures and for planning construction techniques. When buildings impose very heavy loads and the zone of influence is very deep, it would be desirable to invest some amount on sub-surface exploration than to overdesign the building and make it costlier. For complex projects involving heavy structures, such as bridges, dams, multi-storey buildings, it is essential to have detail exploration. The purpose of detailed explorations is to determine the engineering properties of the soils for different strata.

Different researchers explained that the capability of a soil to support a loading from a structure, or to support its overburden, or to sustain a slope in equilibrium is governed by its shear strength. The shear strength of a soil is of prime importance for foundation design, earth and rock fill dam design, highway and airfield design, stability of slopes and cuts, and lateral earth pressure problems. It is highly complex because of various factors involved in it such as the heterogeneous nature of the soil, the water table location, the drainage facility, the type and nature of construction, the stress history, time, chemical action, or environmental conditions.

To determine the relevant geotechnical parameters in a design situation, laboratory tests that simulate the in-situ loading conditions as closely as possible should be performed. A

consensus was developed during the late 1930's that the tri axial device is superior to the other existing test equipment and that view tends to persist today as the first modern equipment of tri axial was developed apparently under the direction of Karl Terzaghi.

The geotechnical centrifuge is a special facility capable of replicating on reduced scale models the same stress field existing in-situ increasing the gravity field by rotation. This condition is fundamental in geo-technics because the mechanical behavior of soils is strongly dependent on the stress-field. On observing the extreme emerging worldwide importance of geo-technical centrifuges, our aimed to develop a custom centrifuge capable of replicating the field stresses on soil samples and give a reasonable idea of the shear strength.

We further worked on the co-relations development of the custom self- designed centrifuge and the most reliable standard tri-axial test by testing a number of soil samples on both the apparatuses and developed a standard for the machine operation.

LITERATURE REVIEW

Geotechnical properties of soils influence the stability of civil engineering structures. One must understand the nature of shearing resistance in order to analyze soil stability problems such as bearing capacity, slope stability, and lateral pressure on earth retaining structures.

2.1 Shear Strength of Soil

Soils consist of individual particles that can slide and roll relative to one another. Shear strength of a soil is equal to the maximum value of shear stress that can be mobilized within a soil mass without failure taking place.

The shear strength of a soil is a function of the stresses applied to it as well as the manner in which these stresses are applied.

2.1.1 Importance of Shear Strength of Soil

The knowledge of shear strength is very important some of the uses are provided below:

- In the design of foundations the evaluation of bearing capacity is dependent on the shear strength.
- For the design of embankments for dams, roads, pavements, excavations, levees etc. The analysis of the stability of the slope is done using shear strength.
- In the design of earth retaining structures like retaining walls, sheet pile coffer dams, bulks heads, and other underground structures etc.

2.1.2 Components of Shear Strength of Soil

The shear strength of a soil mass is essentially made up of:

- Due to the interlocking of the grains the structural resistance of the movement of the soil is very essential.

- Another important component is the frictional resistance between the individual soil grains at their contact point on sliding.
- The resistance due to the forces which hold the particles together or the cohesion.

2.1.3 Mohr Circle of Stresses

In soil testing, cylindrical samples are commonly used in which radial and axial stresses act on principal planes. The vertical plane is usually the minor principal plane whereas the horizontal plane is the major principal plane. The radial stress (σ_r) is the minor principal stress (σ_3), and the axial stress (σ_a) is the major principal stress (σ_1).
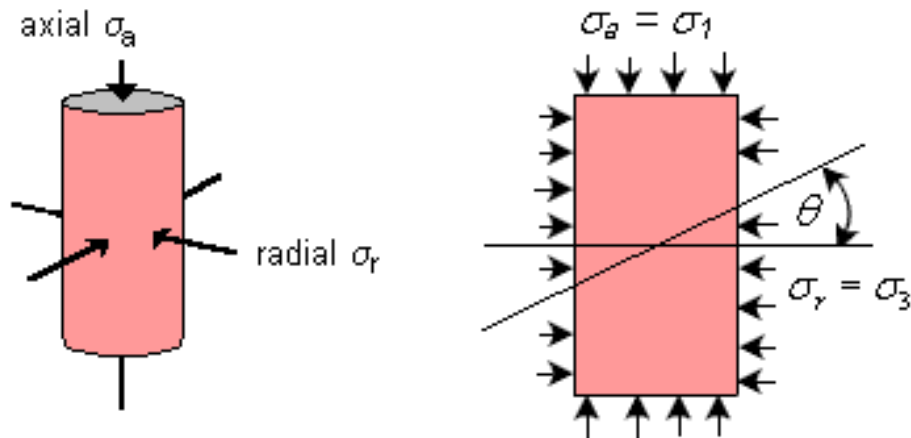
Fig 1: Mohr Circle of Stresses

To visualize the normal and shear stresses acting on any plane within the soil sample, a graphical representation of stresses called the Mohr circle is obtained by plotting the principal stresses. The sign convention in the construction is to consider compressive stresses as positive and angles measured counter-clockwise also positive.
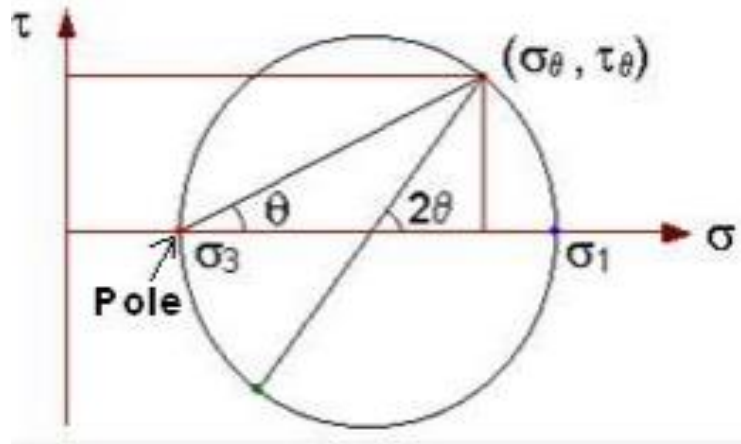
Fig 2: Mohr Coulomb Sign Convention

2.1.4 Mohr Coulomb Failure Criterion

When the soil sample has failed, the shear stress on the failure plane defines the shear strength of the soil. Thus, it is necessary to identify the failure plane.

For the present, it can be assumed that a failure plane exists and it is possible to apply principal stresses and measure them in the laboratory by conducting a triaxial test. Then, the Mohr circle of stress at failure for the sample can be drawn using the known values of the principal stresses.

If data from several tests, carried out on different samples up to failure is available, a series of Mohr circles can be plotted. It is convenient to show only the upper half of the Mohr circle. A line tangential to the Mohr circles can be drawn, and is called the Mohr-Coulomb failure envelope.
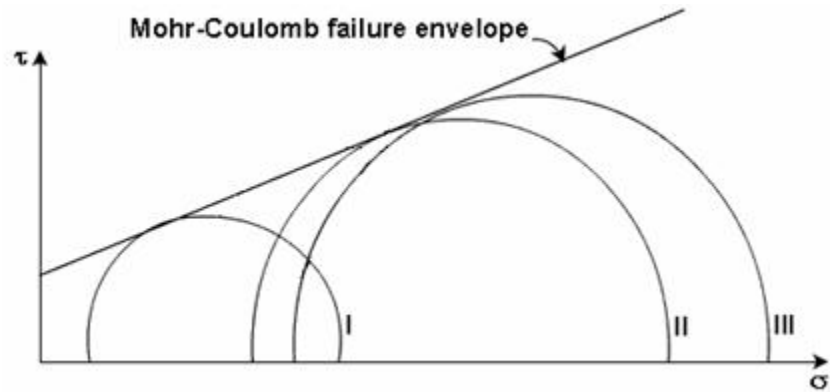
Fig 3: Mohr-Coulomb Failure Envelope

2.2 Conventional Testing Procedures Available

2.2.1 Direct Shear Testing

➢   The direct shear device is used to determine failure envelopes for soils. The device is not suitable for determination of stress-strain properties of soils.

➢   Direct shear testing is covered in ASTM standard D-3080, "Standard Method for Direct Shear Test on Soils under Consolidated Drained Conditions".

Fig 4: Direct Shear Apparatus

6

Overall Review of Testing Procedure

- **Introduction**

  It is assumed that the test is to be fully drained and the sample is undisturbed and cohesive, and is in a sampling tube. Minor modifications cover other cases.

- **Trimming the Sample**

  The soil sample is extruded from the sampling tube. The extruded sample must typically be trimmed to fit into the shear box. The soil cannot conveniently be trimmed directly into most direct shear devices because the shear box is typically too large and heavy to be handled conveniently. Instead, a special trimming ring is used. The trimming ring has a height that is standard for that laboratory. If a thinner sample is desired, then after the soil has been trimmed into the ring and one face has been trimmed, a spacer plate is used on the surface just trimmed, to push the soil up into the ring an appropriate distance, and then the other face is trimmed.

  The trimmings can be used to obtain initial water content but they tend to dry out so fast that such water contents usually turn out to be significantly too low. It is better to weigh the soil in the trimming ring, subtract out the known weight of the ring, and then dry the sample after the test, being sure not to lose any sample.
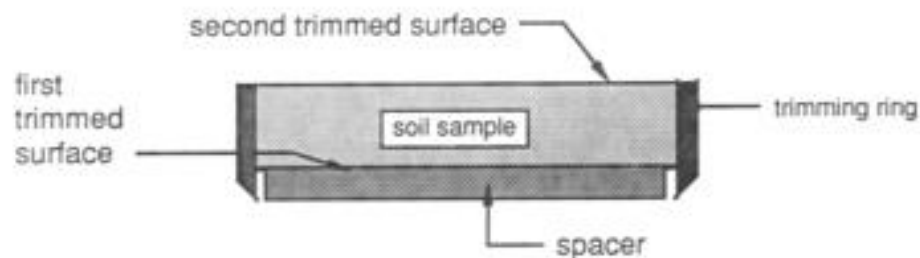
Fig 5: Trimming the Sample to a Height Less Than That of the Trimming Ring

- **Apparatus Assembly**

The shear box is then assembled with the top and the bottom halves of the box screwed (or rigidly attached) together. The inside of the shear box is typically lightly greased to minimize side friction, just as for consolidation tests. The lower porous stone is placed in the shear box. Sometimes spacer disks are placed below this stone to adjust the elevation of its top to accommodate soil samples of different thicknesses. The trimming ring is then carefully aligned with the top of the shear box. Sometimes the trimming ring and top shear box have been machined so the ring fits into the shallow slot in the top of the shear box, to provide proper alignment. The sample is then slowly extruded into the shear box by pressing on its top surface, typically using the top porous stone or a suitable disk. The upper porous stone and loading cap are placed in the shear box, and the system to apply the normal-toad is brought into place and a small normal load (seating load) is applied.

- **Consolidation Stage**

A dial indicator, or other suitable device for measuring the change in thickness of the sample, is quickly mounted and a zero reading taken. A consolidation pressure is then added to the top of the sample using the load-application system of the apparatus (typically a lever arm or a pneumatic system). The consolidation stage proceeds as for a standard incremental one dimensional consolidation test. Loads are typically applied with a load increment ratio of one, to minimize problems with soil extrusion. Readings of settlement or expansion are taken as a function of time to allow appropriate calculation of consolidation coefficients and to ensure that the sample has come to equilibrium prior to the start of shear.

- **Preparation for the Shearing Stage**

During the consolidation stage, the upper and lower halves of the shear box have been tightly screwed together to prevent the soil from extruding out from between the boxes. Typically, only two locking screws are used. Prior to shearing the

sample, the upper half of the box is typically raised to provide a small separation between the boxes and ensure that the shearing and normal stresses are actually transmitted through the soil rather than from box to box. The boxes are usually separated before the final shearing stage by removing the locking screws, and then using screws that are threaded through the top box but not the bottom box, to lift the upper box.

For normally consolidated samples, of the order of 5-8% of the applied load has been transferred into side shear in the, upper half of the box so lifting the box momentarily reverses the side shear and causes a small amount of sample disturbance, thus causing a small amount of additional time-dependent consolidation. Prior to starting the shearing stage, the screws used to lift the top box must be withdrawn so the full applied stress plus the weight of the upper half of the shear box, acts on the soil in the potential failure zone, and another stage of a small amount of consolidation begins. If the top half of the shear box is heavy, and not counterbalanced, and the sample is soft, a significant amount of additional consolidation may result. To minimize the time during this stage of the test, the top half of the box is usually raised and then it is released at once; and then readings of sample thickness are continued until the sample has come back to equilibrium.
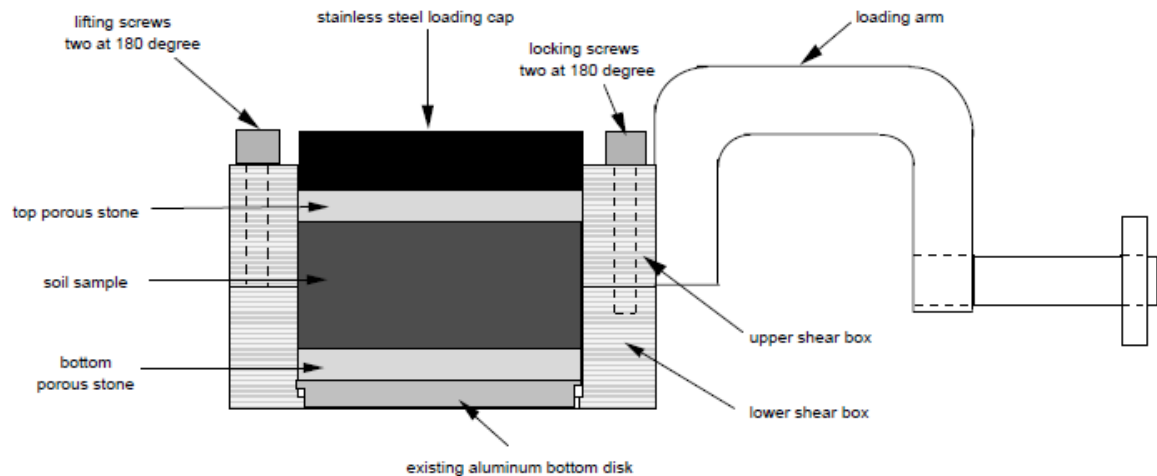
Fig 6: Assembly Drawing of Direct Shear Box

- **Shearing Stage**

  The shearing stage is usually performed at a constant rate of deformation. Methods of selecting the deformation rate will be discussed subsequently. A rate is selected and the shearing stage begins. Readings are taken of horizontal displacement, vertical movement of the top cap, and shearing force, as a function of time. Stress conditions in the sample become increasingly uncertain as deformation continues so the test is usually stopped at a horizontal deflection of about 0.25 inch even if the shearing stress has not reached a peak value.

- **Dismantling Stage**

  When the test is over, the shearing stress is reduced to zero. Equipment for measuring deformations is removed. The normal load is then reduced to zero as quickly as possible and the apparatus dismantled. The soil sample starts to rebound as soon as the normal load begins to decrease so the dismantling stage must be quite rapid if there is any desire to measure the water content at the failure stage. Once the apparatus has been dismantled, the two halves of the shear box are separated. Often, a water content sample is taken from the shear zone, and then the water content sample and the rest of the specimen are dried to obtain a final dry weight (and thus initial water content).

- **Data Reduction**

  The data are reduced by calculating the normal and shearing stresses, plotting a curve of shearing force vs. horizontal movement, and perhaps plotting change in sample thickness vs. horizontal movement. The failure condition is plotted in a Coulomb diagram.

  There are numerous options in the above procedure, e.g., it may be desired to determine the residual strength as well as, or in place of, the peak strength.

2.2.2 Unconfined Compression Test

The purpose of this laboratory is to determine the unconfined compressive strength of a cohesive soil sample.

Fig 7: Unconfined Compression Test Apparatus

Overall Review of Testing Procedure

- **Introduction**

The unconfined compression test is by far the most popular method of soil shear testing because it is one of the fastest and cheapest methods of measuring shear strength. The method is used primarily for saturated, cohesive soils recovered from thin-walled sampling tubes. The unconfined compression test is inappropriate for dry sands or crumbly clays because the materials would fall apart without some land of lateral confinement.

To perform an unconfined compression test, the sample is extruded from the sampling tube. A cylindrical sample of soil is trimmed such that the ends are reasonably smooth and the

11

length-to-diameter ratio is on the order of two. The soil sample is placed in a loading frame on a metal plate; by turning a crank, the operator raises the level of the bottom plate. The top of the soil sample is restrained by the top plate, which is attached to a calibrated proving ring. As the bottom plate is raised, an axial load is applied to the sample. The operator turns the crank at a specified rate so that there is constant strain rate. The load is gradually increased to shear the sample, and readings are taken periodically of the force applied to the sample and the resulting deformation. The loading is continued until the soil develops an obvious shearing plane or the deformations become excessive. The measured data are used to determine the strength of the soil specimen and the stress-strain characteristics. Finally, the sample is oven dried to determine its water content. The maximum load per unit area is defined as the unconfined compressive strength, qu.

In the unconfined compression test, we assume that no pore water is lost from the sample during set-up or during the shearing process. A saturated sample will thus remain saturated during the test with no change in the sample volume, water content, or void ratio. More significantly, the sample is held together by an effective confining stress that results from negative pore water pressures (generated by menisci forming between particles on the sample surface). Pore pressures are not measured in an unconfined compression test; consequently, the effective stress is unknown. Hence, the un-drained shear strength measured in an unconfined test is expressed in terms of the total stress.

- **Apparatus**

The loading frame consists of two metal plates. The top plate is stationary and is attached to the load-measuring device. The bottom plate is raised and lowered by means of a crank on the front of the loading frame. After the soil sample has been placed between the plates, the bottom plate is gradually raised; the resistance provided by the stationary top plate applies an axial force to the sample. Although the loading frames in our laboratory are hand operated, electric motor-driven and hydraulic load frames are common. Loads are measured with a calibrated proving ring or an electronic load cell. Vertical deformations are measured with a dial gauge; the dial gauge is attached to the top plate and measures the

relative movement between the top and bottom plates. We will be performing a strain-controlled test, in which the load is applied at a constant rate of strain or deformation.

- **Procedure**

The procedure for the test is as follows: -

1. Extrude the soil sample from Shelby tube sampler. Cut a soil specimen so that the ratio (L/d) is approximately between 2 and 2.5, where L and d are the length and diameter of soil specimen, respectively.

2. Measure the exact diameter of the top of the specimen at three locations 120° apart, and then make the same measurements on the bottom of the specimen. Average the measurements and record the average as the diameter on the data sheet.

3. Measure the exact length of the specimen at three locations 120° apart, and then average the measurements and record the average as the length on the data sheet.

4. Weigh the sample and record the mass on the data sheet.

5. Calculate the deformation (A_l) corresponding to 15% strain (£).

6. Where L_o = Original specimen length (as measured in step 3).

7. Carefully place the specimen in the compression device and center it on the bottom plate. Adjust the device so that the upper plate just makes contact with the specimen and set the load and deformation dials to zero.

8. Apply the load so that the device produces an axial strain at a rate of 0.5% to 2.0% per minute, and then record the load and deformation dial readings on the data sheet at every 20 to 50 divisions on deformation the dial.

9. Keep applying the load until (1) the load (load dial) decreases on the specimen significantly, (2) the load holds constant for at least four deformation dial readings, or (3) the deformation is significantly past the 15% strain that was determined in step 5.

10. Draw a sketch to depict the sample failure.

11. Remove the sample from the compression device and obtain a sample for water content determination.

- **Sources of Errors in the Unconfined Compression Test**

There are a number of sources of error in the unconfined compression test. One of the largest sources is the use of an unrepresentative sample of soil. The soil may be unrepresentative because it is not the same as, or perhaps even similar to the bulk of the soil found in the ground. The sample can also be unrepresentative if it has been disturbed or changed from its original slate. A common cause for disturbance is the soil sampling process. Disturbance usually has the effect of lowering the strength of the soil and reducing the slope of the stress-strain curve Fig 8.
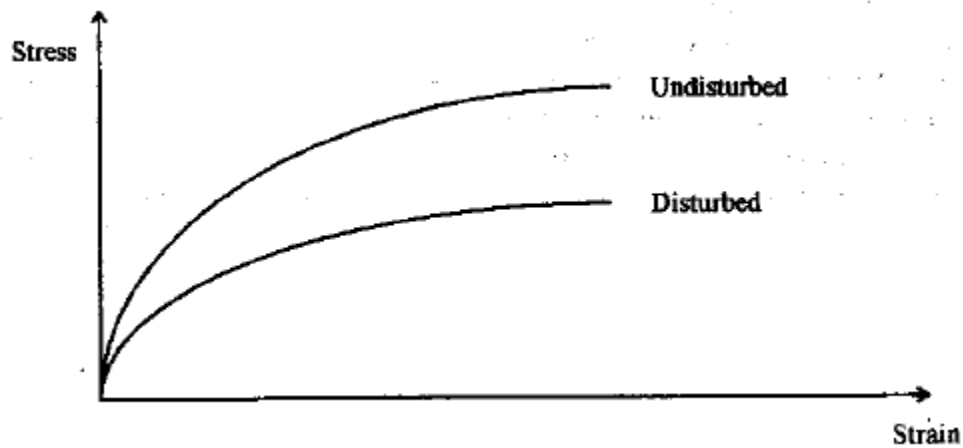
Fig 8: Effect of Disturbance on the Stress-Strain Behavior

If the sample is too short there will be significant end effects. End effects are caused by the top and bottom loading plates that grip the sample. They can increase the strength of a soil sample by preventing the formation of the weakest failure plane. If the sample is too long, we find that it tends to buckle. A length-to-width ratio of two to three is recommended to avoid this problem. The effect of length-to-width ratio on the unconfined compressive strength is shown in Figure 9.
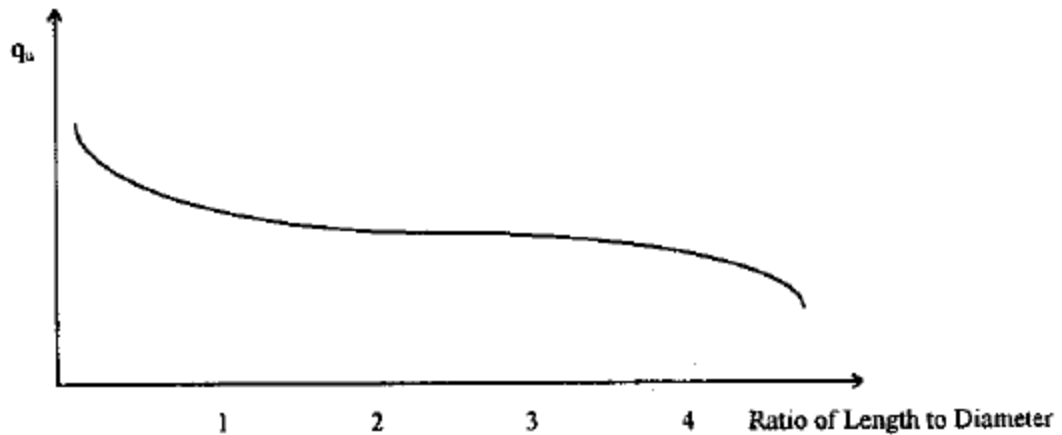
Fig 9: Effect of Length to Diameter Ratio on Unconfined Compressive Strength of Soil

Another source of error is that the soil is not confined during shear but will be confined in the field if the soil is located at a depth of a few feet or more. The problem is most severe with fissured soils (soils that contain cracks). In the ground, the cracks are held closed by the confining pressure due to the weight of soil above it. The soil is much stronger in this state than it is with no confining pressure in an unconfined compression test.

2.2.3 Tri-Axial Test

The tri-axial shear test is one of the most reliable methods available for determining shear strength parameters. It is used widely for research and conventional testing.

Fig 10: Tri-Axial Test Apparatus

Typical Layout of Tri-Axial Test Apparatus

A diagram of the tri-axial test layout is shown in Figure 11.

In this test, a soil specimen about 36 mm (1.4 in.) in diameter and 76 mm (3 in.) long generally is used. The specimen is encased by a thin rubber membrane and placed inside a plastic cylindrical chamber that usually is filled with water or glycerine. The specimen is subjected to a confining pressure by compression of the fluid in the chamber. Air is sometimes used as a compression medium. To cause shear failure in the specimen, one must apply axial stress through a vertical loading ram sometimes called *deviator stress*.

This stress can be applied in one of two ways:

1. Application of dead weights or hydraulic pressure in equal increments until the specimen fails. (Axial deformation of the specimen resulting from the load applied through the ram is measured by a dial gauge.)

2. Application of axial deformation at a constant rate by means of a geared or hydraulic loading press. This is a strain-controlled test.

The axial load applied by the loading ram corresponding to a given axial deformation is measured by a proving ring or load cell attached to the ram.
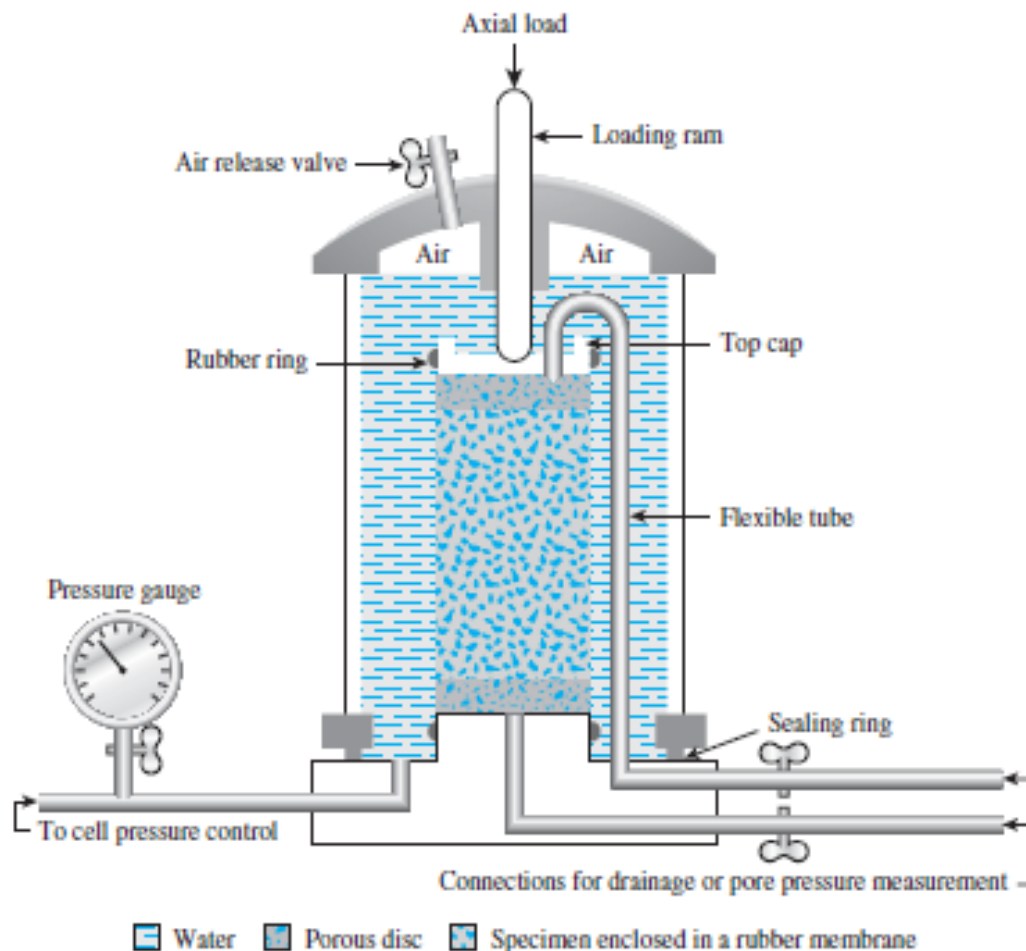
Fig 11: Typical Layout of Tri-Axial Test Apparatus (After Bishop and Bjerrum, 1960. With permission from ASCE.)

Connections to measure drainage into or out of the specimen, or to measure pressure in the pore water (as per the test conditions), also are provided. The following three standard types of tri-axial tests generally are conducted:

1. Consolidated-drained test or drained test (CD test)
2. Consolidated-undrained test (CU test)
3. Unconsolidated-undrained test or undrained test (UU test)

The general procedures and implications for each of the tests in *saturated soils* are described in the following sections.

2.2.3.1 Consolidated-Drained Tri-Axial Test

In the CD test, the saturated specimen first is subjected to an all - around confining pressure σ_3, by compression of the chamber fluid (Figure 12). As confining pressure is applied, the pore water pressure of the specimen increases by Uc (if drainage is prevented). This increase in the pore water pressure can be expressed as a non-dimensional parameter in the form:

$$B = Uc \div \sigma_3$$

where
B = Skempton's Pore Pressure Parameter (Skempton, 1954).

For saturated soft soils, B is approximately equal to 1; however, for saturated stiff soils, the magnitude of B can be less than 1. Black and Lee (1973) gave the theoretical values of B for various soils at complete saturation.

Now, if the connection to drainage is opened, dissipation of the excess pore water pressure, and thus consolidation, will occur. With time, Uc will become equal to 0. In saturated soil, the change in the volume of the specimen (Vc) that takes place during consolidation can be obtained from the volume of pore water drained (Figure 12 a). Next, the deviator stress σ_d,

on the specimen is increased very slowly (Figure 12 b). The drainage connection is kept open, and the slow rate of deviator stress application allows complete dissipation of any pore water pressure that developed as a result ($Ud = 0$).
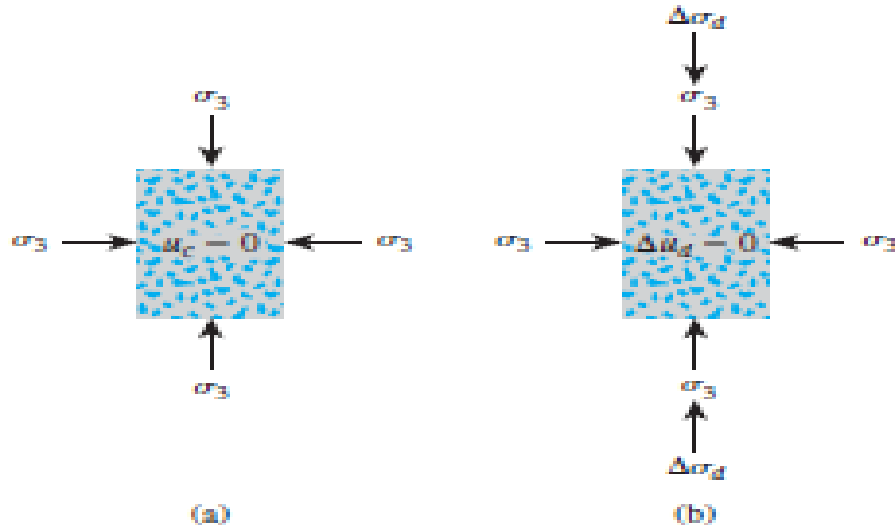
Fig 12: Consolidated-drained tri-axial test: (a) specimen under chamber confining pressure; (b) deviator stress application

2.2.3.2 Consolidated-Undrained Tri-Axial Test

The consolidated-undrained test is the most common type of tri-axial test. In this test, the saturated soil specimen is first consolidated by an all-around chamber fluid pressures σ_3, that results in drainage (Figures 13a and 13b). After the pore water pressure generated by the application of confining pressure is dissipated, the deviator stress σd, on the specimen is increased to cause shear failure (Figure 13c). During this phase of the test, the drainage line from the specimen is kept closed. Because drainage is not permitted, the pore water pressure Ud, will increase. During the test, simultaneous measurements of σd and Ud are made.
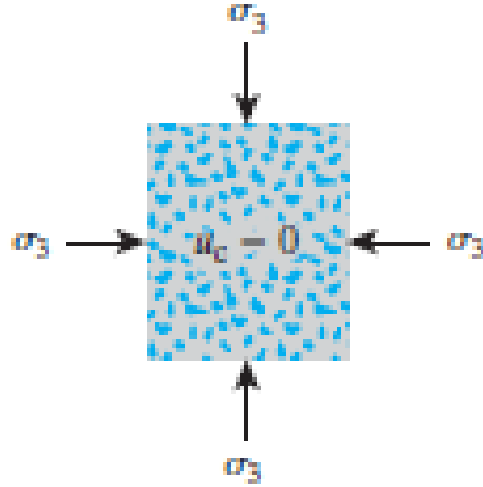
Fig 13a: Consolidated un-drained test: (a) specimen under chamber confining pressure
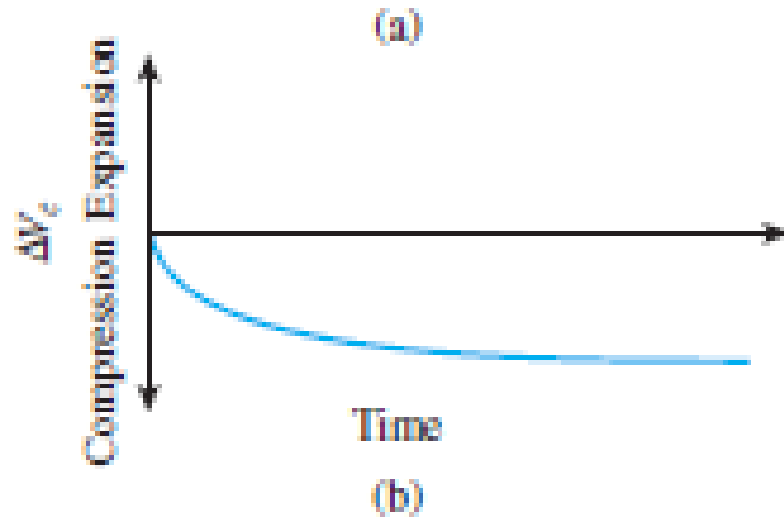
Fig 13b: Consolidated un-drained test: (b) volume change in specimen caused by confining pressure
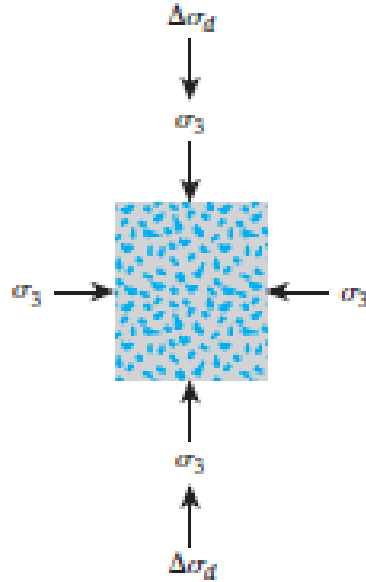
Fig 13c: Consolidated un-drained test: (c) deviator stress application

2.2.3.3 Unconsolidated-Undrained Tri-Axial Test

In unconsolidated-undrained tests, drainage from the soil specimen is not permitted during the application of chamber pressure σ_3. The test specimen is sheared to failure by the application of deviator stress, σ_d and drainage is prevented. Because drainage is not allowed at any stage, the test can be performed quickly. Because of the application of chamber confining pressures σ_3, the pore water pressure in the soil specimen will increase by U_c. A further increase in the pore water pressure (U_d) will occur because of the deviator stress application. Hence, the total pore water pressure U in the specimen at any stage of deviator stress application can be given as:

$$U = U_c + \Delta U_d$$

This test usually is conducted on clay specimens and depends on a very important strength concept for cohesive soils if the soil is fully saturated. The added axial stress at failure $(\sigma_d)_f$ is practically the same regardless of the chamber confining pressure.

21

The failure envelope for the total stress Mohr's circles becomes a horizontal line and hence is called a ϕ=0 condition. For $\phi = 0$ condition,

$$T_f = c = c_u$$

where cu is the un-drained shear strength and is equal to the radius of the Mohr's circles. The $\phi = 0$ concept is applicable to only saturated clays and silts.
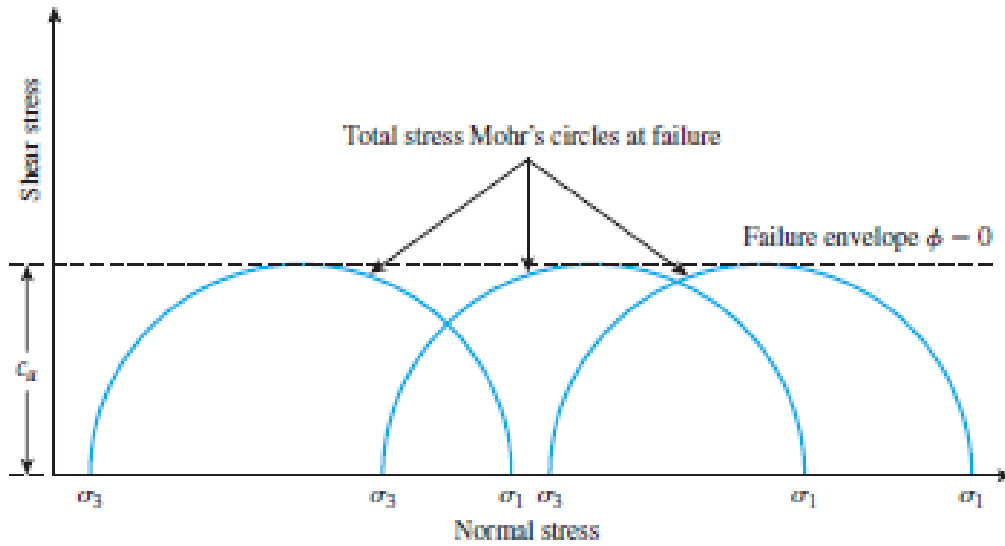
Fig 14: Total stress Mohr's circles and failure envelope (ϕ=0) obtained from unconsolidated un-drained tri-axial tests on fully saturated cohesive soil

Summary of the standard types of Tri-Axial Test is given in Table 1 as follows:

Sr. No.	Type	Attribute	Procedure
1	Consolidated Drained (CD)	S-test (Slow)	• Drainage permitted during consolidation as well as shearing • Slow shearing rate to ensure complete pore water pressure dissipation
2	Consolidated Undrained (CU)	R-test (Rapid)	• Drainage permitted during consolidation but not during shearing. • Relatively faster shearing rate • Pore pressures are also measured
3	Unconsolidated Undrained (UU)	Q-test (Quick)	• Sample is sheared directly after saturation without consolidation

Table 1: Summary of Standard Types of Tri-axial test

Summary of the conventional testing procedures as explained in above sections is provided in Table 2 as:

Sr. No.	Procedure	Standard	Purpose	Shortcomings
1	Direct Shear Test	ASTM Standard D-3080 "Standard Method for Direct Shear Test on soils under Consolidated Drained Conditions"	• CD shear strength	• failure plane defined • stress conditions unknown
2	Tri-axial Test	1. ASTM Standard D-2850 "UU compressive strength of cohesive soils in tri-axial compression" 2. D-4767 "CU compression test on cohesive soils"	• Shear strength parameters for CD, CU, UU conditions	• Leakage through membranes
3	Unconfined Compression test	ASTM Standard D-2166 "Standard Test Method for Unconfined Compressive Strength of Cohesive Soil"	• To determine undrained shear strength of cohesive soils	• Inappropriate for dry sands or crumbly clays

Table 2: Summary of conventional testing procedures

2.3 Centrifuge as a Testing Equipment

2.3.1 Centrifuge

A machine using *centrifugal* force for separating substances of different densities, for removing moisture, or for simulating gravitational effects.

2.3.2 Geotechnical Centrifuge

A geotechnical centrifuge is used to conduct model tests to study geotechnical problems.
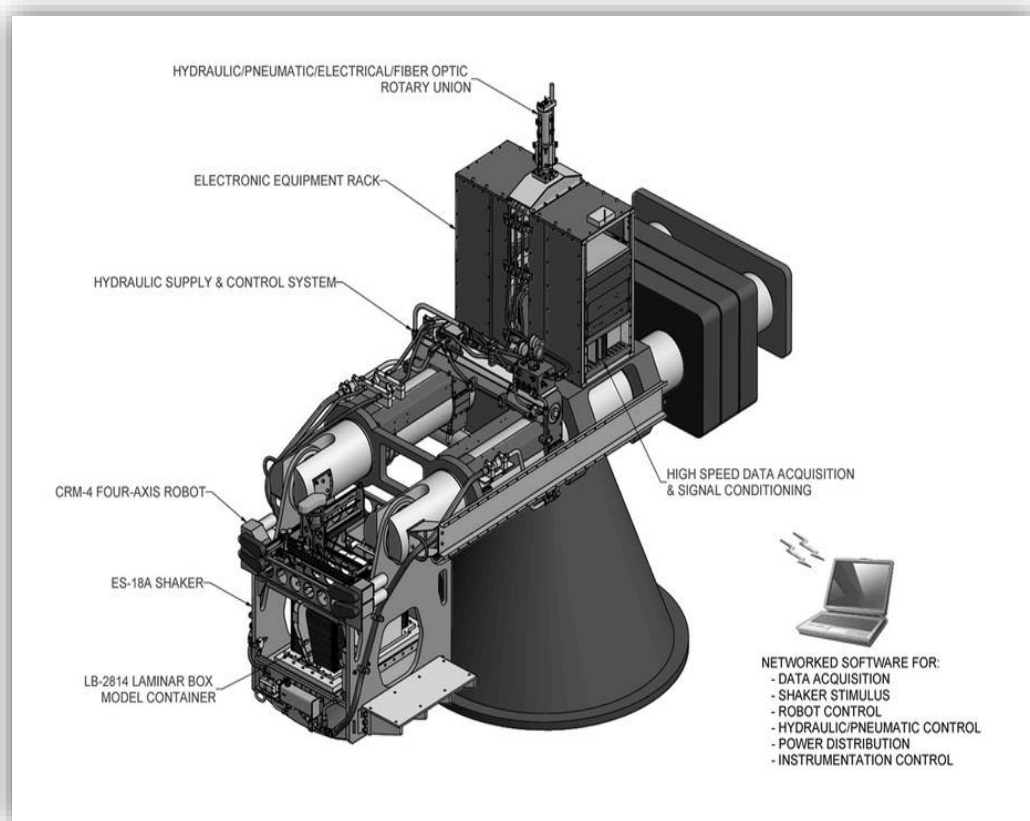
Fig 15: Geotechnical Centrifuge

There are two main types of geotechnical centrifuges:

- Beam centrifuges that are composed by beam as an arm, which in the end has an assembled swing where the model is located.
- Drum centrifuges that are composed by a simple drum that inside of it the model took place.

Both of them have size, maximum acceleration, model mass defined by user.

Fig 16: Beam Centrifuge
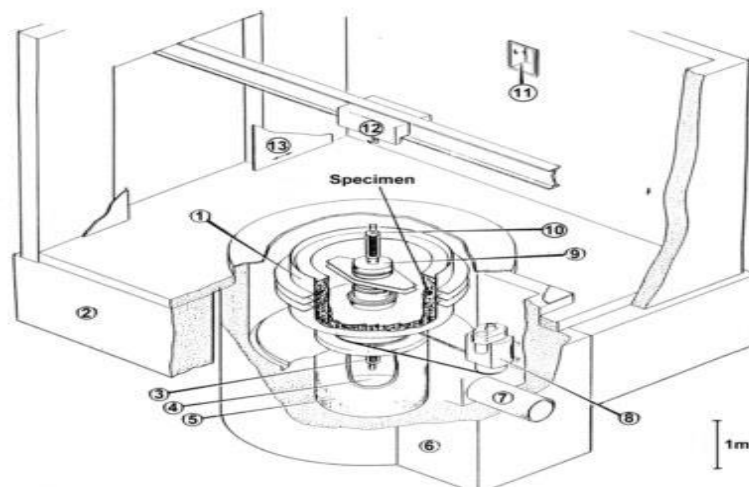
Fig 17: Drum Centrifuge

RESEARCH GAP

3.1 The NEES Geotechnical Centrifuge at UC Davis:

The UC Davis centrifuge has the largest radius and largest platform area of any geotechnical centrifuge in the US. It is one of the top few in these categories in the world. The 9-m radius centrifuge at UC Davis can carry five-ton payloads to accelerations of 75g.

An earthquake simulator, mounted on the end of the centrifuge, is designed to operate in either a biaxial (horizontal-vertical) or uniaxial (horizontal) shaking mode. The servo-hydraulic shaking tables are capable of simulating broad-spectrum earthquake events as well as step- and sinusoidal-wave type motions, and can vary intensity from micro-tremors to extreme shaking events.

Fig 18: The NEES Geotechnical Centrifuge at UC Davis

The large centrifuge has been used for many earthquake engineering research projects in the past ten years. Research projects have included soil-pile interaction in liquefying sands, liquefaction and ground improvement, dynamic response of tire shreds and void redistribution in liquefying sands.

With NEES, the Center for Geotechnical Modeling is working to implement advanced instrumentation, digital video, robotics, and geophysical testing to increase the quality and quantity of data that can be collected; to increase the capacity of the centrifuge; and to develop a biaxial shaking capability. These improvements will allow us to extract more detailed and more accurate information from experiments and simulations, maximizing the information and knowledge that can be gained.

3.2 Geotechnical Centrifuge from Nueva Granada Military University:

The Geotechnical group of Nueva Granada Military University designed a project whose main objective is design, modelling and building a geotechnical centrifuge with a specification as effective spin radius, mass and volume of specimen over the swing, maximum acceleration, par and others. The Geotechnical Group at the Nueva Granada Military University designed, modelled and it is building a Geotechnical centrifuge type beam, with a central spindle supporting a pair of parallel arms with 2.4 meters radio, maximum acceleration 200 Earth gravity and 500 Kg mass of the model.
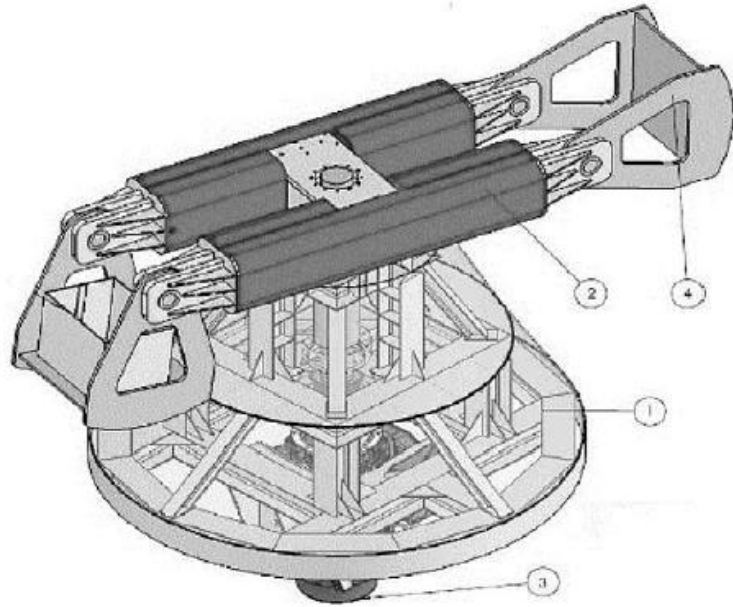
Fig 19: Geotechnical Centrifuge from Nueva Granada Military University

To design the geotechnical centrifuge of Geotechnical group from Military University the main design parameters are as follows:

- Maximum acceleration 200g
- Effective diameter 2.4 m
- Maximum load specimen 500Kg

Beam geotechnical centrifuge is composed by: two arms of pipe, a shaft of 4341 steel, two swing A572 steel of 1 m x 1 m x 90, a structure steel base to avoid vibration from movement, besides a box of aluminum to keep instrumentation and data logger on the top. Lastly the bunker where the machine will be installed is around 8 meter diameter and 4 meter high.

3.3 The National Geotechnical Centrifuge facility at IIT Bombay:

Sponsored jointly by the Department of Science and Technology, Defence Research and Development Organization and the Ministry of Human Resources Development, the centrifuge has been indigenously fabricated and commissioned at IIT Bombay. NGCF is a true MADE IN INDIA indigenous equipment.

Fig 20: The National Geotechnical Centrifuge facility at IIT Bombay

3.3.1 Features

- Configuration: Beam type
- Platform radius: 4.5 m
- Model area: 1.0 m x 1.2 m (up to 0.66 m height)
- 0.7 m x 1.2 m (up to 1.2 m height)
- Acceleration range: 10 g to 200 g
- Payload: 2.5 tons at 100g
- Capacity: 250 g-tons
- Run-up time to 200g: 6 minutes
- In-flight balancing range: 0 to ± 100 kN

29

- In-flight balancing time: 60 seconds
- Cost-effective cooling system
- Good swing-out at g-level
- Low power consumption
- Indigenously built

3.3.2 Selected application areas

- Slope stabilization techniques
- Reinforced soil structures
- Landslides
- Ground improvement techniques
- Environmental geotechnics
- Deep excavations and retention systems
- Geotechnical structures subjected to earthquake (under development)
- Subsidence
- Tunnels/Tunnel lining
- Foundations/Anchors

Going through the literature, we came to know that there exists a research gap in working on centrifuge in our country as compared to other countries. To play our part as an effort to fill this void we had undertaken this project and developed our problem statement.

SELF-DESIGNED CENTRIFUGE MACHINE

A self-designed centrifuge machine was developed by our seniors of batch 2014.
This self-designed centrifuge machine was capable of:

- Simulating the depth through confinement produced by rotating the cylinder at an RPM.
- Simulation of ground temperature at different depths by inclusion of temperature sensors inside the cylinder.

Fig 21: Self-Designed Centrifuge Machine

4.1 Specifications:

- Cylinder (Height = 14", Diameter = 7")

- Capacity = 14kg

- Electric Motor (0.75Hp, 1400RPM, 150G's)

- Moment Arm = 6"

4.2 Shortcomings:

As we started working on our project, we found out that there were certain shortcomings in the apparatus that were being a hindrance to our project.

The main issue with this self-designed machine was the presence of instability. The factors that we figured out that were causing the instability were eccentricity and vibrations:

- Eccentricity was present due to the mis-alignment of the center of rotation i.e. the motor and the center of mass i.e. the cylinder being rotated by the motor.
- Moreover, there were uncontrolled vibrations caused as result of this eccentricity which restricted the continuous rotation of the centrifuge.

CHAPTER 5

MACHINE STABILITY USING STRUCTURAL DYNAMICS

5.1 Background:

Man has been designing machines since beginning of civilization. Those machines grew complex with passing time and automation resulted in machines that had inherent motion that was initiated by power supply to internal components of the machine and not by an external force. These machines grew powerful producing stronger vibrations and hence necessitated well-designed foundations to keep them stable.

5.2 Type of foundation required:

There are three types of machines for which foundations are required:
1. Reciprocating
2. Impact
3. Rotating

Our centrifuge is the third type, rotating machine, that rotates at 1350 rpm. The foundation generally provided for rotating machines is block foundation that is also provided below this centrifuge machine.

5.3 Design Standard:

The IS:2974 (Part-1)-1969 standard was used to design the foundation, using which 3 criteria had to be fulfilled to stabilize the machine against the translational and rotational vibrations as shown in figure 22.
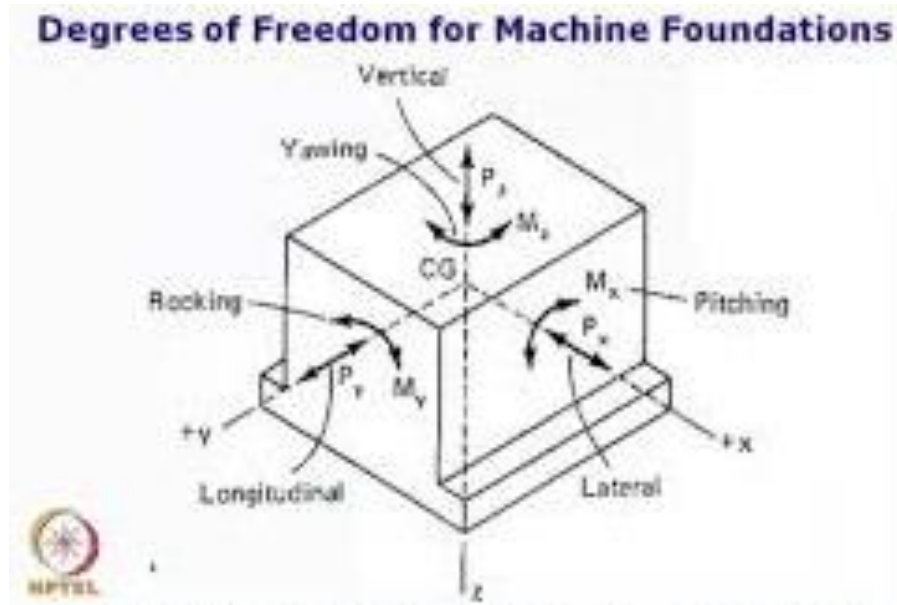
Fig 22: Degrees of Freedom for Machine Foundations

5.3.1 Dimensional Criterion:

The foundation is larger than the base of the machine with 150mm clearance and placed on a good bearing strata. Combined center of gravity of machine and its foundation is below the top of the foundation.

5.3.2 Displacement Criteria:

The vibration of the machine are not so large as to cause disturbances to the operator and other people in the surroundings and does not produce intolerable noise.

5.3.3 Vibration Criteria:

Vibrations of the frame were recorded against time using the setup shown in figure 23 with a dial gauge and stopwatch. The data was plotted to obtain a sine function for the harmonic vibrations of the frame induced by the harmonic loading due to rotations.
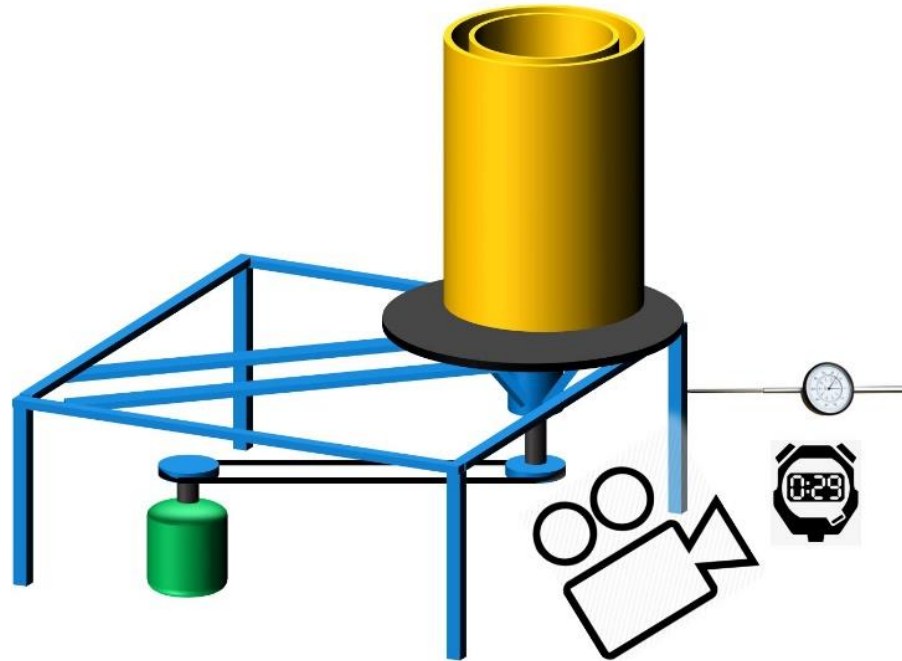
Fig 23: Proposed arrangement for recording vibrations

Fig 24: Actual arrangement for recording vibrations

35

Figure 24 shows how the investigation was actually carried out to obtain graphs in figure 25, 26 and 27.

0.62 s ω_1 = 10.11 Hz
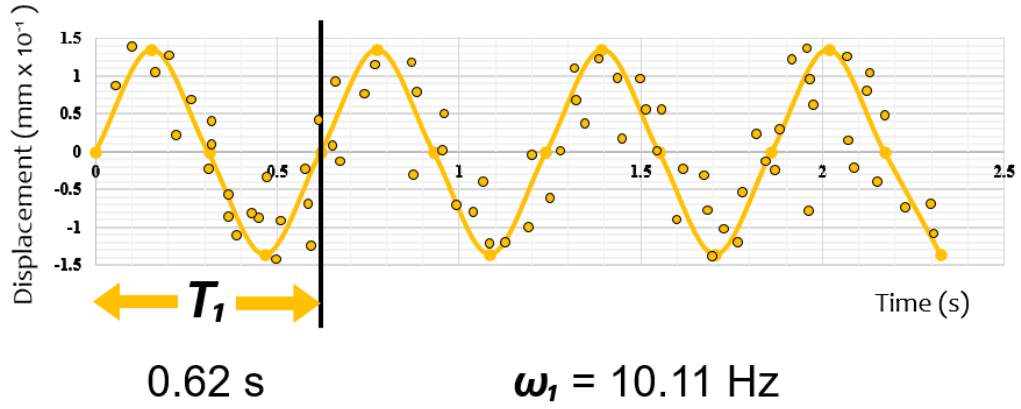
Fig 25: External Frequency 1

0.67 s ω_2 = 9.42 Hz
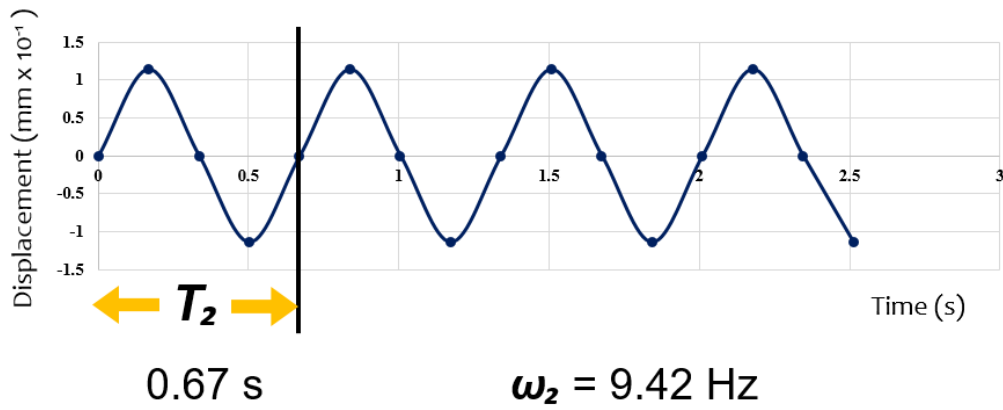
Fig 26: External frequency 2

2.35 s ω_v = 2.67 Hz
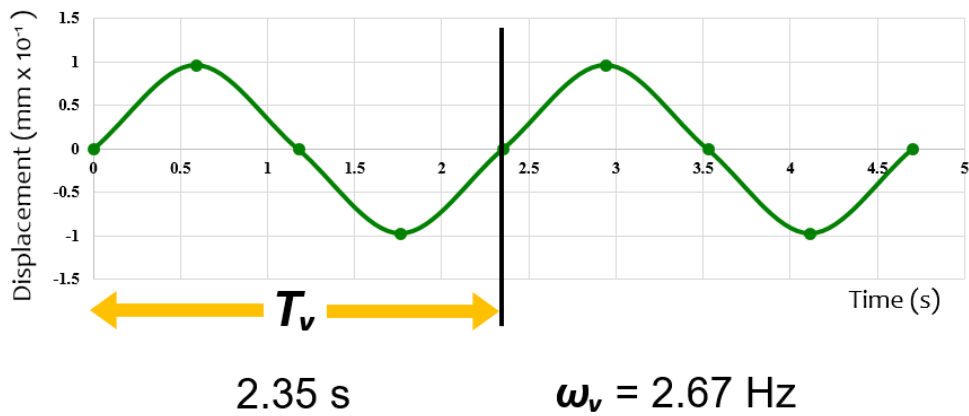
Fig 27: Natural Frequency

Motor was used to provide the external force for obtaining two of the externally applied frequencies as shown in figure 28. By removing the belt and allowing the cylinder to rotate freely, natural time period was determined. This is shown in figure 29.

Externally Applied
Frequency
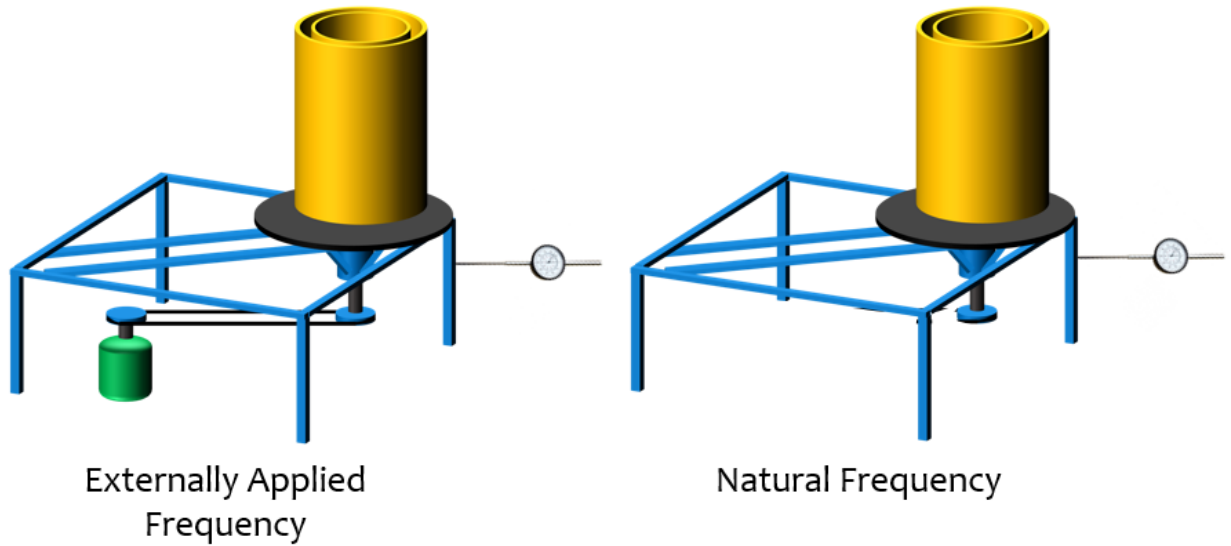
Natural Frequency

Fig 28: Externally Applied Frequency　　　　　**Fig 29: Natural Frequency**

The time periods determined using the graphs were used to calculate frequencies which were then subsequently used for calculation of the DMF ratio for the machine.

By plotting these calculated values (Figure 30 and Figure 31), it was figured out that our machine operates in the mass-controlled zone. This means that a massive foundation is sufficient to cause damping and no additional damping system is required.

$$\frac{1}{2\eta\sqrt{1-\eta^2}} = 2.00$$
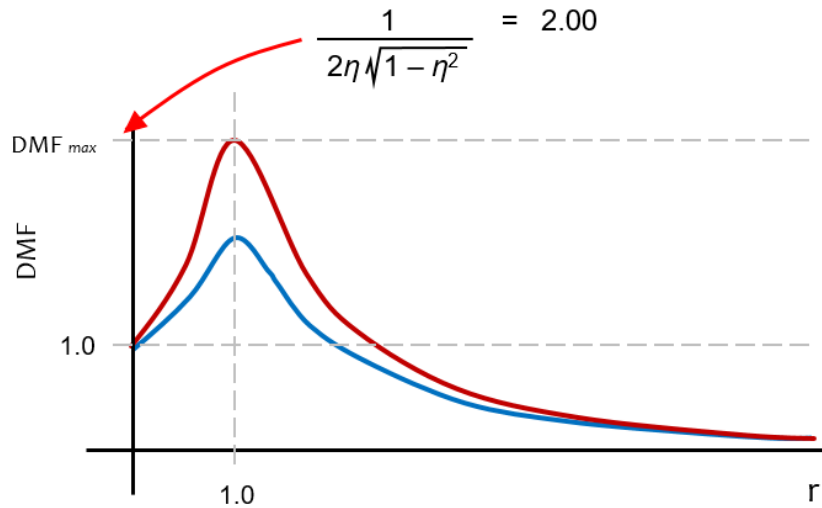
Fig 30: Typical DMF vs r (red), Centrifuge DMF vs r (blue)

$\eta = 0.258$ r = 3.78   DMF = 0.074
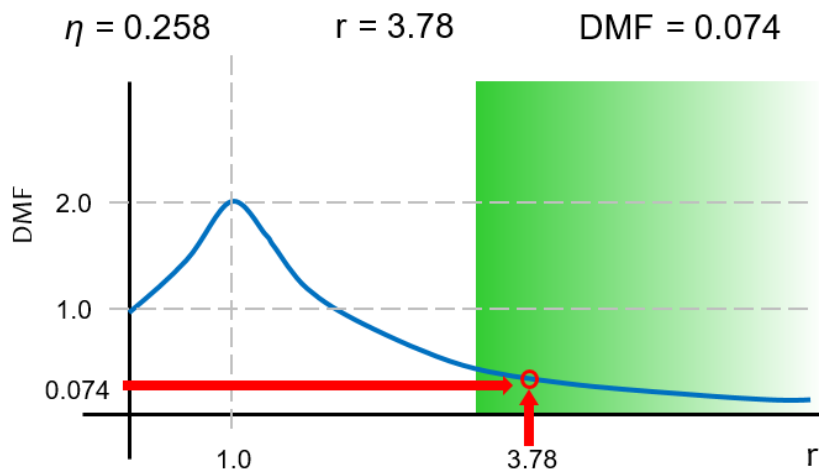
Fig 31: Machine operates in mass controlled zone (green)

5.4 Foundation Design using Tschebotarioff's Method:

The procedure for required depth of foundation is below. The depth provided was 5 inches. Other dimensions of the foundation block are shown in figure 32.

Tschebotarioff's Method

rpm	= 1350
depth of foundation	= 5"
area of foundation	= 20.25 ft^2
mass of machine and foundation	= 50 kg + 1266 kg
	= 1316 kg
bearing pressure , q_o	= 0.065 tons/ft^2

$$A = \left(\frac{1}{\tan \theta \cdot f_n \cdot q_o} \right)^4 = 7.14 \times 10^{-4} \text{ ft}^2$$
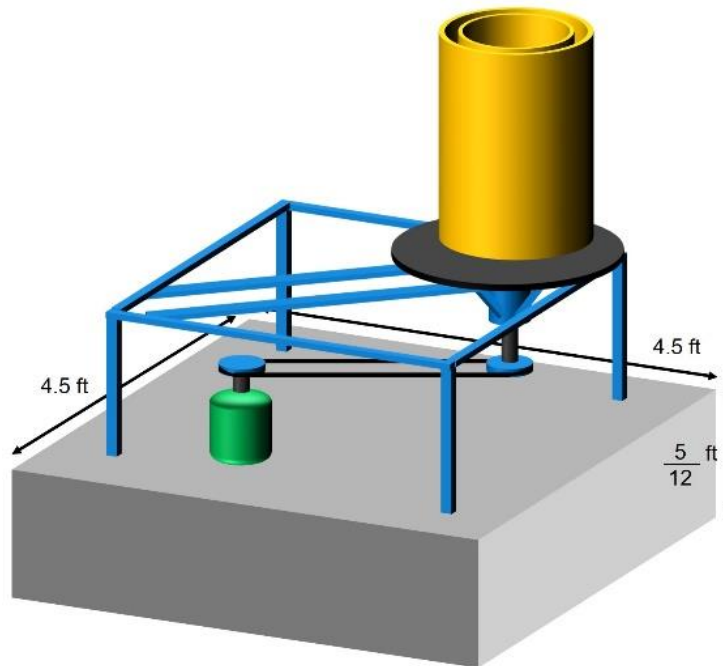
Fig 32: Dimensions of the foundation block

This concludes the stability study of this centrifuge machine and ensures that the vibrations caused by rotating parts will cause no stability problem in the long run.

CHAPTER 6

SIMULATION OF IN-SITU CONDITIONS

For any geotechnical investigation on any soil sample, the best and the most accurate results could only be obtained if the provision of in situ soil conditions like the stresses, densities etc. is done as close as possible. As mentioned already the determination of all the index and engineering properties of any soil sample is a must to determine its geotechnical properties and behaviour precisely and for that we need to provide the in-situ stress conditions of soil in the lab as well. Now to provide the in-situ soil conditions in lab we firstly must know the ins itu soil conditions so that they could be accurately simulated in lab and in our case in the centrifuge as well. For the determination of in situ stresses we have considered our centrifuge as a model and the actual field conditions where the soil sample has been taken from as prototype. To determine those field stresses, we have used the following mathematical expressions:

$$\sigma_{vp} = \rho \cdot g \cdot h_p$$

In the above equation we have to determine the field depth of our soil sample from which we have taken the sample in the field. And using the value of gravitational acceleration we find out the stress and this stress is the stress that a soil experiences at a particular depth.

Now the next important thing we have to do is to simulate the field stresses we have calculated using the above mathematical expression in our centrifuge so we could be able to determine the geotechnical properties of soil precisely and accurately. The only thing we could variate and control in our centrifuge is its revolutions per minute and variating these rpms we can simulate different field stresses in the centrifuge . Using the following mathematical expression we firstly determine the angular velocity of our centrifuge that we could provide at a certain value of rpms.

$$\omega \ (= 2\pi \cdot RPM / 60)$$

The only variable we have to put in the above mathematical expression is the value of rpm of our centrifuge machine and putting that we get the angular velocity of our machine which we later use to simulate the in situ stresses in the centrifuge and also to simulate the field depth at which we obtained the soil sample. Now to simulate the field stresses we use following mathematical expressions

$$Ng = \omega^2 R_e$$

$$\sigma_{vm} = \rho \cdot N \cdot g \cdot h_m = \rho \cdot \omega^2 \cdot R_e \cdot h_m$$

Once the simulation of In-situ stresses has been done we needed to verify whether our centrifuge is capable enough for geotechnical testings. Since it was a custom made centrifuge thus no machine standards were available readily but reviewing the literature and relating it with the most closely related available centrifuge we found out that if we satisfy certain conditions for our centrifuge we would be very sure about its validity. The conditions we must have to satisfy include the following:

1. The exact scaling relationship between the filed and the centrifuge must be satisfied. The developed strains in both the centrifuge and the field must be same if the same material with identical mechanical properties is used. This could be written mathematically as:

$$\frac{h_p}{h_m} = N$$

2. When N times the earth's gravity is applied on the centrifuge it behaves exactly like the field conditions at 1g because the material properties do not change at higher g values

3. The centrifuge machine must continue to provide N times the Earth's gravity during the tests.

As our centrifuge satisfied all these three conditions so we had verified its use for the determination of geotechnical properties of soil samples.

METHODOLOGY

The project methodology comprises of two phases (a) Lab Testing Phase, involving the conventional testing procedures and (b) The Centrifuge Testing Phase, involving tests carried out on the custom self- designed centrifuge apparatus.

7.1 Lab Testing

Lab Testing was conducted in 3 stages (a) Material Procurement, (b) Preparation and Testing and (c) Results and Analysis

7.1.1 Material Procurement

Easily available NUST Clay and a sample of Sand for the newly proposed construction of 132kV Grid Station at Sangor, Jhelum was procured.

7.1.1.1 Sieve Analysis

Sieve Analysis was carried out on the procured materials as per the specifications and respective grain size distribution curves were generated.

Given below in Fig is the grain size distribution curve of NUST Clay. As obvious from the curve distribution the sample contained around 69% gravel, 15.5% sand and 77.6% fines and was classified as a clay of low plasticity or lean clay as per the Unified Soil Classification System.

Similarly, in Fig the grain size distribution curve of Jhelum Sand is shown. Curve Analysis showed that the sample contained no gravel, around 95.89 % sand and 4.11% fines as per the Unified Soil Classification System.

Specific Gravity Test was carried out on both the samples i.e the NUST Clay and the Jhelum Sand as per the specifications the results of which are shown in the listed tables.

Sieve No	Sieve Dia	Mass of Soil Retained	Cumulative Mass Retained	Cummulative %age Retained	%age Passing	Remarks	
	(mm)	gm					
		gm					
2.5"	63.5	**0**	0	0.00	100.00		
2"	50.8		0	0.00	100.00		
1.5"	38.1		0	0.00	100.00		
1"	25.4		0	0.00	100.00		
3/4"	19.05		0	0.00	100.00		
1/2"	12.7		0	0.00	100.00		
3/8"	9.52		0	0.00	100.00		
4	4.75	**34.5**	34.5	6.90	93.10	6.90	**GRAVEL %**
10	2	**21.4**	55.9	11.18	88.82		
16	1.18	**6.3**	62.2	12.44	87.56		
30	0.6	**0**	62.2	12.44	87.56		
40	0.425	**0**	62.2	12.44	87.56		
50	0.3	**0**	62.2	12.44	87.56		
100	0.15	**22.5**	84.7	16.94	83.06	15.50	**SAND %**
200	0.074	**27.3**	112	22.40	77.60		
pan		**388**	500	100.00	0.00	77.60	**FINES %**

Table 3: Sieve Analysis on NUST Clay
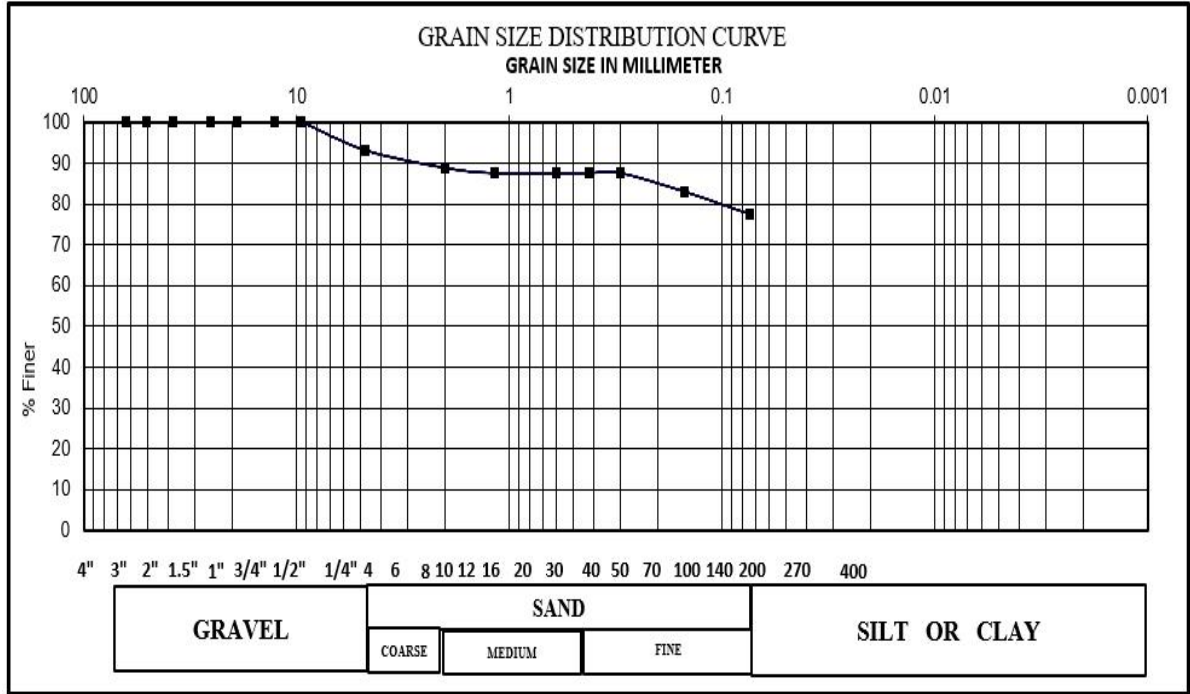
Fig 33: Grain Size Distribution Curve for NUST Clay

Sieve No	Sieve Dia	Mass of Soil Retained	Cumulative Mass Retained	Cummulative %age Retained	%age Passing	Remarks	
	(mm)	gm					
		gm					
2.5"	63.5		0	0.00	100.00		
2"	50.8		0	0.00	100.00		
1.5"	38.1		0	0.00	100.00		
1"	25.4		0	0.00	100.00		
3/4"	19.05		0	0.00	100.00		
1/2"	12.7		0	0.00	100.00		
3/8"	9.52		0	0.00	100.00		
4	4.75		0	0.00	100.00	0.00	**GRAVEL %**
10	2		0	0.00	100.00		
16	1.18		0	0.00	100.00		
30	0.6	**0.3**	0.3	0.07	99.93		
40	0.425	**6.4**	6.7	1.65	98.35		
50	0.3	**18.5**	25.2	6.21	93.79		
100	0.15	**316.3**	341.5	84.11	15.89	95.89	**SAND %**
200	0.074	**47.8**	389.3	95.89	4.11		
pan		**16.7**	406	100.00	0.00	4.11	**FINES %**

Table 4: Sieve Analysis Results for Jhelum Sand

45
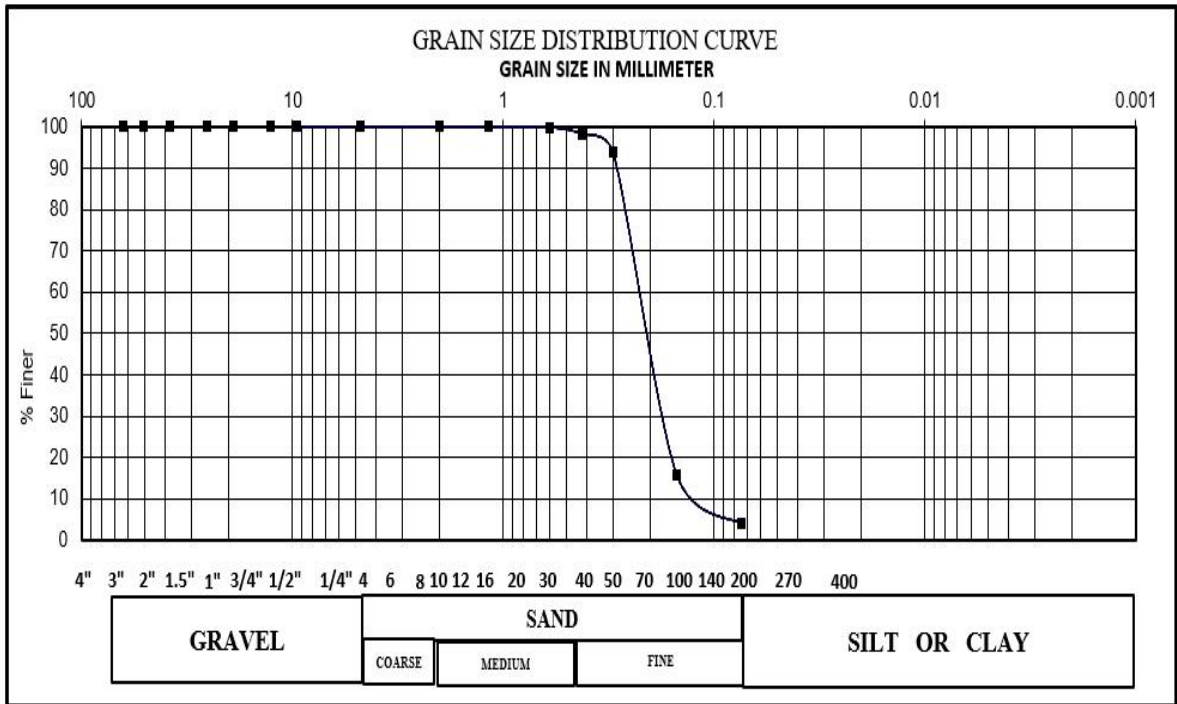
Fig 34: Grain Size Distribution of Jhelum Sand

7.1.1.2 Specific Gravity Test

Mass of flask	W1	89	gm
Mass of flask + dry soil	W2	130	gm
Mass of flask+soil+water	W3	303	gm
Mass of flask+water	W4	291	gm
Specific Gravity	Gs	2.71	

Table 5: Specific Gravity Test Results for NUST Clay

7.1.1.3 Proctor Test

Proctor Test was performed on the NUST Clay in order to get an idea of the Optimum Moisture Content (OMC) and Maximum Dry Density of the Clayey Sample.

For Sand, there's no proctor application thus the moisture content was estimated by taking into consideration the bulk density and the ratio of voids.

Denity				Trial No				
Observation				1	2	3	4	5
Wt of mould+Compacted soil (gm)	W1			3272	3500	3676	3558	3516
Wt of mould (gm)	W2			1442	1442	1442	1442	1442
Wt of compacted soil (gm)	W3			1830	2058	2234	2116	2074
Voulme of mould (cm^3)	V			943	943	943	943	943
Wet density of soil, γwet (gm/Cc)	W3/V			1.94	2.18	2.37	2.24	2.2
Wet density of soil, γdry (gm/Cc)	γwet/(1+mc/100)			1.83	2.05	2.19	1.99	1.88

Table 6: Results for MDD (Proctors Test)

Moisture Content								
Observation				1	2	3	4	5
Wt of container+wet soil (gm)	W1			3272	3500	3676	3558	3516
Wt of container+dry soil (gm)	W2			1442	1442	1442	1442	1442
Wt of container(gm)	W3			1830	2058	2234	2116	2074
Wt of water (gm)	Ww			943	943	943	943	943
Wt of dry soil (gm)	Ws			1.94	2.18	2.37	2.24	2.2
Moisture Content (M.C)%	(Ww/Ws)*100			1.83	2.05	2.19	1.99	1.88

Table 7: Results for OMC (Proctors Test)

7.1.2 Preparation and Testing

Samples were prepared as per the specifications for the Unconfined Compression Test and The Tri-Axial Test was carried out.

7.1.2.1 Tri-Axial Test

Unconsolidated Undrained Tri- Axial Test was performed on NUST Clay. The samples were prepared as per the specifications in the Tri-Axial Apparatus mold with height to Diameter Ratio (H/D) = 2 and was encased by a thin rubber membrane.

Sample prepared for the Tri-Axial Test can be seen in Fig.

Fig 35: Sample Preparation for the Tri-Axial Test

After preparing the sample as per the specifications, it was placed in the Tri-Axial Test Apparatus and after filling the cylindrical chamber with water the test was started.

Fig 36: Sample Placement

After having the sample placed, carried out by saturation the sample shearing was also done.

Following figures clearly indicate the shearing process and the sheared sample.

Fig 37: Sample Shearing
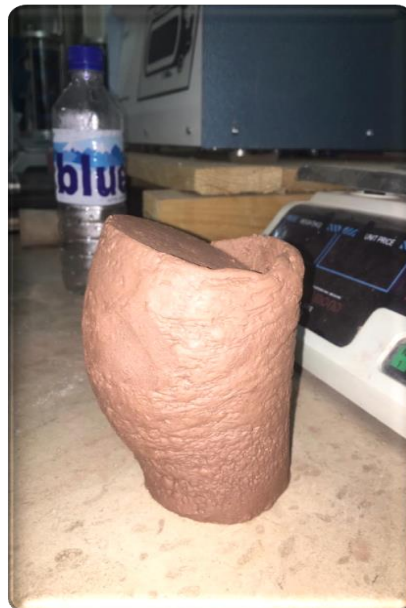
Fig 38: Sheared Sample

7.1.2.1 Unconfined Compression Test

A number of trials for the Unconfined Compression Test were carried out on the NUST Clay.

For Unconfined Compression Test, the samples were again prepared as per the specifications of the test at OMC and then placed in UCS Apparatus.

Test was carried out and sample was sheared by load application. Several trials were carried out in order to develop co-relations for the **"c"** values.

These stages can be clearly seen in the subsequent figures.
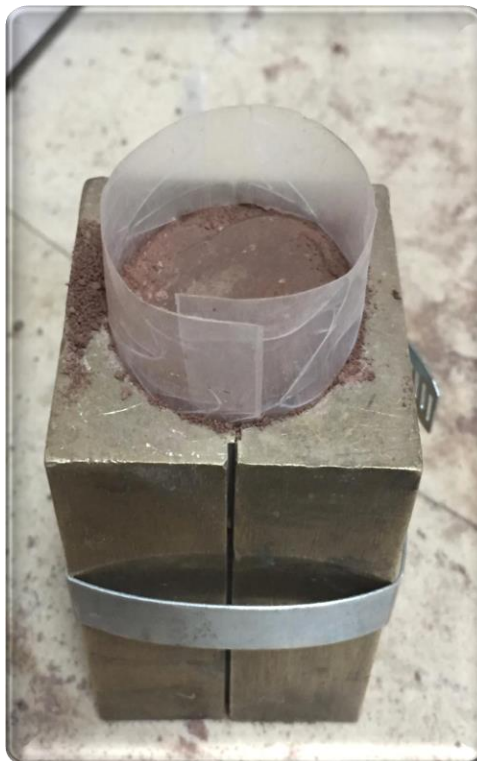
Fig 39: Sample Preparation

Fig 40: Sample Testing

Fig 41: Sample Shearing

7.1.3 Results and Analysis

Results for both the testing procedures were compiled and respective graphs were formed.

7.1.3.1 Tri-Axial Test Results

The results of the Unconsolidated Un-drained Tri-Axial Test trials are provided in following tables and the failure envelopes for the respective trials have also been attached.

D=70mm	L=140mm	Area=	3848.45 mm^2	0.00384845	m^2						
	L=0.14m			TRI AXIAL TEST RESULTS TRIAL # 01							
Deformation	Deformation ΔL	Strain	Corrected Area	P.R.R	Load P	Deviatoric Stress	Pore Pressure	Cell Pressure	Effective Cell Pressure	б1=б3+Δб	б1'=б3'+Δб
D.R	D.R*0.01 (mm)	ε	C.A=A/(1-e) (mm^2)		(KN)	Δб	u (kPa)	б3	б'3 (kPa)		
0	0	0	3848.45	0	0	0	0	120	120	120	120
100	1	0.007142857	3876.136691	25	0.1025	26.63409944	0	120	120	146.6340994	146.6340994
200	2	0.014285714	3904.224638	29	0.1189	30.89555535	3	120	117	150.8955554	147.8955554
300	3	0.021428571	3932.722628	29	0.1189	30.89555535	4	120	116	150.8955554	146.8955554
400	4	0.028571429	3961.639706	30	0.123	31.96091933	5	120	115	151.9609193	146.9609193
500	5	0.035714286	3990.985185	31	0.1271	33.02628331	5	120	115	153.0262833	148.0262833
600	6	0.042857143	4020.768657	32	0.1312	34.09164729	5	120	115	154.0916473	149.0916473
700	7	0.05	4051	34	0.1394	36.22237524	6	120	114	156.2223752	150.2223752
800	8	0.057142857	4081.689394	34	0.1394	36.22237524	7	120	113	156.2223752	149.2223752
900	9	0.064285714	4112.847328	35	0.1435	37.28773922	10	120	110	157.2877392	147.2877392
1000	10	0.071428571	4144.484615	35	0.1435	37.28773922	10	120	110	157.2877392	147.2877392
1100	11	0.078571429	4176.612403	35	0.1435	37.28773922	12	120	108	157.2877392	145.2877392
1200	12	0.085714286	4209.242188	37	0.1517	39.41846718	12	120	108	159.4184672	147.4184672
1300	13	0.092857143	4242.385827	43	0.1763	45.81065104	14	120	106	165.810651	151.810651
1400	14	0.1	4276.055556	43	0.1763	45.81065104	14	120	106	165.810651	151.810651
1500	15	0.107142857	4310.264	43	0.1763	45.81065104	14	120	106	165.810651	151.810651
1600	16	0.114285714	4345.024194	43	0.1763	45.81065104	18	120	102	165.810651	147.810651
1700	17	0.121428571	4380.349593	45	0.1845	47.941379	19	120	101	167.941379	148.941379
1800	18	0.128571429	4416.254098	46	0.1886	49.00674297	19	120	101	169.006743	150.006743
1900	19	0.135714286	4452.752066	46	0.1886	49.00674297	19	120	101	169.006743	150.006743
2000	20	0.142857143	4489.858333	46	0.1886	49.00674297	20	120	100	169.006743	149.006743
2100	21	0.15	4527.588235	47	0.1927	50.07210695	21	120	99	170.072107	149.072107
2200	22	0.157142857	4565.957627	48	0.1968	51.13747093	21	120	99	171.1374709	150.1374709
2300	23	0.164285714	4604.982906	48	0.1968	51.13747093	24	120	96	171.1374709	147.1374709
2400	24	0.171428571	4644.681034	49	0.2009	52.20283491	24	120	96	172.2028349	148.2028349
2500	25	0.178571429	4685.069565	49	0.2009	52.20283491	26	120	94	172.2028349	146.2028349
2600	26	0.185714286	4726.166667	49	0.2009	52.20283491	26	120	94	172.2028349	146.2028349
2700	27	0.192857143	4767.99115	49	0.2009	52.20283491	27	120	93	172.2028349	145.2028349
2800	28	0.2	4810.5625	49	0.2009	52.20283491	28	120	92	172.2028349	144.2028349
2900	29	0.207142857	4853.900901	49	0.2009	52.20283491	28	120	92	172.2028349	144.2028349
3000	30	0.214285714	4898.027273	50	0.205	53.26819889	31	120	89	173.2681989	142.2681989
3100	31	0.221428571	4942.963303	50	0.205	53.26819889	31	120	89	173.2681989	142.2681989
3200	32	0.228571429	4988.731481	50	0.205	53.26819889	33	120	87	173.2681989	140.2681989
3300	33	0.235714286	5035.35514	50	0.205	53.26819889	35	120	85	173.2681989	138.2681989
3400	34	0.242857143	5082.858491	50	0.205	53.26819889	35	120	85	173.2681989	138.2681989
3500	35	0.25	5131.266667	50	0.205	53.26819889	36	120	84	173.2681989	137.2681989
3600	36	0.257142857	5180.605769	53	0.2173	56.46429082	38	120	82	176.4642908	138.4642908
3700	37	0.264285714	5230.902913	54	0.2214	57.5296548	38	120	82	177.5296548	139.5296548
3800	38	0.271428571	5282.186275	56	0.2296	59.66038275	39	120	81	179.6603828	140.6603828
3900	39	0.278571429	5334.485149	59	0.2419	62.85647468	42	120	78	182.8564747	140.8564747
4000	40	0.285714286	5387.83	61	0.2501	64.98720264	42	120	78	184.9872026	142.9872026
4100	41	0.292857143	5442.252525	64	0.2624	68.18329457	44	120	76	188.1832946	144.1832946
4200	42	0.3	5497.785714	67	0.2747	71.37938651	44	120	76	191.3793865	147.3793865
4300	43	0.307142857	5554.463918	70	0.287	74.57547844	44	120	76	194.5754784	150.5754784
4400	44	0.314285714	5612.322917	71	0.2911	75.64084242	48	120	72	195.6408424	147.6408424
4500	45	0.321428571	5671.4	75	0.3075	79.90229833	48	120	72	199.9022983	151.9022983
4600	46	0.328571429	5731.734043	77	0.3157	82.03302628	48	120	72	202.0330263	154.0330263
4700	47	0.335714286	5793.365591	80	0.328	85.22911822	51	120	69	205.2291182	154.2291182
4800	48	0.342857143	5856.336957	82	0.3362	87.35984617	51	120	69	207.3598462	156.3598462
4900	49	0.35	5920.692308	84	0.3444	89.49057413	51	120	69	209.4905741	158.4905741
5000	50	0.357142857	5986.477778	86	0.3526	91.62130208	54	120	66	211.6213021	157.6213021
5100	51	0.364285714	6053.741573	89	0.3649	94.81739402	55	120	65	214.817394	159.817394

Table 8: Tri-Axial Test Results (Trial 1)

				TRI AXIAL TRIAL 02							
Deformation	Deformation ΔL	Strain	Corrected Area	P.R.R	Load P	Deviatoric Stress	Pore Pressure	Cell Pressure	Effective Cell Pressure	61=63+Δ6	61'=63'+Δ6
D.R	D.R*0.01 (mm)	ε	C.A=A/(1-ε) (mm^2)		(KN)	Δ6	u (kPa)	63	6'3 (kPa)		
0	0	0	3848.45	0	0	0	0	120	120	120	120
100	1	0.007142857	3876.136691	28	0.1148	29.83019138	0	120	120	149.8301914	149.8301914
200	2	0.014285714	3904.224638	29	0.1189	30.89555535	1	120	119	150.8955554	149.8955554
300	3	0.021428571	3932.722628	40	0.164	42.61455911	2	120	118	162.6145591	160.6145591
400	4	0.028571429	3961.639706	44	0.1804	46.87601502	4	120	116	166.876015	162.876015
500	5	0.035714286	3990.985185	46	0.1886	49.00674297	5	120	115	169.006743	164.006743
600	6	0.042857143	4020.768657	47	0.1927	50.07210695	6	120	114	170.072107	164.072107
700	7	0.05	4051	50	0.205	53.26819889	6	120	114	173.2681989	167.2681989
800	8	0.057142857	4081.689394	51	0.2091	54.33356286	6	120	114	174.3335629	168.3335629
900	9	0.064285714	4112.847328	52	0.2132	55.39892684	6	120	114	175.3989268	169.3989268
1000	10	0.071428571	4144.484615	55	0.2255	58.59501877	8	120	112	178.5950188	170.5950188
1100	11	0.078571429	4176.612403	55	0.2255	58.59501877	9	120	111	178.5950188	169.5950188
1200	12	0.085714286	4209.242188	56	0.2296	59.66038275	9	120	111	179.6603828	170.6603828
1300	13	0.092857143	4242.385827	57	0.2337	60.72574673	9	120	111	180.7257467	171.7257467
1400	14	0.1	4276.055556	58	0.2378	61.79111071	11	120	109	181.7911107	170.7911107
1500	15	0.107142857	4310.264	59	0.2419	62.85647468	11	120	109	182.8564747	171.8564747
1600	16	0.114285714	4345.024194	61	0.2501	64.98720264	11	120	109	184.9872026	173.9872026
1700	17	0.121428571	4380.349593	62	0.2542	66.05256662	13	120	107	186.0525666	173.0525666
1800	18	0.128571429	4416.254098	63	0.2583	67.1179306	15	120	105	187.1179306	172.1179306
1900	19	0.135714286	4452.752066	64	0.2624	68.18329457	15	120	105	188.1832946	173.1832946
2000	20	0.142857143	4489.858333	65	0.2665	69.24865855	17	120	103	189.2486586	172.2486586
2100	21	0.15	4527.588235	65	0.2665	69.24865855	20	120	100	189.2486586	169.2486586
2200	22	0.157142857	4565.957627	68	0.2788	72.44475048	22	120	98	192.4447505	170.4447505
2300	23	0.164285714	4604.982906	69	0.2829	73.51011446	25	120	95	193.5101145	168.5101145
2400	24	0.171428571	4644.681034	70	0.287	74.57547844	27	120	93	194.5754784	167.5754784
2500	25	0.178571429	4685.069565	71	0.2911	75.64084242	29	120	91	195.6408424	166.6408424
2600	26	0.185714286	4726.166667	72	0.2952	76.70620639	29	120	91	196.7062064	167.7062064
2700	27	0.192857143	4767.99115	73	0.2993	77.77157037	32	120	88	197.7715704	165.7715704
2800	28	0.2	4810.5625	75	0.3075	79.90229833	34	120	86	199.9022983	165.9022983
2900	29	0.207142857	4853.900901	75	0.3075	79.90229833	36	120	84	199.9022983	163.9022983
3000	30	0.214285714	4898.027273	76	0.3116	80.96766231	38	120	82	200.9676623	162.9676623
3100	31	0.221428571	4942.963303	77	0.3157	82.03302628	41	120	79	202.0330263	161.0330263
3200	32	0.228571429	4988.731481	78	0.3198	83.09839026	43	120	77	203.0983903	160.0983903
3300	33	0.235714286	5035.35514	79	0.3239	84.16375424	45	120	75	204.1637542	159.1637542
3400	34	0.242857143	5082.858491	80	0.328	85.22911822	45	120	75	205.2291182	160.2291182
3500	35	0.25	5131.266667	81	0.3321	86.29448219	47	120	73	206.2944822	159.2944822
3600	36	0.257142857	5180.605769	83	0.3403	88.42521015	52	120	68	208.4252101	156.4252101
3700	37	0.264285714	5230.902913	84	0.3444	89.49057413	53	120	67	209.4905741	156.4905741
3800	38	0.271428571	5282.186275	84	0.3444	89.49057413	54	120	66	209.4905741	155.4905741
3900	39	0.278571429	5334.485149	85	0.3485	90.5559381	57	120	63	210.5559381	153.5559381
4000	40	0.285714286	5387.83	87	0.3567	92.68666606	59	120	61	212.6866661	153.6866661
4100	41	0.292857143	5442.252525	88	0.3608	93.75203004	61	120	59	213.75203	152.75203
4200	42	0.3	5497.785714	89	0.3649	94.81739402	63	120	57	214.817394	151.817394
4300	43	0.307142857	5554.463918	90	0.369	95.88275799	65	120	55	215.882758	150.882758
4400	44	0.314285714	5612.322917	91	0.3731	96.94812197	68	120	52	216.948122	148.948122
4500	45	0.321428571	5671.4	93	0.3813	99.07884993	70	120	50	219.0788499	149.0788499
4600	46	0.328571429	5731.734043	96	0.3936	102.2749419	75	120	45	222.2749419	147.2749419
4700	47	0.335714286	5793.365591	99	0.4059	105.4710338	76	120	44	225.4710338	149.4710338

Table 9: Tri-Axial Test Results (Trial 2)
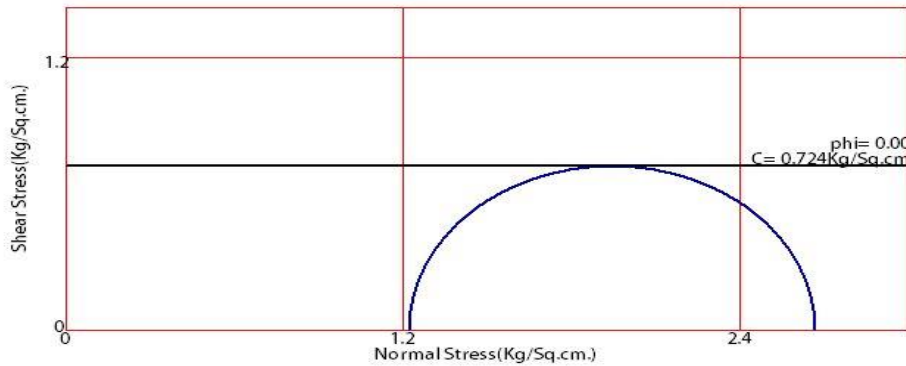
Fig 42: Failure Envelope (Tri-Axial Test trial 1)
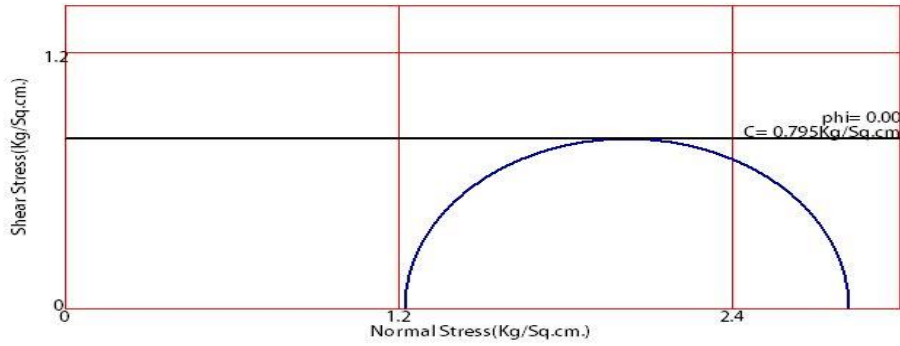
Fig 43: Failure Envelope (Tri-Axial Test trial 2)

7.1.3.2 Unconfined Compression Test Results

The tabulated test results are given in following tables:

TRIAL #01		L=80mm	Area =	1256.637				
Deformation ΔL (mm)	Strain ϵ=ΔL/L		Corrected Area Ac=A/(1-ϵ) m^2		P.R.R	Load P (kN)	Stress б=P/A	
0	0		0.001256637		0	0	0	
0.25	0.003125		0.001260576		314	0.0314	24.90924	
0.5	0.00625		0.00126454		3180	0.318	251.4748	
0.75	0.009375		0.001268529		3750	0.375	295.6179	
1	0.0125		0.001272544		3995	0.3995	313.9381	
1.25	0.015625		0.001276584		4018	0.4018	314.7463	
1.5	0.01875		0.001280649		2624	0.2624	204.8961	
1.75	0.021875		0.001284741		2120	0.212	165.0138	
2	0.025		0.001288858		1570	0.157	121.8132	
2.25	0.028125		0.001293003		1325	0.1325	102.4747	
2.5	0.03125		0.001297174		1180	0.118	90.967	
2.75	0.034375		0.001301372		1140	0.114	87.59988	
3	0.0375		0.001305597		970	0.097	74.29552	
3.25	0.040625		0.00130985		966	0.0966	73.74892	
3.5	0.04375		0.00131413		942	0.0942	71.6824	

Table 10: Unconfined Compression Test Results (Trial 1)

TRIAL #02		L=80mm	Area =	1256.637				
Deformation ΔL (mm)	Strain ϵ=ΔL/L		Corrected Area Ac=A/(1-ϵ) m^2		P.R.R	Load P (kN)	Stress б=P/A	
0	0		0.001256637		0	0	0	
0.25	0.003125		0.001260576		88	0.0088	6.980934	
0.5	0.00625		0.00126454		282	0.0282	22.30059	
0.75	0.009375		0.001268529		516	0.0516	40.67702	
1	0.0125		0.001272544		854	0.0854	67.10967	
1.25	0.015625		0.001276584		1224	0.1224	95.88091	
1.5	0.01875		0.001280649		1422	0.1422	111.0374	
1.75	0.021875		0.001284741		1326	0.1326	103.2115	
2	0.025		0.001288858		1216	0.1216	94.34705	
2.25	0.028125		0.001293003		1150	0.115	88.94026	
2.5	0.03125		0.001297174		1054	0.1054	81.25358	
2.75	0.034375		0.001301372		998	0.0998	76.68832	
3	0.0375		0.001305597		924	0.0924	70.77223	
3.25	0.040625		0.00130985		866	0.0866	66.11446	

Table 11: Unconfined Compression Test Results (Trial 2)

TRIAL #03		L=80mm	Area =	1256.637				
Deformation ΔL (mm)	Strain ϵ=ΔL/L		Corrected Area Ac=A/(1-ϵ) m^2		P.R.R	Load P (kN)	Stress б=P/A	
0	0		0.001256637		0	0	0	
0.25	0.003125		0.001260576		482	0.0482	38.23648	
0.5	0.00625		0.00126454		925	0.0925	73.14911	
0.75	0.009375		0.001268529		1543	0.1543	121.6369	
1	0.0125		0.001272544		2236	0.2236	175.711	
1.25	0.015625		0.001276584		2895	0.2895	226.7772	
1.5	0.01875		0.001280649		3465	0.3465	270.5659	
1.75	0.021875		0.001284741		3814	0.3814	296.8692	
2	0.025		0.001288858		3906	0.3906	303.0589	
2.25	0.028125		0.001293003		3624	0.3624	280.2778	
2.5	0.03125		0.001297174		3217	0.3217	248.0007	
2.75	0.034375		0.001301372		2742	0.2742	210.7008	
3	0.0375		0.001305597		1828	0.1828	140.0126	
3.25	0.040625		0.00130985		1442	0.1442	110.089	

Table 12: Unconfined Compression Test Results (Trial 3)

TRIAL #04		L=80mm	Area =	1256.637				
Deformation ΔL (mm)	Strain ε=ΔL/L		Corrected Area Ac=A/(1-ε) m^2		P.R.R	Load P (kN)	Stress б=P/A	
0	0		0.001256637		0	0	0	
0.25	0.003125		0.001260576		260	0.026	20.62549	
0.5	0.00625		0.00126454		860	0.086	68.0089	
0.75	0.009375		0.001268529		1230	0.123	96.96267	
1	0.0125		0.001272544		1830	0.183	143.8064	
1.25	0.015625		0.001276584		2390	0.239	187.2184	
1.5	0.01875		0.001280649		2950	0.295	230.3519	
1.75	0.021875		0.001284741		3440	0.344	267.7583	
2	0.025		0.001288858		3640	0.364	282.4205	
2.25	0.028125		0.001293003		4170	0.417	322.5051	
2.5	0.03125		0.001297174		4310	0.431	332.2608	
2.75	0.034375		0.001301372		4360	0.436	335.0311	
3	0.0375		0.001305597		4240	0.424	324.7557	
3.25	0.040625		0.00130985		3900	0.39	297.7441	
3.5	0.04375		0.00131413		3680	0.368	280.0331	
3.75	0.046875		0.001318439		3570	0.357	270.7748	
4	0.05		0.001322776		3210	0.321	242.6715	

Table 13: Unconfined Compression Test Results (Trial 4)

TRIAL #05		L=80mm	Area =	1256.637				
Deformation ΔL (mm)	Strain ε=ΔL/L		Corrected Area Ac=A/(1-ε) m^2		P.R.R	Load P (kN)	Stress б=P/A	
0	0		0.001256637		0	0	0	
0.25	0.003125		0.001260576		245	0.0245	19.43555	
0.5	0.00625		0.00126454		812	0.0812	64.21305	
0.75	0.009375		0.001268529		1212	0.1212	95.5437	
1	0.0125		0.001272544		1789	0.1789	140.5846	
1.25	0.015625		0.001276584		2415	0.2415	189.1768	
1.5	0.01875		0.001280649		2850	0.285	222.5434	
1.75	0.021875		0.001284741		3340	0.334	259.9746	
2	0.025		0.001288858		3510	0.351	272.334	
2.25	0.028125		0.001293003		4010	0.401	310.1308	
2.5	0.03125		0.001297174		4410	0.441	339.9699	
2.75	0.034375		0.001301372		4355	0.4355	334.6469	
3	0.0375		0.001305597		4210	0.421	322.4579	
3.25	0.040625		0.00130985		3945	0.3945	301.1796	
3.5	0.04375		0.00131413		3780	0.378	287.6427	
3.75	0.046875		0.001318439		3690	0.369	279.8765	
4	0.05		0.001322776		3450	0.345	260.8152	

Table 14: Unconfined Compression Test Results (Trial 5)

TRIAL #06		L=80mm	Area =	1256.637				
Deformation ΔL (mm)	Strain ε=ΔL/L		Corrected Area Ac=A/(1-ε) m^2		P.R.R	Load P (kN)	Stress б=P/A	
0	0		0.001256637		0	0	0	
0.25	0.003125		0.001260576		240	0.024	19.03891	
0.5	0.00625		0.00126454		820	0.082	64.8457	
0.75	0.009375		0.001268529		1270	0.127	100.1159	
1	0.0125		0.001272544		1840	0.184	144.5923	
1.25	0.015625		0.001276584		2400	0.24	188.0018	
1.5	0.01875		0.001280649		2860	0.286	223.3242	
1.75	0.021875		0.001284741		3450	0.345	268.5367	
2	0.025		0.001288858		3750	0.375	290.9551	
2.25	0.028125		0.001293003		4050	0.405	313.2244	
2.5	0.03125		0.001297174		4425	0.4425	341.1263	
2.75	0.034375		0.001301372		4270	0.427	328.1153	
3	0.0375		0.001305597		4100	0.41	314.0326	
3.25	0.040625		0.00130985		3800	0.38	290.1096	
3.5	0.04375		0.00131413		3695	0.3695	281.1746	
3.75	0.046875		0.001318439		3590	0.359	272.2917	
4	0.05		0.001322776		3200	0.32	241.9155	

Table 15: Unconfined Compression Test Results (Trial 6)

TRIAL #07		L=80mm	Area =	1256.637				
Deformation ΔL (mm)	Strain ε=ΔL/L		Corrected Area Ac=A/(1-ε) m^2		P.R.R	Load P (kN)	Stress б=P/A	
0	0		0.001256637		0	0	0	
0.25	0.003125		0.001260576		240	0.024	19.03891	
0.5	0.00625		0.00126454		830	0.083	65.6365	
0.75	0.009375		0.001268529		1130	0.113	89.07952	
1	0.0125		0.001272544		1750	0.175	137.5198	
1.25	0.015625		0.001276584		2325	0.2325	182.1267	
1.5	0.01875		0.001280649		2890	0.289	225.6668	
1.75	0.021875		0.001284741		3345	0.3345	260.3638	
2	0.025		0.001288858		3790	0.379	294.0587	
2.25	0.028125		0.001293003		4070	0.407	314.7712	
2.5	0.03125		0.001297174		4315	0.4315	332.6463	
2.75	0.034375		0.001301372		4420	0.442	339.6416	
3	0.0375		0.001305597		4210	0.421	322.4579	
3.25	0.040625		0.00130985		3820	0.382	291.6365	
3.5	0.04375		0.00131413		3430	0.343	261.0091	
3.75	0.046875		0.001318439		3215	0.3215	243.849	

Table 16: Unconfined Compression Test Results (Trial 7)

TRIAL #08		L=80mm	Area =	1256.637				
Deformation ΔL (mm)	Strain $\epsilon=\Delta L/L$		Corrected Area $Ac=A/(1-\epsilon)$ m^2		P.R.R	Load P (kN)	Stress $б=P/A$	
0	0		0.001256637		0	0	0	
0.25	0.003125		0.001260576		270	0.027	21.41877	
0.5	0.00625		0.00126454		840	0.084	66.4273	
0.75	0.009375		0.001268529		1250	0.125	98.5393	
1	0.0125		0.001272544		1690	0.169	132.8049	
1.25	0.015625		0.001276584		2160	0.216	169.2016	
1.5	0.01875		0.001280649		2890	0.289	225.6668	
1.75	0.021875		0.001284741		3230	0.323	251.4126	
2	0.025		0.001288858		3650	0.365	283.1963	
2.25	0.028125		0.001293003		4190	0.419	324.0519	
2.5	0.03125		0.001297174		4420	0.442	340.7408	
2.75	0.034375		0.001301372		4350	0.435	334.2627	
3	0.0375		0.001305597		4240	0.424	324.7557	
3.25	0.040625		0.00130985		3910	0.391	298.5075	
3.5	0.04375		0.00131413		3700	0.37	281.5551	
3.75	0.046875		0.001318439		3410	0.341	258.6392	

Table 17: Unconfined Compression Test Results (Trial 8)

TRIAL #09		L=80mm	Area =	1256.637				
Deformation ΔL (mm)	Strain $\epsilon=\Delta L/L$		Corrected Area $Ac=A/(1-\epsilon)$ m^2		P.R.R	Load P (kN)	Stress $б=P/A$	
0	0		0.001256637		0	0	0	
0.25	0.003125		0.001260576		220	0.022	17.45234	
0.5	0.00625		0.00126454		760	0.076	60.10089	
0.75	0.009375		0.001268529		1130	0.113	89.07952	
1	0.0125		0.001272544		1740	0.174	136.734	
1.25	0.015625		0.001276584		2210	0.221	173.1183	
1.5	0.01875		0.001280649		2870	0.287	224.1051	
1.75	0.021875		0.001284741		3240	0.324	252.191	
2	0.025		0.001288858		3650	0.365	283.1963	
2.25	0.028125		0.001293003		4070	0.407	314.7712	
2.5	0.03125		0.001297174		4210	0.421	324.5518	
2.75	0.034375		0.001301372		4450	0.445	341.9469	
3	0.0375		0.001305597		4190	0.419	320.926	
3.25	0.040625		0.00130985		3870	0.387	295.4538	
3.5	0.04375		0.00131413		3520	0.352	267.8578	
3.75	0.046875		0.001318439		3210	0.321	243.4698	

Table 18: Unconfined Compression Test Results (Trial 9)

TRIAL #10		L=80mm	Area =	1256.637				
Deformation ΔL (mm)	Strain ε=ΔL/L		Corrected Area Ac=A/(1-ε) m^2		P.R.R	Load P (kN)	Stress б=P/A	
0	0		0.001256637		0	0	0	
0.25	0.003125		0.001260576		280	0.028	22.21206	
0.5	0.00625		0.00126454		790	0.079	62.47329	
0.75	0.009375		0.001268529		1240	0.124	97.75098	
1	0.0125		0.001272544		1885	0.1885	148.1285	
1.25	0.015625		0.001276584		2290	0.229	179.385	
1.5	0.01875		0.001280649		3100	0.31	242.0647	
1.75	0.021875		0.001284741		3560	0.356	277.0987	
2	0.025		0.001288858		3895	0.3895	302.2054	
2.25	0.028125		0.001293003		4210	0.421	325.5987	
2.5	0.03125		0.001297174		4400	0.44	339.199	
2.75	0.034375		0.001301372		4590	0.459	352.7048	
3	0.0375		0.001305597		4100	0.41	314.0326	
3.25	0.040625		0.00130985		3860	0.386	294.6903	
3.5	0.04375		0.00131413		3685	0.3685	280.4136	
3.75	0.046875		0.001318439		3480	0.348	263.9485	
4	0.05		0.001322776		3140	0.314	237.3796	

Table 19: Unconfined Compression Test Results (Trial 10)

The plots for the results are as follows:
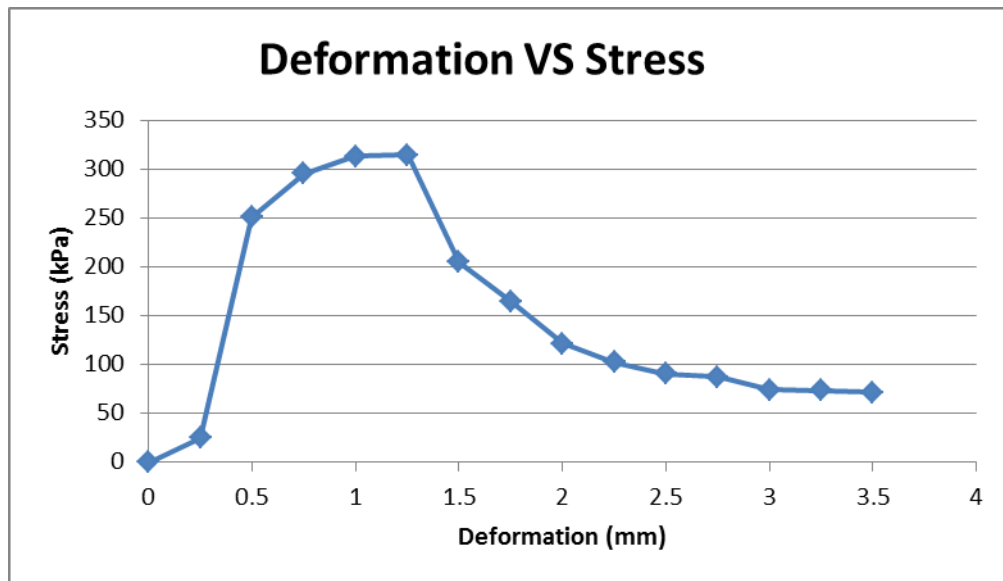
Fig 44: Plot of Stress VS Deformation (Trial 1)
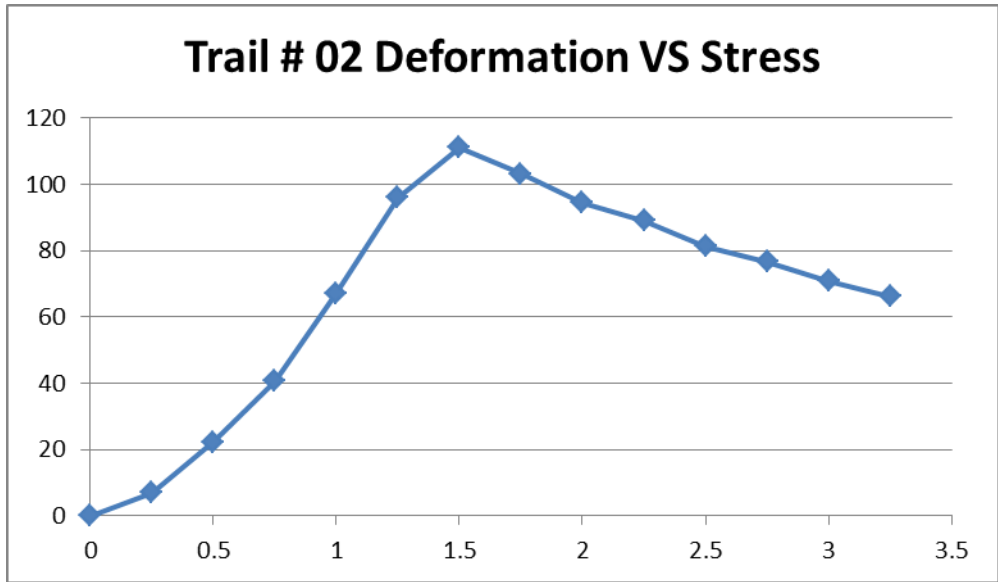
Fig 45: Plot of Stress VS Deformation (Trial 2)
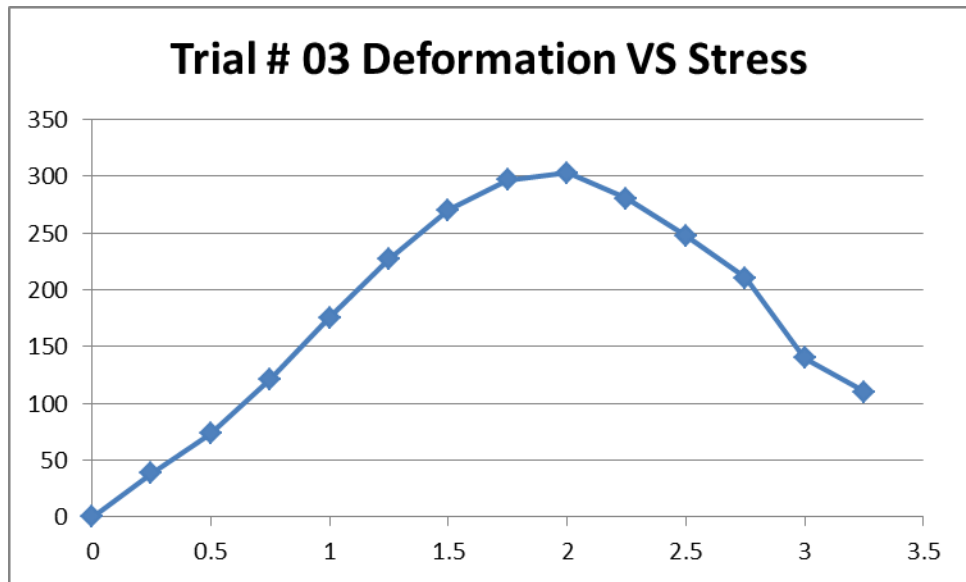
Fig 46: Plot of Stress VS Deformation (Trial 3)
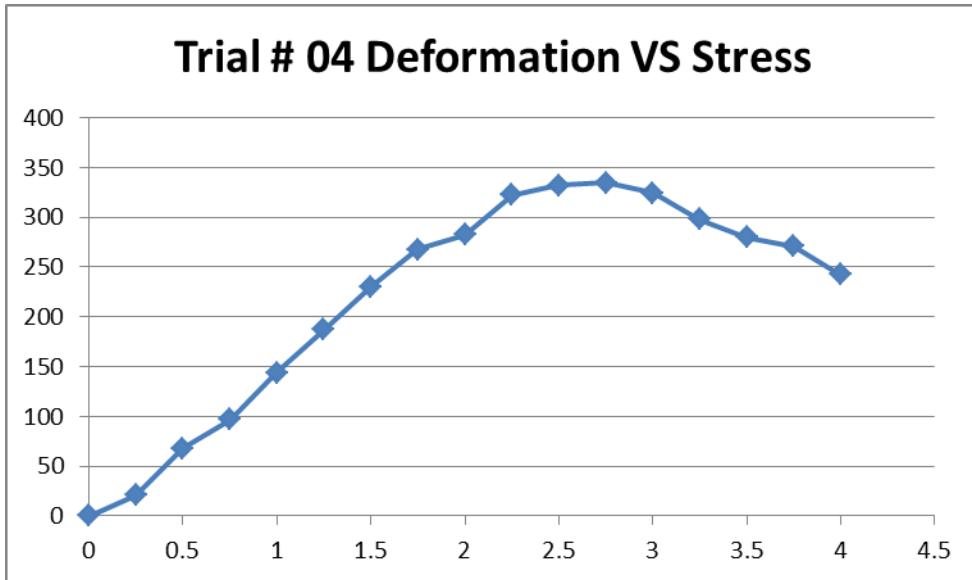
Fig 47: Plot of Stress VS Deformation (Trial 4)
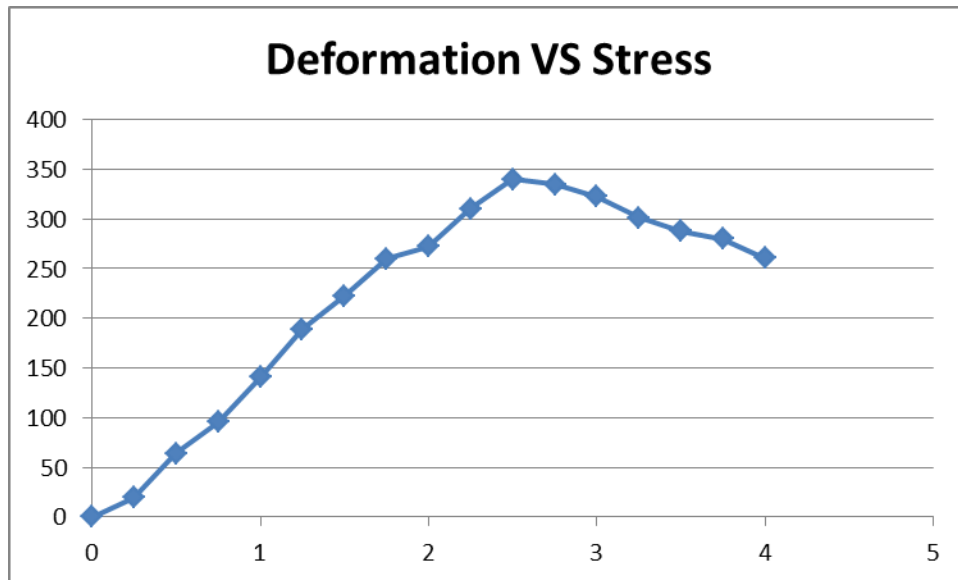
Fig 48: Plot of Stress VS Deformation (Trial 5)
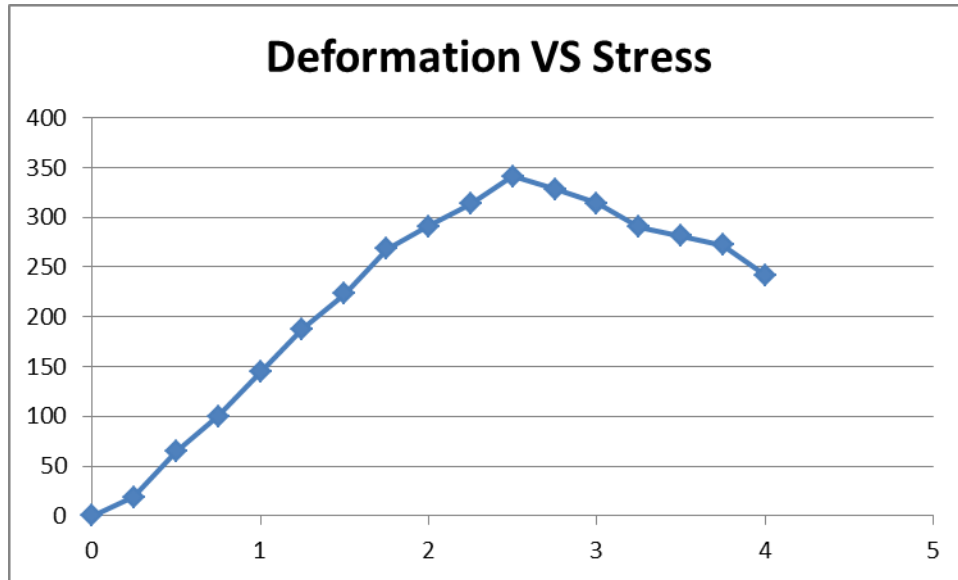
Fig 49: Plot of Stress VS Deformation (Trial 6)
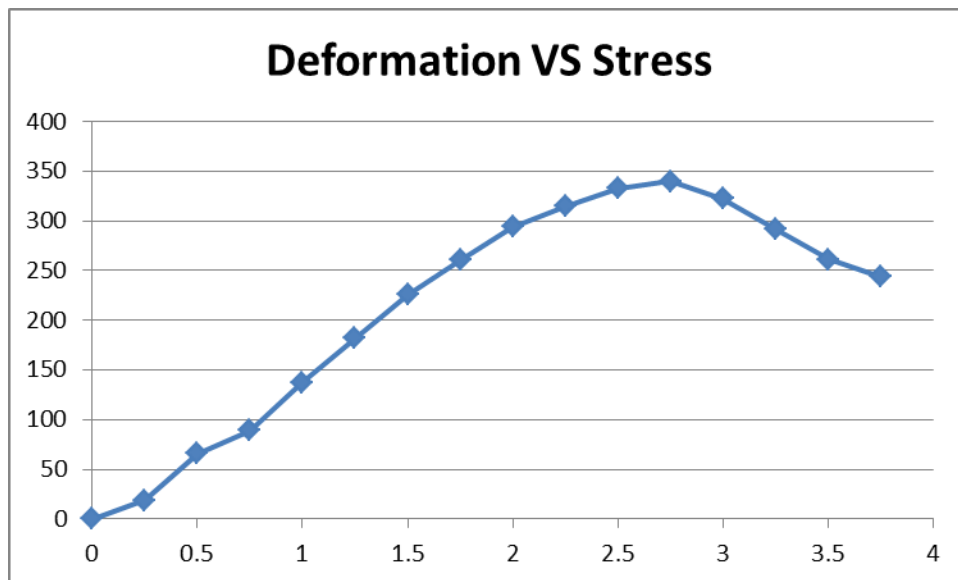
Fig 50: Plot of Stress VS Deformation (Trial 7)
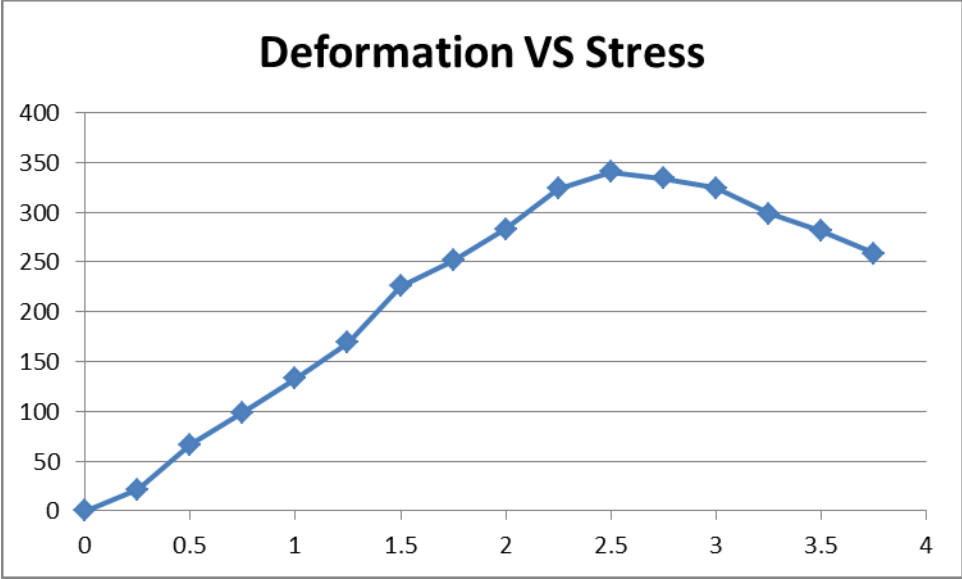
Fig 51: Plot of Stress VS Deformation (Trial 8)
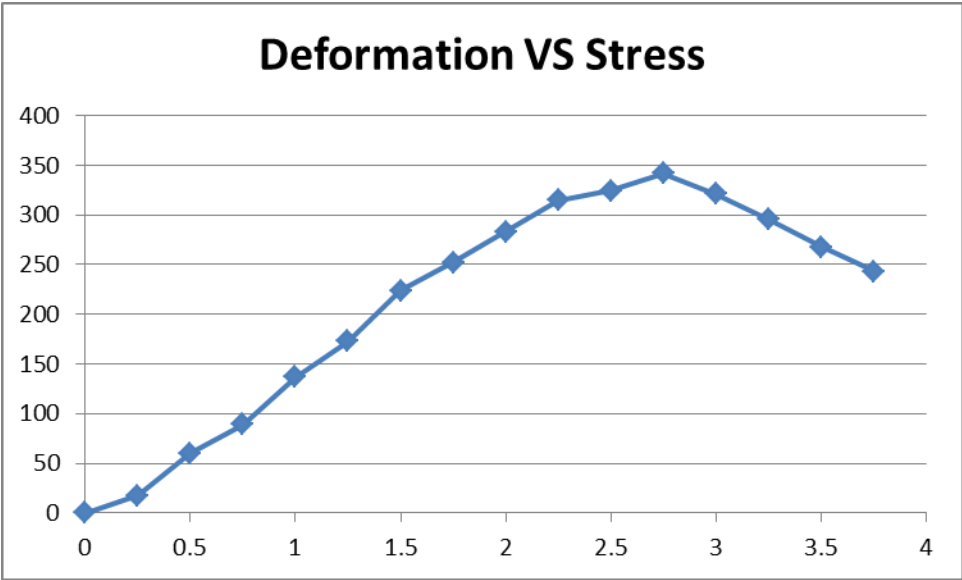
Fig 52: Plot of Stress VS Deformation (Trial 9)
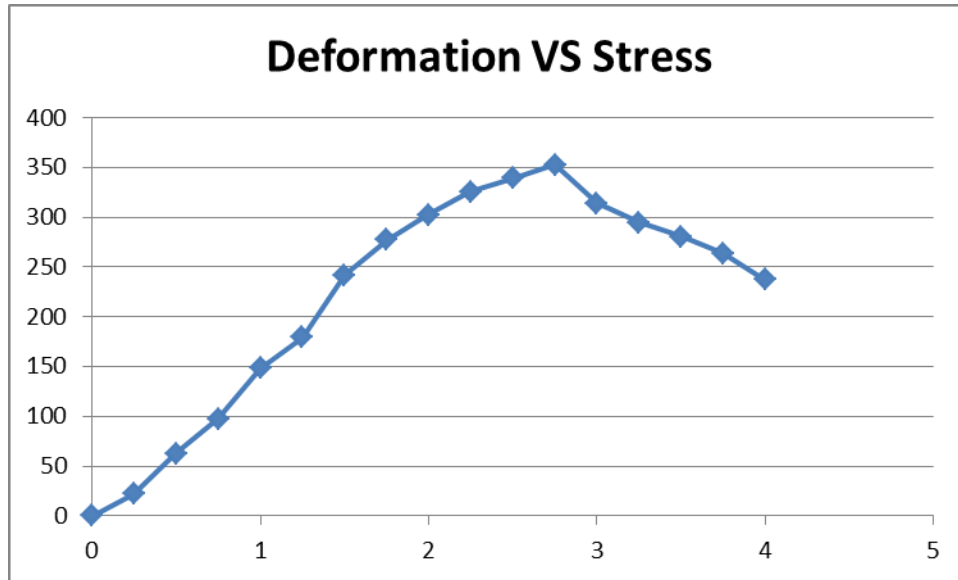
Fig 53: Plot of Stress VS Deformation (Trial 10)

The combined bar chart for the trials is given as follows to work out for the range of c obtained from the test results after discarding the abnormalities in the results.
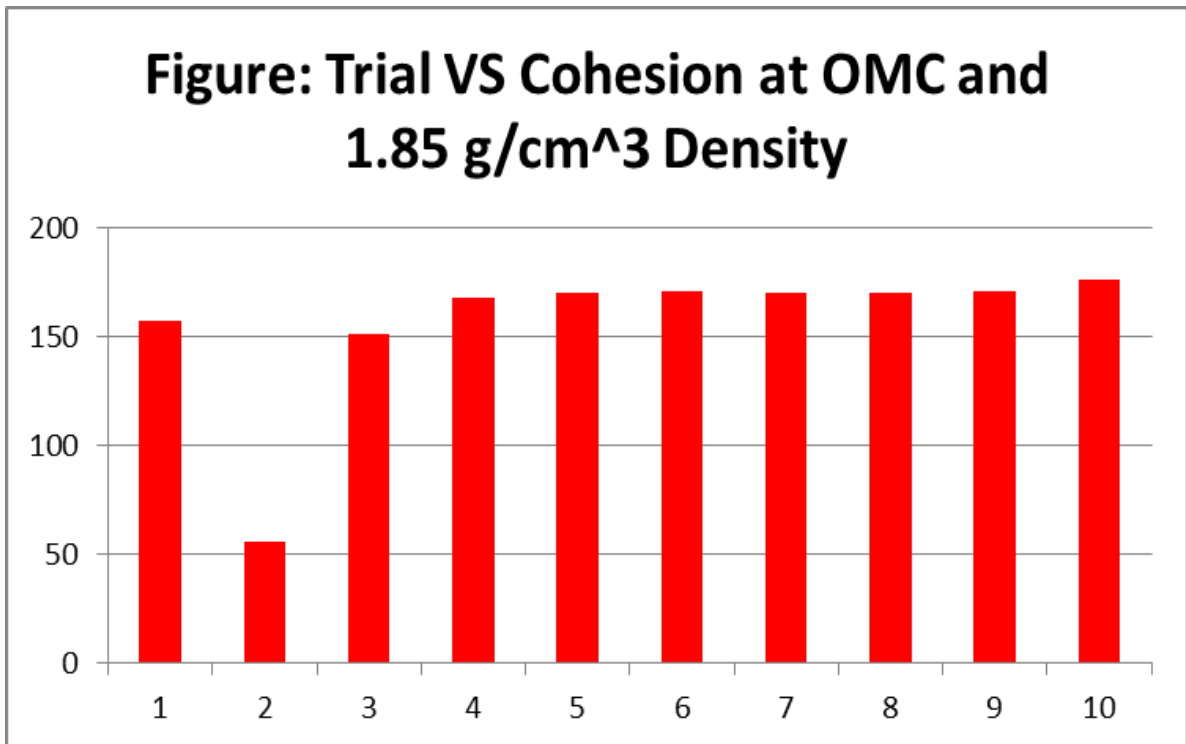
Fig 54: Bar Chart presenting the combined results

7.2 Centrifuge Testing

The testing on the self-designed Centrifuge Apparatus comprises of 4 stages namely (a) Preparation of the Sample at OMC, (b) Densification, (c) Saturation, (c) Shearing. The description of these stages is given below.

7.2.1 Preparation of the Sample at OMC

Samples were prepared at Optimum Moisture Content of 8% as determined before by assuring proper uniformity in the mixing procedures for both the acquired samples in order to proceed with Densification Process.

The process of preparation is shown in the following figures.

Fig 55: Sample Preparation at OMC

7.2.2 Densification

Densification was performed on both the acquired soil samples for the development of co-relations of increase in the percentage densification of the sample with revolutions per minute.

Densification that was carried out on both the soil samples comprised of 4 stages that are explained in the subsequently

7.2.2.1 Sample Placement

After mixing the samples with 8% water by weight of the samples they were properly placed in the detachable wire mesh cylindrical mold by means of a scoop in subsequent layers and weight of the samples were noted down.

Sample Placement is shown in the following figure.

Fig 56: Sample Placement

7.2.2.2 Initial Density

Height from top was noted down to calculate the volume of the samples and to get an estimate of the initial density.

Following figure shows the initial density measurement.

Fig 57: Initial Density Measurement

7.2.2.3 Densification Process

After calculating the initial densities of both the soil samples, the detachable mold was placed in the Centrifuge Apparatus and the densification process was started by operating the centrifuge for 15, 30, 45 and 60 seconds to obtain a trend of the % Densification.

Densification Process is shown in the following figure.

Fig 58: Densification Process

7.2.2.4 Final Density

Height from the top was again noted down for both the soil samples after each trial for the respective time duration and the final density was calculated.

This procedure was carried out on both the soil samples to get an idea of trend of %age densification.

Here are the results of the %age densification for NUST Clay achieved after 15, 30, 45 and 60 seconds.
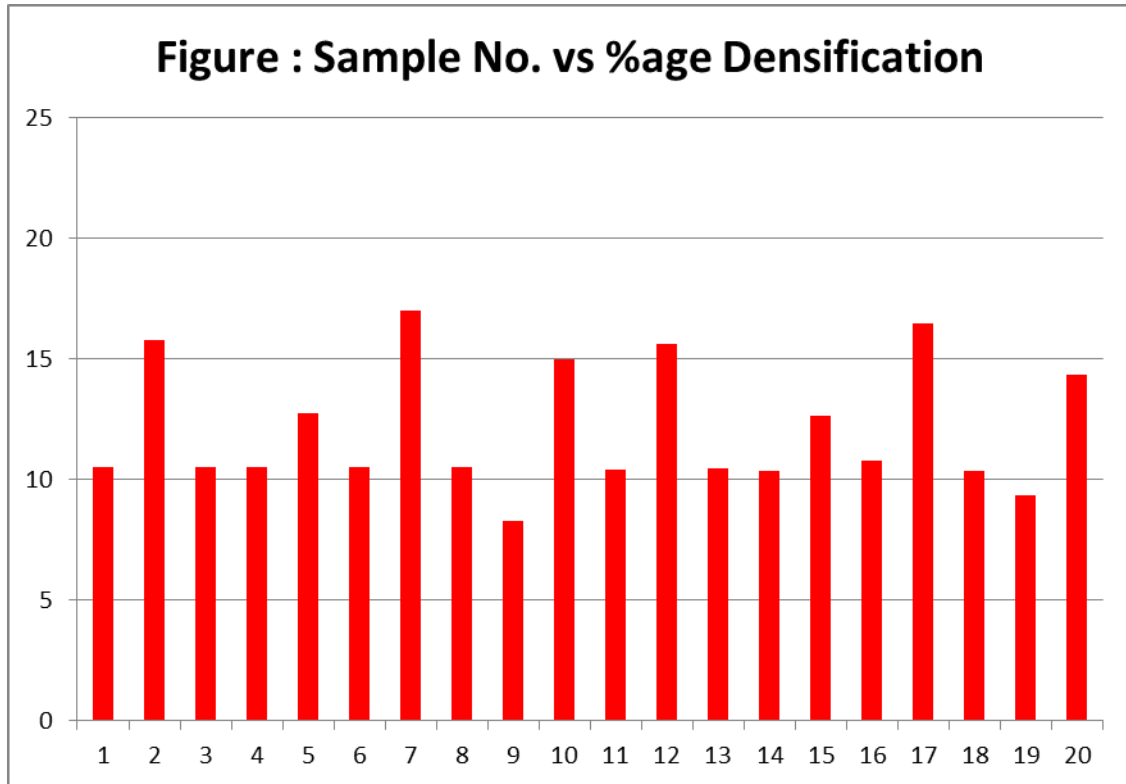
Fig 59: %age Densification after 15 seconds
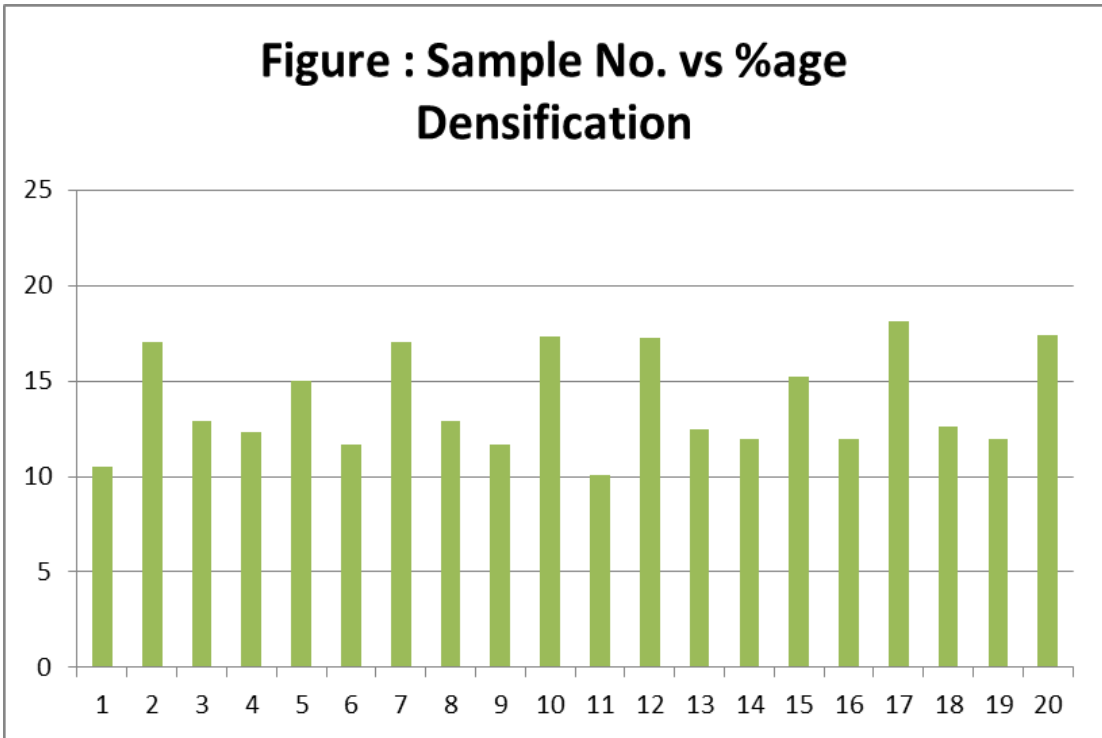
Fig 60: %age Densification after 30 seconds
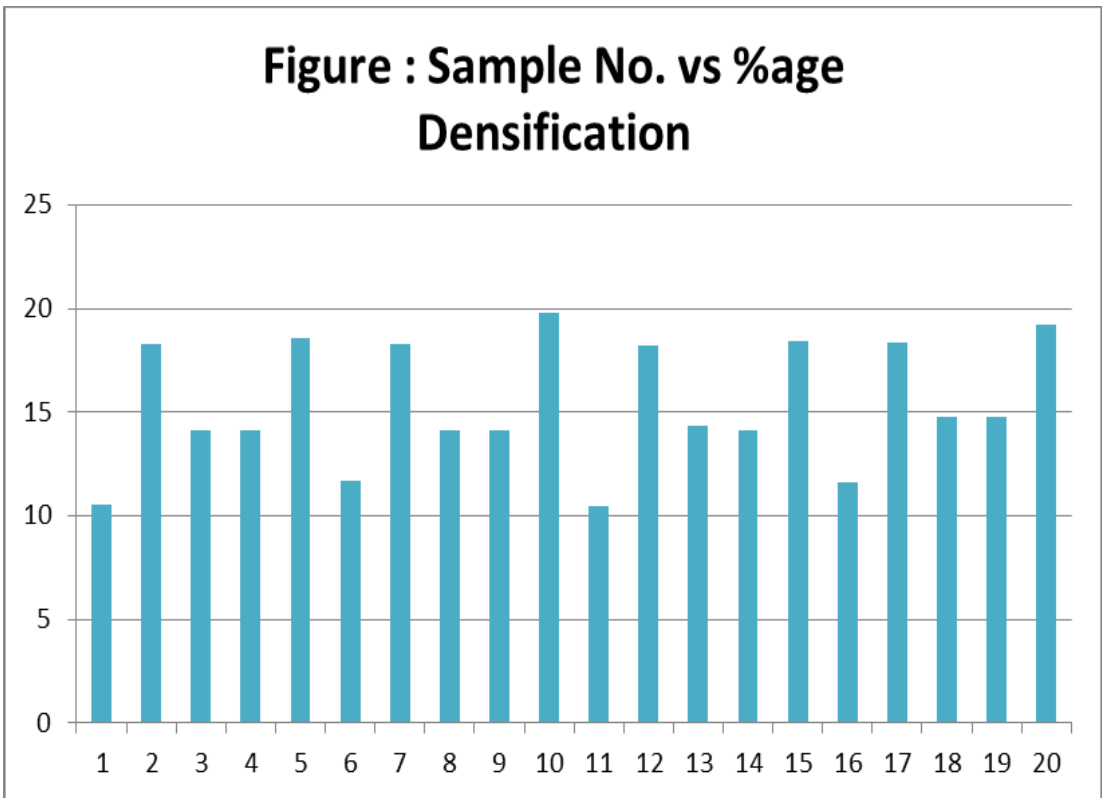
Fig 61: %age Densification after 45 seconds

70
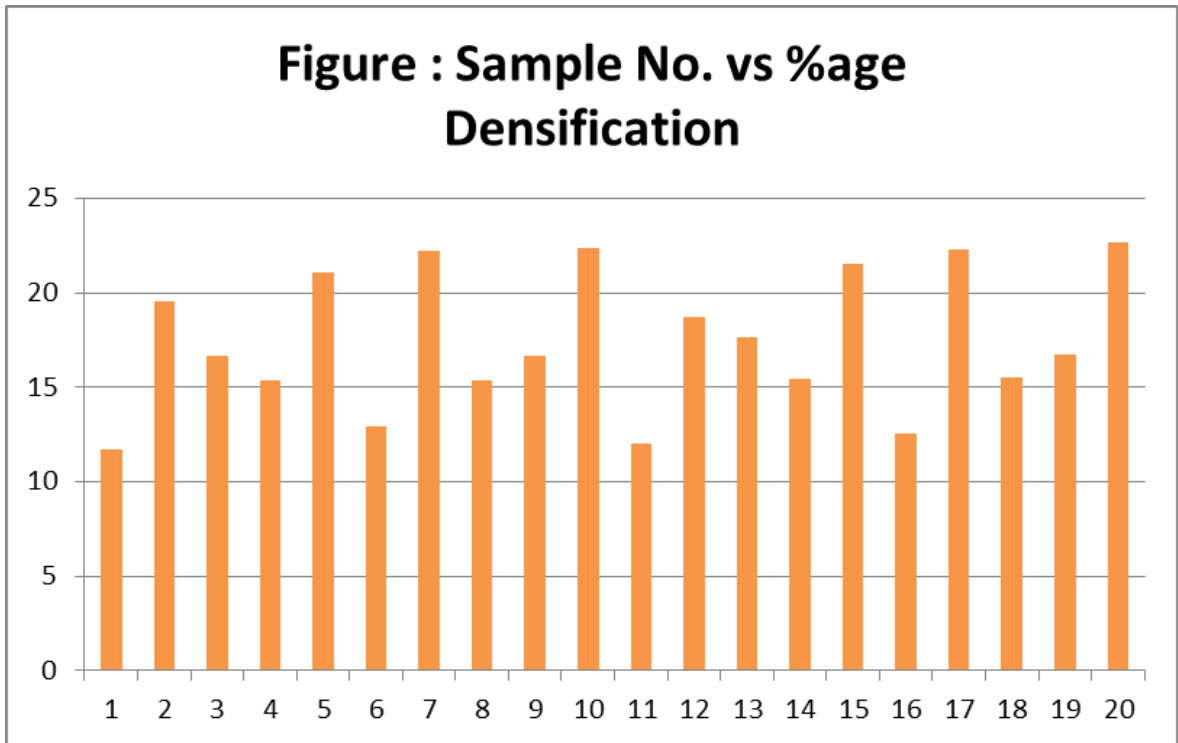
Fig 62: %age Densification after 60 seconds

Similarly here are the results for the Jhelum Sand for 15, 30, 45 and 60 seconds.
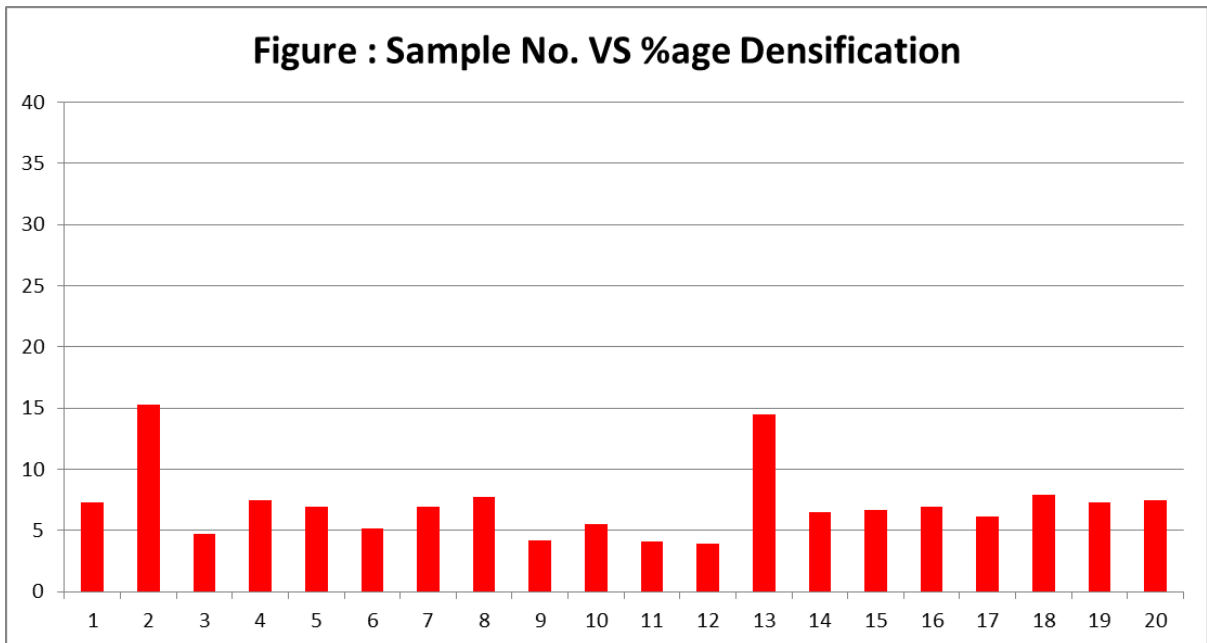
Fig 63: %age Densification after 15 seconds
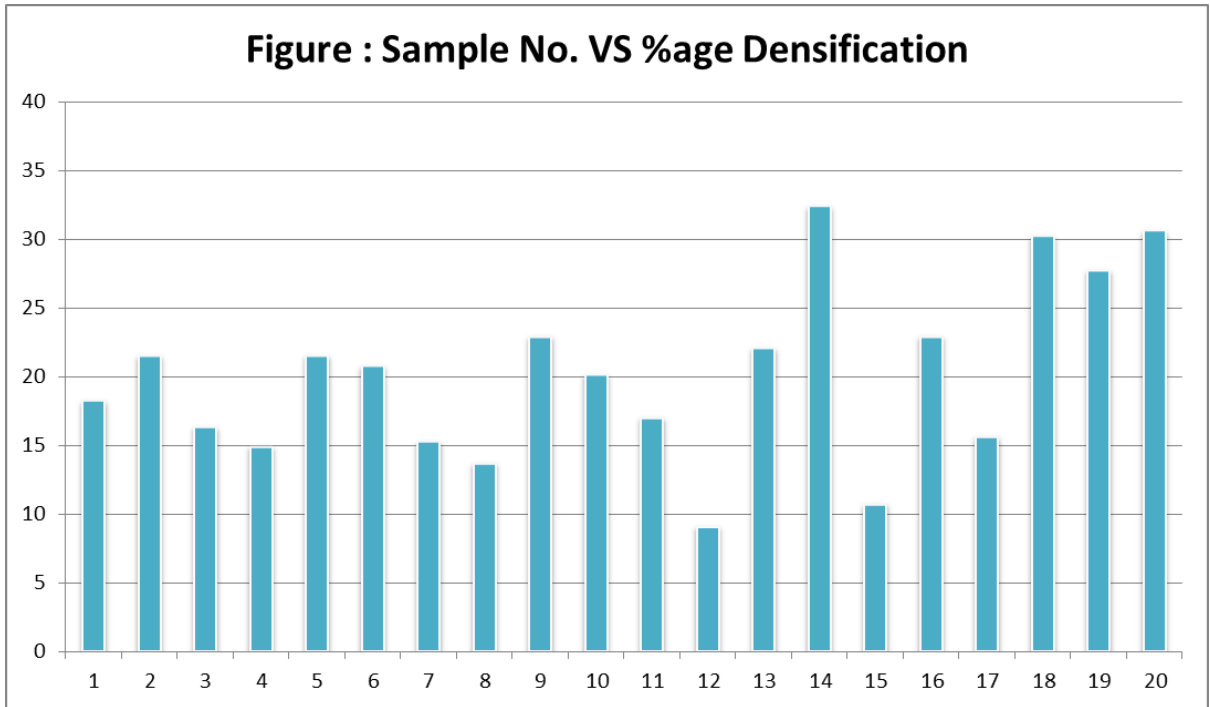
Fig 64: %age Densification after 30 seconds
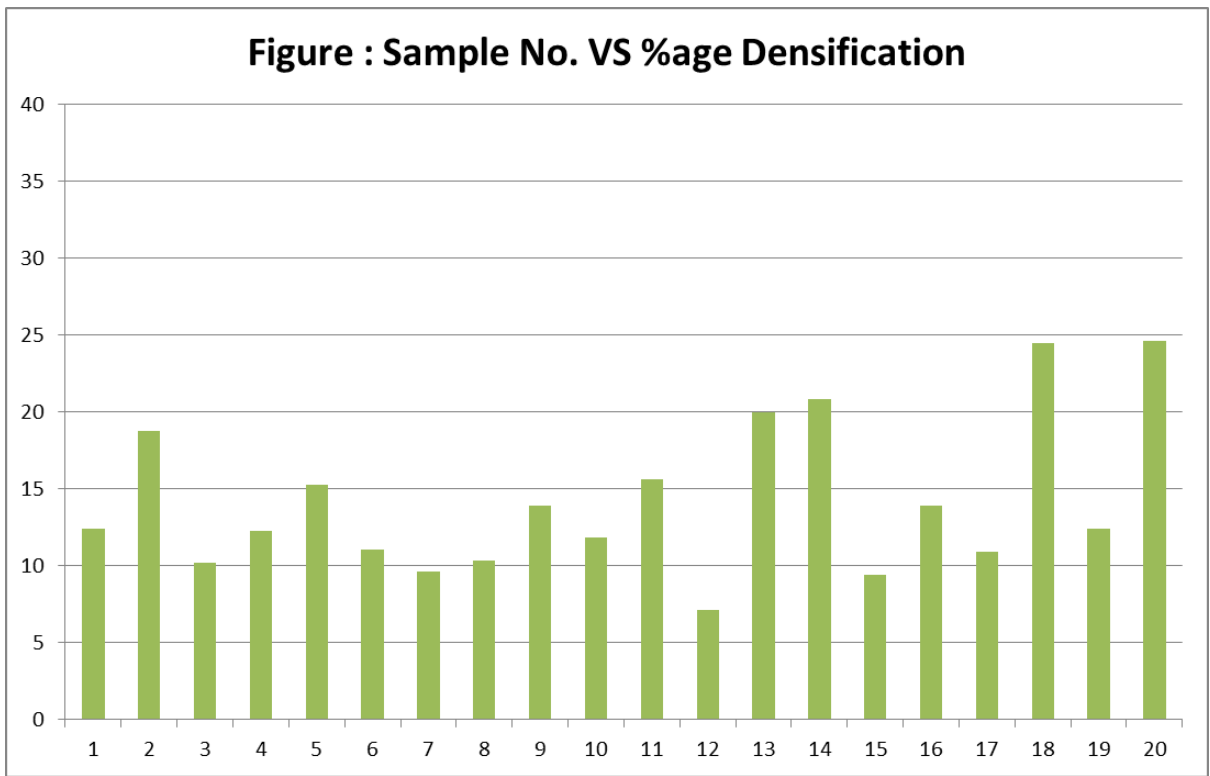
Fig 65: %age Densification after 45 seconds
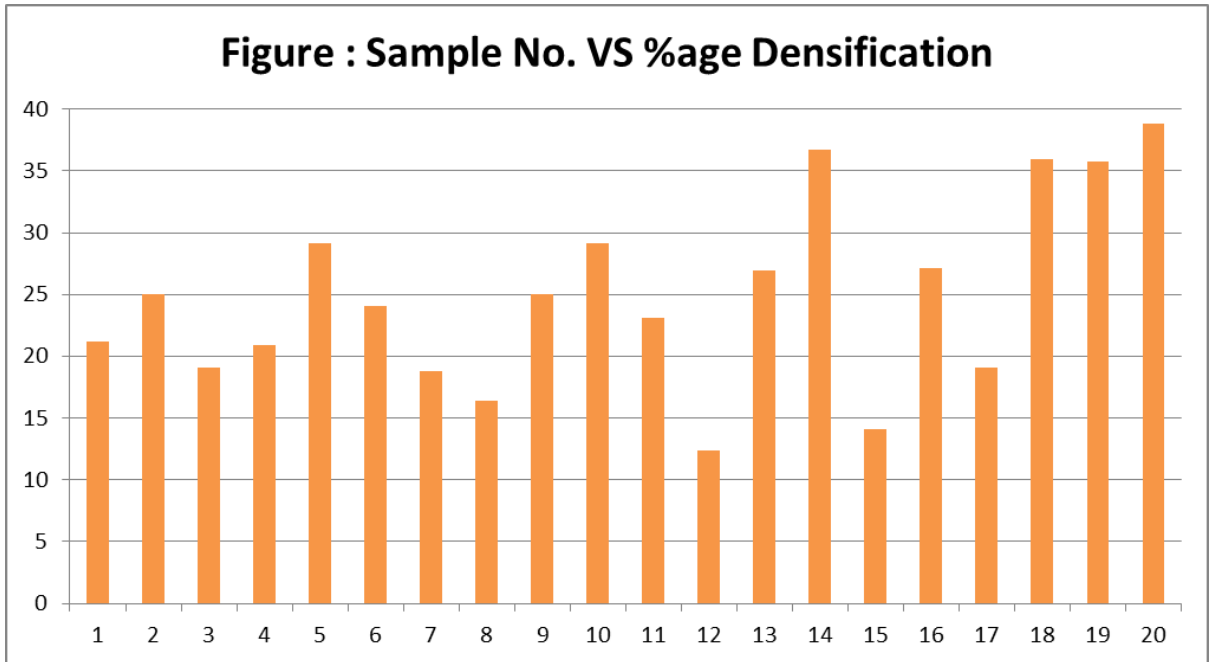
Fig 66: %age Densification after 60 seconds

Here are the combined trends for the increase in density for the both the soil samples at 15. 30, 45 and 60 seconds clearly indicating the increase in the density after 1 minute of the densification process.
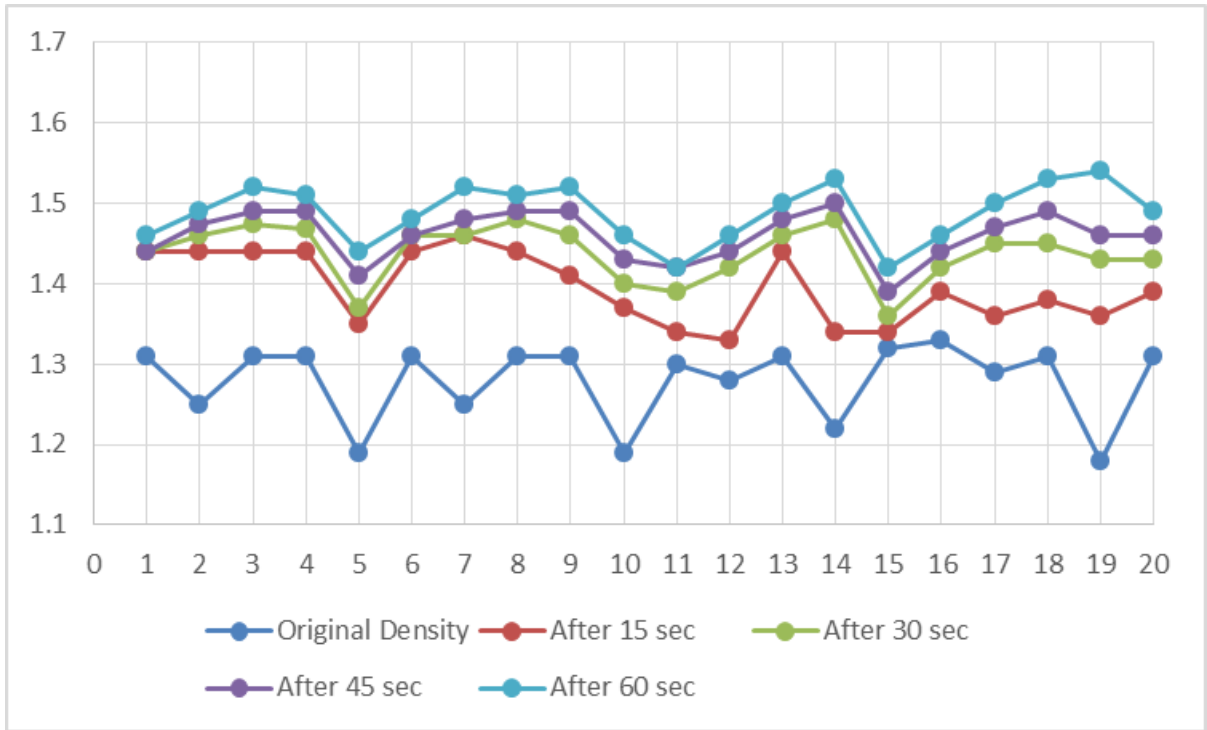
Fig 67: Density Increment for NUST Clay

It is pretty obvious from the trend of Clay that initially it densifies to a greater extent but then stabilizes.
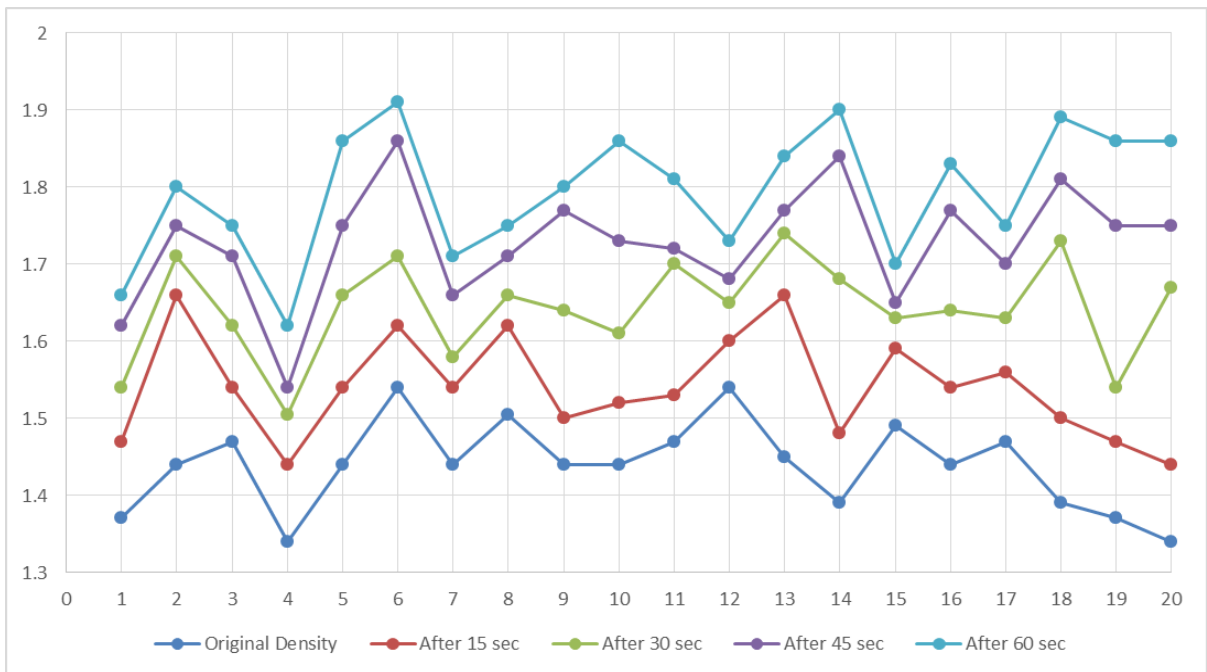
Fig 68: Density Increment for Jhelum Sand

But for Sandy Sample, the density keeps on increasing gradually.

7.2.3 Saturation

Time efficient saturation was obtained from the self-designed Centrifuge Apparatus. The Saturation Process carried out on the "Clayey Sample" comprised of 4 stages that listed below with relevant figures.

7.2.3.1 Provision of Holes

After densifying the Clayey Sample for 2 minutes, holes were provided in the confined soil sample by means of a steel rod up till the base of the cylinder.

Following figure clearly shows this stage.

Fig 69: Provision of holes

7.2.3.2 Water Injection

Water was then injected in the provided holes to achieve uniform saturation by means of rubber tubes.

Following figure clearly shows this stage.

Fig 70: Water Injection

7.2.3.3 Saturation Process

The cylinder was properly covered and rotated for 2 minutes to achieve effective saturation. Following figure clearly shows this stage.

Fig 71: Saturation Process

7.2.3.4 Tensiometer Application

Tensiometer was placed in the sample to get an idea of the soil saturation. When the dial reading approached near zero indicating that saturation has been achieved, some sample was acquired in a can to calculate the moisture content and ultimately the final degree of saturation from the calculated moisture content.

Following figure clearly shows this stage.
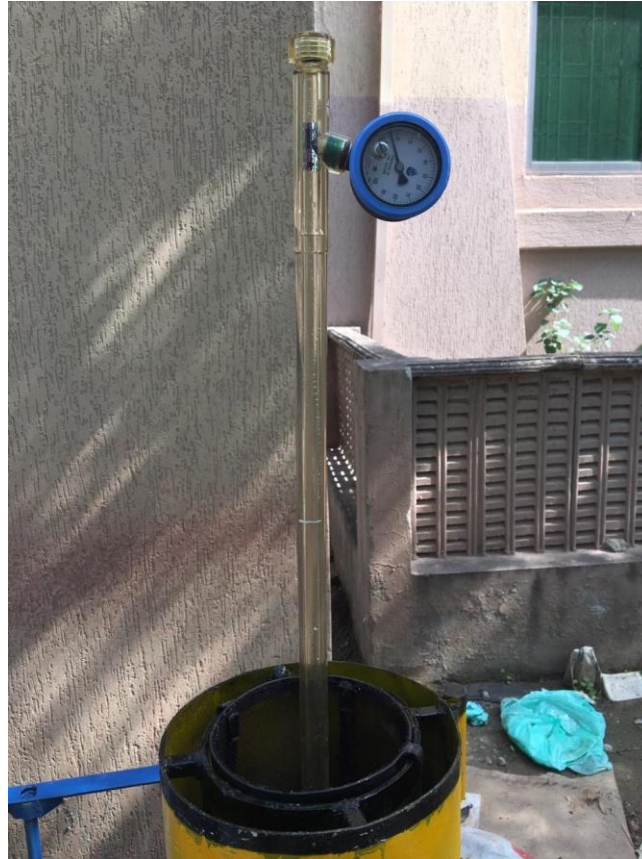
Fig 72: Tensiometer Application

The tabulated saturation results are provided in the table.

TRIAL #	MASS (g)	BULK DENSITY (g/cm3)	DRY DENSITY (g/cm3)	M.C %	SAT %
1	208.98	2.08	1.81	14.81	89.13
2	189.39	1.88	1.54	22.22	84.60
3	212.46	2.11	1.85	14.00	91.32
4	210.82	2.10	1.83	14.29	89.92
5	199.84	1.99	1.69	17.86	86.35
6	202.01	2.01	1.70	18.52	90.91
7	209.63	2.09	1.83	14.00	87.17
8	200.85	2.00	1.69	18.37	89.01
9	208.98	2.08	1.79	16.00	93.06
10	191.57	1.91	1.53	24.44	91.56

Table 20: Results for Degree of Saturation (Joseph E. Bowles)

7.2.4 Shearing

The shearing stages further comprises of 4 stages that are described below with the pictorial presentation.

7.2.4.1 Manual Loading Mechanism

We did devise a manual loading mechanism to shear the sample in the Centrifuge Apparatus but to the unavailability of the failure identification mechanism we switched to the Unconfined Compression Test Apparatus to carry out the shearing of the Saturated Sample.

The devised loading mechanism is shown in the following figure.

Fig 73: Devised Manual Loading Mechanism

7.2.4.2 Sample Extraction

To carry out shearing of the saturated sample in the UCS apparatus, undisturbed saturated sample was extracted from the centrifuge apparatus by means of a Shelby Tube.

Following figure shows the sample extraction.

Fig 74: Sample Extraction using Shelby Tube

7.2.4.3 Sample Shearing Process

The extracted sample was then trimmed and placed in the UCS apparatus for the shearing process.

Sample was sheared by axial load application and the readings were noted down. Following figure shows the sheared sample.

Fig 75: Sample Shearing in UCS Apparatus

7.2.4.4 Sample Failure

Sample failed in a similar manner as it does so in the Tri-Axial Apparatus.
The sample bulged sample is shown in the following figure.

Fig 76: Sheared Sample

The tabulated results and the plots for all the 10 trials performed are given below.

TRIAL #01		L=80mm	Area =	1256.637				
Deformation ΔL (mm)	Strain ε=ΔL/L		Corrected Area Ac=A/(1-ε) m^2		P.R.R	Load P (kN)	Stress б=P/A	
0	0		0.001256637		0	0	0	
0.25	0.003125		0.001260576		64	0.0064	5.077043	
0.5	0.00625		0.00126454		130	0.013	10.28042	
0.75	0.009375		0.001268529		164	0.0164	12.92836	
1	0.0125		0.001272544		194	0.0194	15.24505	
1.25	0.015625		0.001276584		216	0.0216	16.92016	
1.5	0.01875		0.001280649		254	0.0254	19.83369	
1.75	0.021875		0.001284741		266	0.0266	20.70457	
2	0.025		0.001288858		296	0.0296	22.96606	
2.25	0.028125		0.001293003		328	0.0328	25.36731	
2.5	0.03125		0.001297174		358	0.0358	27.59846	
2.75	0.034375		0.001301372		384	0.0384	29.50733	
3	0.0375		0.001305597		412	0.0412	31.55645	
3.25	0.040625		0.00130985		436	0.0436	33.28626	
3.5	0.04375		0.00131413		468	0.0468	35.61291	
4	0.05		0.001322776		494	0.0494	37.34571	
4.5	0.05625		0.001331536		536	0.0536	40.25427	
5	0.0625		0.001340413		584	0.0584	43.56867	
5.5	0.06875		0.001349409		610	0.061	45.20498	
6	0.075		0.001358526		632	0.0632	46.52099	
6.5	0.08125		0.001367768		654	0.0654	47.81512	
7	0.0875		0.001377136		682	0.0682	49.52305	
7.5	0.09375		0.001386634		710	0.071	51.20313	
8	0.1		0.001396263		732	0.0732	52.42564	
8.5	0.10625		0.001406027		752	0.0752	53.48402	
9	0.1125		0.001415929		774	0.0774	54.66376	
9.5	0.11875		0.001425971		794	0.0794	55.68135	
10	0.125		0.001436157		822	0.0822	57.2361	
10.5	0.13125		0.001446489		846	0.0846	58.48646	
11	0.1375		0.00145697		874	0.0874	59.98749	
11.5	0.14375		0.001467605		902	0.0902	61.46067	
12	0.15		0.001478396		1304	0.1304	88.20367	
12.5	0.15625		0.001489348		1338	0.1338	89.838	
13	0.1625		0.001500462		1366	0.1366	91.03862	
13.5	0.16875		0.001511744		1385	0.1385	91.61606	
14	0.175		0.001523196		1390	0.139	91.25547	
14.5	0.18125		0.001534824		1276	0.1276	83.13658	
15	0.1875		0.00154663		1204	0.1204	77.84667	
15.5	0.19375		0.00155862		1172	0.1172	75.19475	

Table 21: Unconfined Compression Test Results (Trial 1)

TRIAL #02		L=80mm	Area =	1256.637				
Deformation ΔL (mm)	Strain ε=ΔL/L		Corrected Area Ac=A/(1-ε) m^2		P.R.R	Load P (kN)	Stress Ϭ=P/A	
0	0		0.001256637		0	0	0	
0.25	0.003125		0.001260576		40	0.004	3.173152	
0.5	0.00625		0.00126454		254	0.0254	20.08635	
0.75	0.009375		0.001268529		490	0.049	38.6274	
1	0.0125		0.001272544		684	0.0684	53.75061	
1.25	0.015625		0.001276584		842	0.0842	65.95729	
1.5	0.01875		0.001280649		690	0.069	53.87892	
1.75	0.021875		0.001284741		1060	0.106	82.50692	
2	0.025		0.001288858		1160	0.116	90.00212	
2.25	0.028125		0.001293003		1222	0.1222	94.5087	
2.5	0.03125		0.001297174		1308	0.1308	100.8346	
2.75	0.034375		0.001301372		1376	0.1376	105.7346	
3	0.0375		0.001305597		1444	0.1444	110.6008	
3.25	0.040625		0.00130985		1510	0.151	115.2804	
3.5	0.04375		0.00131413		1566	0.1566	119.1663	
4	0.05		0.001322776		1616	0.1616	122.1673	
4.5	0.05625		0.001331536		1670	0.167	125.4191	
5	0.0625		0.001340413		1706	0.1706	127.2742	
5.5	0.06875		0.001349409		1724	0.1724	127.7596	
6	0.075		0.001358526		1738	0.1738	127.9327	
6.5	0.08125		0.001367768		1768	0.1768	129.2617	
7	0.0875		0.001377136		1540	0.154	111.8262	
7.5	0.09375		0.001386634		1510	0.151	108.8968	
8	0.1		0.001396263		1485	0.1485	106.3553	
8.5	0.10625		0.001406027		1468	0.1468	104.4076	
9	0.1125		0.001415929		1454	0.1454	102.6888	

Table 22: Unconfined Compression Test Results (Trial 2)

TRIAL #03		L=80mm	Area =	1256.637				
Deformation ΔL (mm)	Strain ϵ=ΔL/L		Corrected Area Ac=A/(1-ϵ) m^2		P.R.R	Load P (kN)	Stress Ƃ=P/A	
0	0		0.001256637		0	0	0	
0.25	0.003125		0.001260576		150	0.015	11.89932	
0.5	0.00625		0.00126454		186	0.0186	14.7089	
0.75	0.009375		0.001268529		220	0.022	17.34292	
1	0.0125		0.001272544		260	0.026	20.43152	
1.25	0.015625		0.001276584		300	0.03	23.50022	
1.5	0.01875		0.001280649		332	0.0332	25.92435	
1.75	0.021875		0.001284741		368	0.0368	28.64391	
2	0.025		0.001288858		402	0.0402	31.19039	
2.25	0.028125		0.001293003		430	0.043	33.25592	
2.5	0.03125		0.001297174		456	0.0456	35.15335	
2.75	0.034375		0.001301372		486	0.0486	37.34521	
3	0.0375		0.001305597		510	0.051	39.06259	
3.25	0.040625		0.00130985		540	0.054	41.22611	
3.5	0.04375		0.00131413		772	0.0772	58.74608	
4	0.05		0.001322776		1472	0.1472	111.2811	
4.5	0.05625		0.001331536		2446	0.2446	183.6976	
5	0.0625		0.001340413		3422	0.3422	255.2945	
5.5	0.06875		0.001349409		4353	0.4353	322.5857	
6	0.075		0.001358526		5348	0.5348	393.6618	
6.5	0.08125		0.001367768		6268	0.6268	458.2648	
7	0.0875		0.001377136		6902	0.6902	501.1849	
7.5	0.09375		0.001386634		7498	0.7498	540.7339	
8	0.1		0.001396263		7716	0.7716	552.6178	
8.5	0.10625		0.001406027		7872	0.7872	559.8753	
9	0.1125		0.001415929		7992	0.7992	564.4351	
9.5	0.11875		0.001425971		7800	0.78	546.9957	
10	0.125		0.001436157		7736	0.7736	538.6599	
10.5	0.13125		0.001446489		7674	0.7674	530.5261	

Table 23: Unconfined Compression Test Results (Trial 3)

TRIAL #04		L=80mm	Area =	1256.637				
Deformation ΔL (mm)	Strain ε=ΔL/L		Corrected Area Ac=A/(1-ε) m^2		P.R.R	Load P (kN)	Stress б=P/A	
0	0		0.001256637		0	0	0	
0.25	0.003125		0.001260576		160	0.016	12.69261	
0.5	0.00625		0.00126454		200	0.02	15.81602	
0.75	0.009375		0.001268529		260	0.026	20.49617	
1	0.0125		0.001272544		310	0.031	24.36065	
1.25	0.015625		0.001276584		360	0.036	28.20027	
1.5	0.01875		0.001280649		415	0.0415	32.40544	
1.75	0.021875		0.001284741		505	0.0505	39.30754	
2	0.025		0.001288858		576	0.0576	44.69071	
2.25	0.028125		0.001293003		612	0.0612	47.33169	
2.5	0.03125		0.001297174		669	0.0669	51.57366	
2.75	0.034375		0.001301372		730	0.073	56.09466	
3	0.0375		0.001305597		812	0.0812	62.19378	
3.25	0.040625		0.00130985		878	0.0878	67.03059	
3.5	0.04375		0.00131413		934	0.0934	71.07363	
4	0.05		0.001322776		1099	0.1099	83.08286	
4.5	0.05625		0.001331536		1234	0.1234	92.67493	
5	0.0625		0.001340413		1678	0.1678	125.1853	
5.5	0.06875		0.001349409		2343	0.2343	173.6316	
6	0.075		0.001358526		3352	0.3352	246.7379	
6.5	0.08125		0.001367768		3989	0.3989	291.643	
7	0.0875		0.001377136		4501	0.4501	326.8376	
7.5	0.09375		0.001386634		4991	0.4991	359.9364	
8	0.1		0.001396263		5548	0.5548	397.3463	
8.5	0.10625		0.001406027		6122	0.6122	435.4111	
9	0.1125		0.001415929		6924	0.6924	489.0076	
9.5	0.11875		0.001425971		7369	0.7369	516.7707	
10	0.125		0.001436157		7890	0.789	549.383	
10.5	0.13125		0.001446489		7548	0.7548	521.8154	
11	0.1375		0.00145697		7432	0.7432	510.0996	

Table 24: Unconfined Compression Test Results (Trial 4)

TRIAL #05		L=80mm	Area =	1256.637				
Deformation ΔL (mm)	Strain ε=ΔL/L		Corrected Area Ac=A/(1-ε) m^2	P.R.R	Load P (kN)	Stress б=P/A	
0	0		0.001256637	0	0	0	
0.25	0.003125		0.001260576	69	0.0069	5.473687	
0.5	0.00625		0.00126454	120	0.012	9.489614	
0.75	0.009375		0.001268529	172	0.0172	13.55901	
1	0.0125		0.001272544	186	0.0186	14.61639	
1.25	0.015625		0.001276584	190	0.019	14.88347	
1.5	0.01875		0.001280649	240	0.024	18.7405	
1.75	0.021875		0.001284741	257	0.0257	20.00404	
2	0.025		0.001288858	277	0.0277	21.49189	
2.25	0.028125		0.001293003	300	0.03	23.20181	
2.5	0.03125		0.001297174	340	0.034	26.21083	
2.75	0.034375		0.001301372	375	0.0375	28.81575	
3	0.0375		0.001305597	396	0.0396	30.33095	
3.25	0.040625		0.00130985	433	0.0433	33.05723	
3.5	0.04375		0.00131413	457	0.0457	34.77585	
4	0.05		0.001322776	483	0.0483	36.51412	
4.5	0.05625		0.001331536	541	0.0541	40.62977	
5	0.0625		0.001340413	579	0.0579	43.19565	
5.5	0.06875		0.001349409	610	0.061	45.20498	
6	0.075		0.001358526	629	0.0629	46.30016	
6.5	0.08125		0.001367768	643	0.0643	47.01089	
7	0.0875		0.001377136	676	0.0676	49.08737	
7.5	0.09375		0.001386634	689	0.0689	49.68867	
8	0.1		0.001396263	728	0.0728	52.13916	
8.5	0.10625		0.001406027	743	0.0743	52.84392	
9	0.1125		0.001415929	765	0.0765	54.02813	
9.5	0.11875		0.001425971	786	0.0786	55.12033	
10	0.125		0.001436157	811	0.0811	56.47017	
10.5	0.13125		0.001446489	853	0.0853	58.97039	
11	0.1375		0.00145697	892	0.0892	61.22293	
11.5	0.14375		0.001467605	921	0.0921	62.75529	
12	0.15		0.001478396	1209	0.1209	81.77779	
12.5	0.15625		0.001489348	1298	0.1298	87.15226	
13	0.1625		0.001500462	1324	0.1324	88.23948	
13.5	0.16875		0.001511744	1367	0.1367	90.42538	
14	0.175		0.001523196	1387	0.1387	91.05852	
14.5	0.18125		0.001534824	1265	0.1265	82.41988	
15	0.1875		0.00154663	1212	0.1212	78.36392	
15.5	0.19375		0.00155862	1165	0.1165	74.74563	

Table 25: Unconfined Compression Test Results (Trial 5)

TRIAL #06		L=80mm	Area =	1256.637				
Deformation ΔL (mm)	Strain ϵ=ΔL/L		Corrected Area Ac=A/(1-ϵ) m^2		P.R.R	Load P (kN)	Stress Ϭ=P/A	
0	0		0.001256637		0	0	0	
0.25	0.003125		0.001260576		30	0.003	2.379864	
0.5	0.00625		0.00126454		102	0.0102	8.066172	
0.75	0.009375		0.001268529		325	0.0325	25.62022	
1	0.0125		0.001272544		426	0.0426	33.47625	
1.25	0.015625		0.001276584		497	0.0497	38.93204	
1.5	0.01875		0.001280649		536	0.0536	41.85377	
1.75	0.021875		0.001284741		856	0.0856	66.62823	
2	0.025		0.001288858		982	0.0982	76.19145	
2.25	0.028125		0.001293003		1197	0.1197	92.57521	
2.5	0.03125		0.001297174		1254	0.1254	96.67171	
2.75	0.034375		0.001301372		1324	0.1324	101.7388	
3	0.0375		0.001305597		1432	0.1432	109.6816	
3.25	0.040625		0.00130985		1522	0.1522	116.1965	
3.5	0.04375		0.00131413		1533	0.1533	116.6551	
4	0.05		0.001322776		1623	0.1623	122.6965	
4.5	0.05625		0.001331536		1654	0.1654	124.2175	
5	0.0625		0.001340413		1723	0.1723	128.5425	
5.5	0.06875		0.001349409		1759	0.1759	130.3534	
6	0.075		0.001358526		1795	0.1795	132.1285	
6.5	0.08125		0.001367768		1754	0.1754	128.2381	
7	0.0875		0.001377136		1523	0.1523	110.5918	
7.5	0.09375		0.001386634		1576	0.1576	113.6565	
8	0.1		0.001396263		1476	0.1476	105.7107	

Table 26: Unconfined Compression Test Results (Trial 6)

TRIAL #07		L=80mm	Area =	1256.637				
Deformation ΔL (mm)	Strain ϵ=ΔL/L		Corrected Area Ac=A/(1-ϵ) m^2		P.R.R	Load P (kN)	Stress б=P/A	
0	0		0.001256637		0	0	0	
0.25	0.003125		0.001260576		120	0.012	9.519455	
0.5	0.00625		0.00126454		143	0.0143	11.30846	
0.75	0.009375		0.001268529		187	0.0187	14.74148	
1	0.0125		0.001272544		217	0.0217	17.05246	
1.25	0.015625		0.001276584		276	0.0276	21.62021	
1.5	0.01875		0.001280649		298	0.0298	23.26945	
1.75	0.021875		0.001284741		346	0.0346	26.9315	
2	0.025		0.001288858		398	0.0398	30.88004	
2.25	0.028125		0.001293003		427	0.0427	33.02391	
2.5	0.03125		0.001297174		478	0.0478	36.84934	
2.75	0.034375		0.001301372		512	0.0512	39.3431	
3	0.0375		0.001305597		537	0.0537	41.13061	
3.25	0.040625		0.00130985		576	0.0576	43.97451	
3.5	0.04375		0.00131413		894	0.0894	68.02979	
4	0.05		0.001322776		953	0.0953	72.04547	
4.5	0.05625		0.001331536		1657	0.1657	124.4428	
5	0.0625		0.001340413		2643	0.2643	197.1781	
5.5	0.06875		0.001349409		3768	0.3768	279.2334	
6	0.075		0.001358526		4983	0.4983	366.7945	
6.5	0.08125		0.001367768		6024	0.6024	440.4255	
7	0.0875		0.001377136		6907	0.6907	501.548	
7.5	0.09375		0.001386634		7323	0.7323	528.1134	
8	0.1		0.001396263		7662	0.7662	548.7504	
8.5	0.10625		0.001406027		7862	0.7862	559.1641	
9	0.1125		0.001415929		7942	0.7942	560.9038	
9.5	0.11875		0.001425971		7917	0.7917	555.2006	
10	0.125		0.001436157		7824	0.7824	544.7874	

Table 27: Unconfined Compression Test Results (Trial 7)

TRIAL #08		L=80mm	Area =	1256.637				
Deformation ΔL (mm)	Strain ϵ=ΔL/L		Corrected Area Ac=A/(1-ϵ) m^2	P.R.R	Load P (kN)	Stress Ϭ=P/A	
0	0		0.001256637	0	0	0	
0.25	0.003125		0.001260576	150	0.015	11.89932	
0.5	0.00625		0.00126454	198	0.0198	15.65786	
0.75	0.009375		0.001268529	254	0.0254	20.02318	
1	0.0125		0.001272544	298	0.0298	23.41766	
1.25	0.015625		0.001276584	354	0.0354	27.73026	
1.5	0.01875		0.001280649	412	0.0412	32.17118	
1.75	0.021875		0.001284741	564	0.0564	43.89991	
2	0.025		0.001288858	582	0.0582	45.15624	
2.25	0.028125		0.001293003	599	0.0599	46.32628	
2.5	0.03125		0.001297174	643	0.0643	49.56931	
2.75	0.034375		0.001301372	712	0.0712	54.7115	
3	0.0375		0.001305597	784	0.0784	60.04916	
3.25	0.040625		0.00130985	853	0.0853	65.12198	
3.5	0.04375		0.00131413	921	0.0921	70.08438	
4	0.05		0.001322776	1012	0.1012	76.50578	
4.5	0.05625		0.001331536	1267	0.1267	95.15327	
5	0.0625		0.001340413	1643	0.1643	122.5742	
5.5	0.06875		0.001349409	1987	0.1987	147.2497	
6	0.075		0.001358526	2765	0.2765	203.5293	
6.5	0.08125		0.001367768	3525	0.3525	257.7191	
7	0.0875		0.001377136	4258	0.4258	309.1923	
7.5	0.09375		0.001386634	4789	0.4789	345.3687	
8	0.1		0.001396263	5156	0.5156	369.2713	
8.5	0.10625		0.001406027	6842	0.6842	486.6192	
9	0.1125		0.001415929	7123	0.7123	503.0619	
9.5	0.11875		0.001425971	7205	0.7205	505.2697	
10	0.125		0.001436157	7927	0.7927	551.9593	
10.5	0.13125		0.001446489	7653	0.7653	529.0743	
11	0.1375		0.00145697	7421	0.7421	509.3446	
11.5	0.14375		0.001467605	7212	0.7212	491.4128	
12	0.15		0.001478396	7119	0.7119	481.5352	

Table 28: Unconfined Compression Test Results (Trial 8)

TRIAL #09		L=80mm	Area =	1256.637				
Deformation ΔL (mm)	Strain ε=ΔL/L		Corrected Area Ac=A/(1-ε) m^2		P.R.R	Load P (kN)	Stress б=P/A	
0	0		0.001256637		0	0	0	
0.25	0.003125		0.001260576		145	0.0145	11.50268	
0.5	0.00625		0.00126454		212	0.0212	16.76498	
0.75	0.009375		0.001268529		270	0.027	21.28449	
1	0.0125		0.001272544		313	0.0313	24.5964	
1.25	0.015625		0.001276584		367	0.0367	28.74861	
1.5	0.01875		0.001280649		434	0.0434	33.88906	
1.75	0.021875		0.001284741		564	0.0564	43.89991	
2	0.025		0.001288858		590	0.059	45.77694	
2.25	0.028125		0.001293003		643	0.0643	49.72921	
2.5	0.03125		0.001297174		692	0.0692	53.34675	
2.75	0.034375		0.001301372		745	0.0745	57.24729	
3	0.0375		0.001305597		794	0.0794	60.8151	
3.25	0.040625		0.00130985		856	0.0856	65.35101	
3.5	0.04375		0.00131413		928	0.0928	70.61705	
4	0.05		0.001322776		1012	0.1012	76.50578	
4.5	0.05625		0.001331536		1269	0.1269	95.30348	
5	0.0625		0.001340413		1345	0.1345	100.3422	
5.5	0.06875		0.001349409		1512	0.1512	112.0491	
6	0.075		0.001358526		1789	0.1789	131.6868	
6.5	0.08125		0.001367768		2459	0.2459	179.7819	
7	0.0875		0.001377136		3589	0.3589	260.6132	
7.5	0.09375		0.001386634		4567	0.4567	329.3587	
8	0.1		0.001396263		5349	0.5349	383.0939	
8.5	0.10625		0.001406027		6290	0.629	447.3597	
9	0.1125		0.001415929		7156	0.7156	505.3926	
9.5	0.11875		0.001425971		7481	0.7481	524.625	
10	0.125		0.001436157		7934	0.7934	552.4467	
10.5	0.13125		0.001446489		7610	0.761	526.1016	
11	0.1375		0.00145697		7290	0.729	500.3533	
11.5	0.14375		0.001467605		6892	0.6892	469.6086	

Table 29: Unconfined Compression Test Results (Trial 9)

Deformation ΔL (mm)	Strain ϵ=ΔL/L	Corrected Area Ac=A/(1-ϵ) m^2	P.R.R	Load P (kN)	Stress б=P/A	
TRIAL #10		L=80mm	Area =	1256.637		
0	0	0.001256637	0	0	0	
0.25	0.003125	0.001260576	175	0.0175	13.88254	
0.5	0.00625	0.00126454	214	0.0214	16.92314	
0.75	0.009375	0.001268529	256	0.0256	20.18085	
1	0.0125	0.001272544	309	0.0309	24.28207	
1.25	0.015625	0.001276584	376	0.0376	29.45361	
1.5	0.01875	0.001280649	412	0.0412	32.17118	
1.75	0.021875	0.001284741	578	0.0578	44.98962	
2	0.025	0.001288858	606	0.0606	47.01835	
2.25	0.028125	0.001293003	647	0.0647	50.03857	
2.5	0.03125	0.001297174	710	0.071	54.73438	
2.75	0.034375	0.001301372	779	0.0779	59.85992	
3	0.0375	0.001305597	824	0.0824	63.1129	
3.25	0.040625	0.00130985	898	0.0898	68.55749	
3.5	0.04375	0.00131413	934	0.0934	71.07363	
4	0.05	0.001322776	1015	0.1015	76.73258	
4.5	0.05625	0.001331536	1190	0.119	89.37048	
5	0.0625	0.001340413	1379	0.1379	102.8788	
5.5	0.06875	0.001349409	1589	0.1589	117.7553	
6	0.075	0.001358526	1799	0.1799	132.4229	
6.5	0.08125	0.001367768	1989	0.1989	145.4194	
7	0.0875	0.001377136	2698	0.2698	195.9138	
7.5	0.09375	0.001386634	3570	0.357	257.458	
8	0.1	0.001396263	4589	0.4589	328.6629	
8.5	0.10625	0.001406027	5674	0.5674	403.5483	
9	0.1125	0.001415929	6870	0.687	485.1938	
9.5	0.11875	0.001425971	7304	0.7304	512.2124	
10	0.125	0.001436157	7814	0.7814	544.0911	
10.5	0.13125	0.001446489	7543	0.7543	521.4697	
11	0.1375	0.00145697	7256	0.7256	498.0197	
11.5	0.14375	0.001467605	6790	0.679	462.6585	

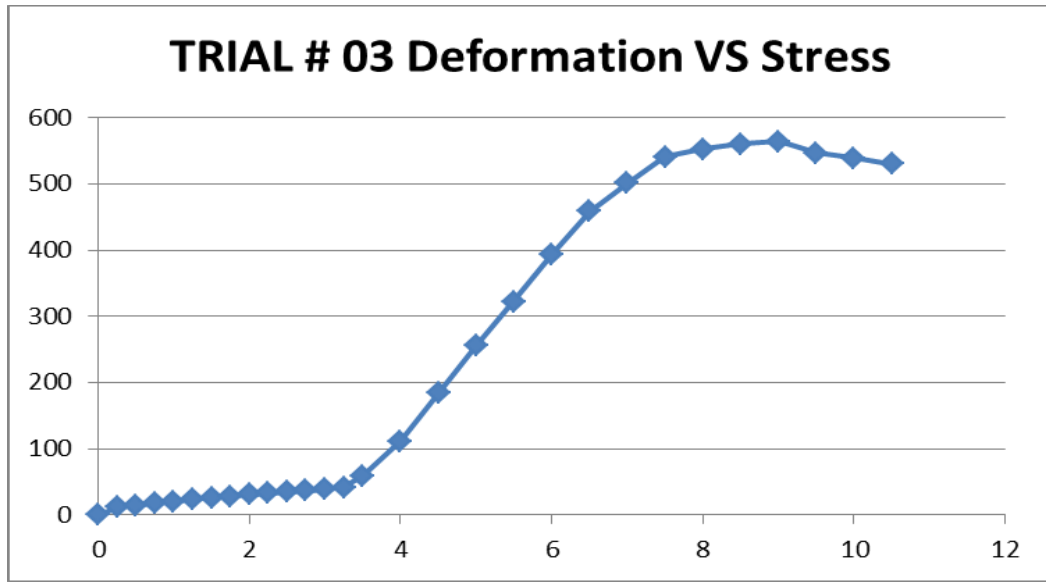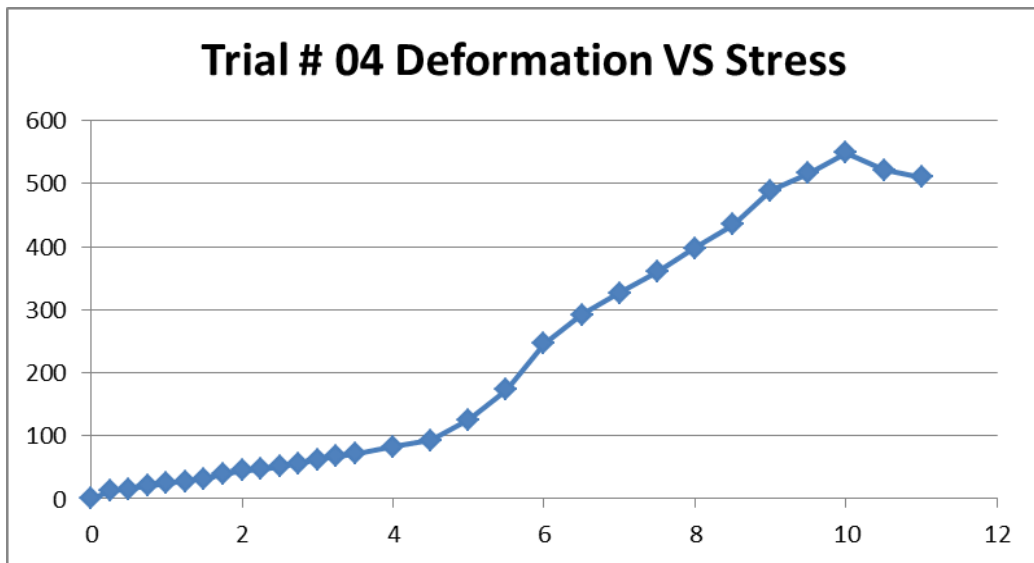**Table 30: Unconfined Compression Test Results (Trial 10)**
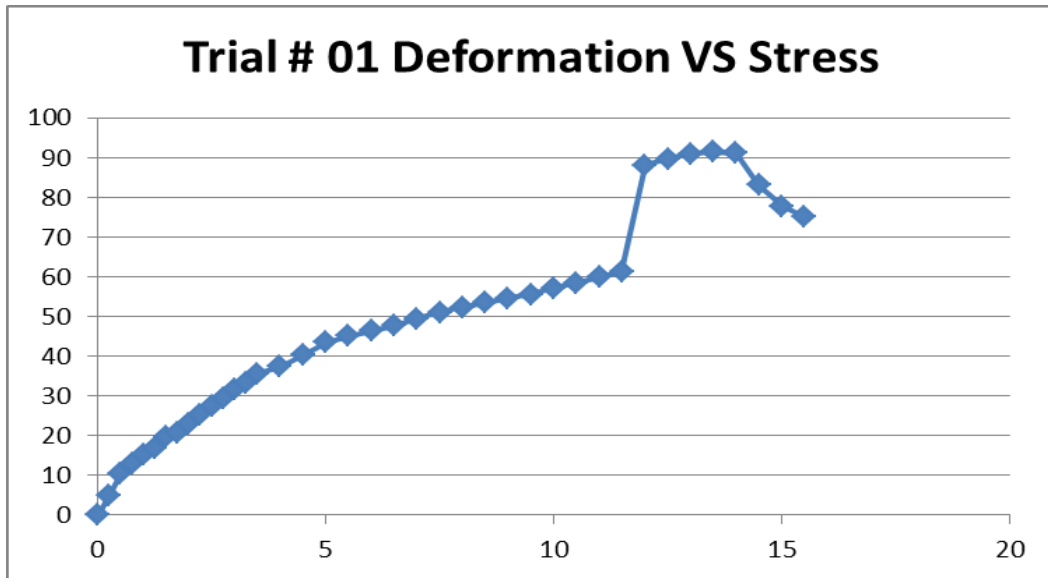
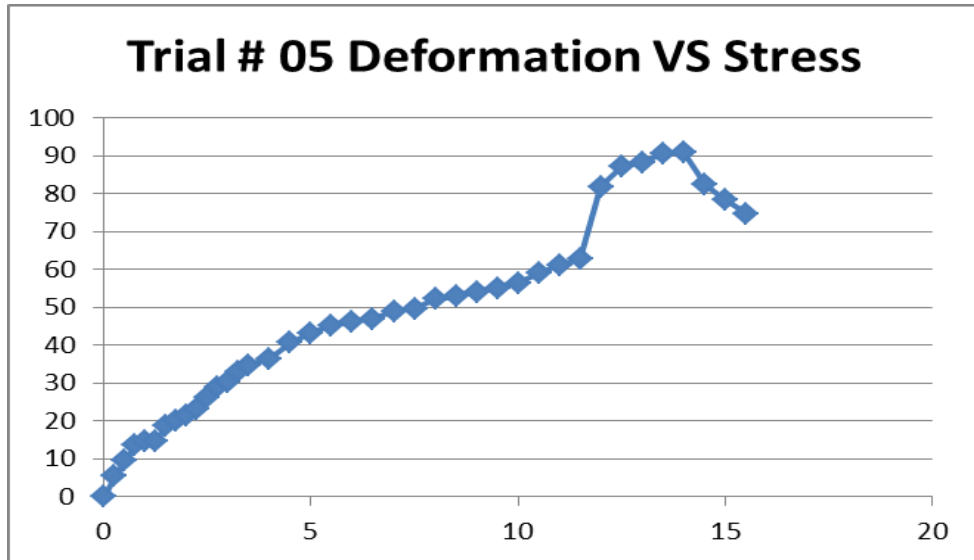**Fig 77: Plot of Stress VS Deformation (Trial 1)**
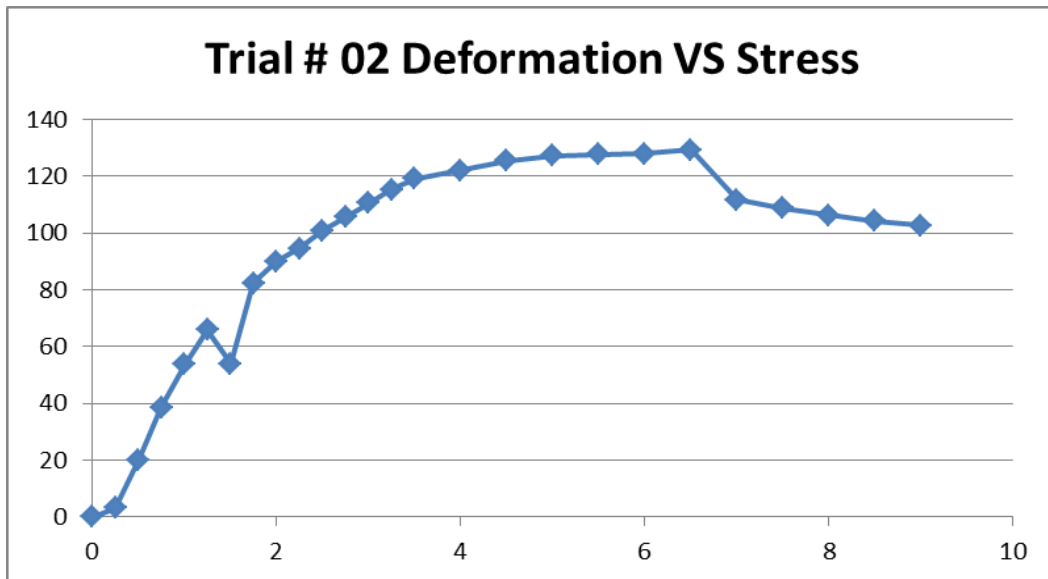
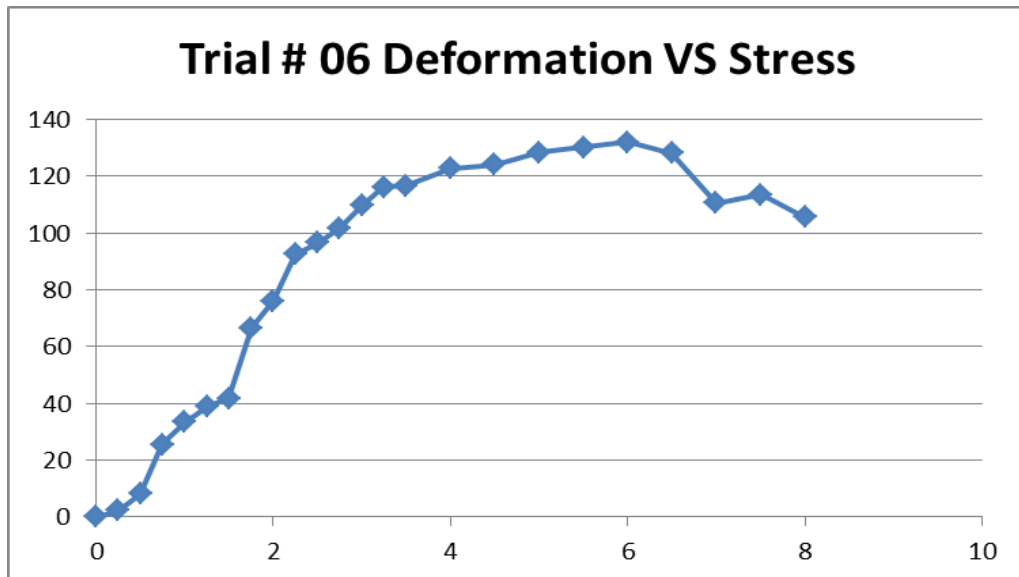**Fig 78: Plot of Stress VS Deformation (Trial 2)**

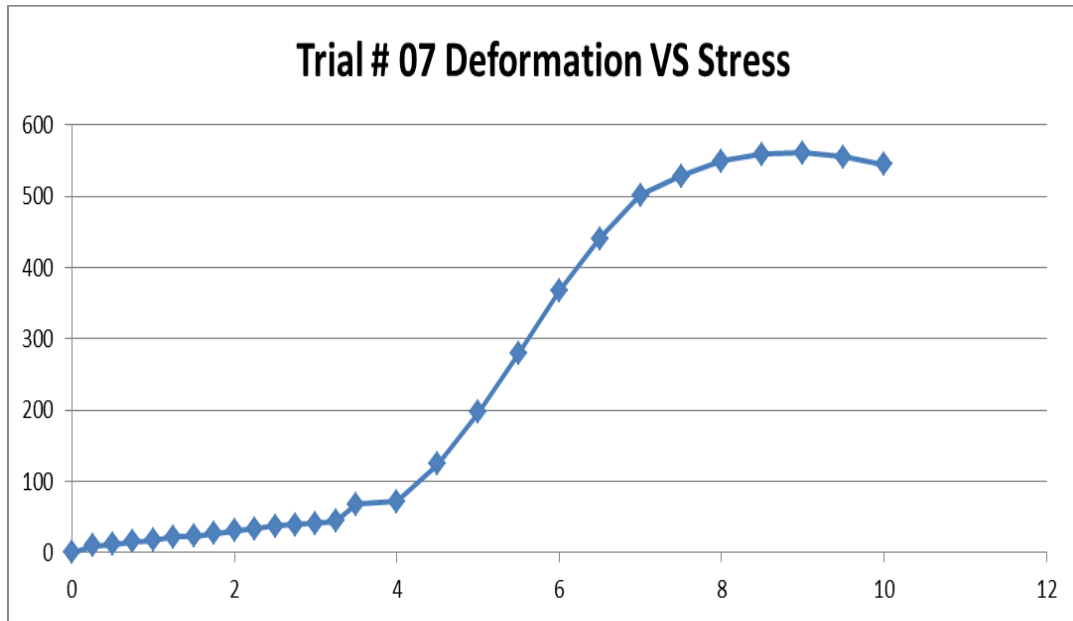**Fig 79: Plot of Stress VS Deformation (Trial 3)**

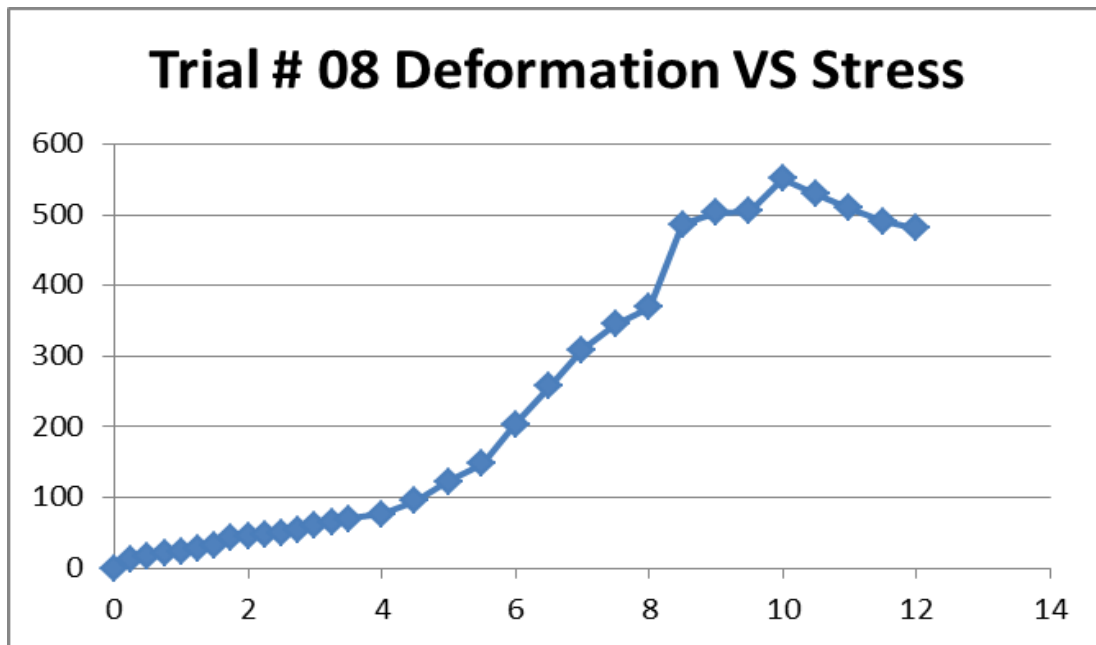**Fig 80: Plot of Stress VS Deformation (Trial 4)**

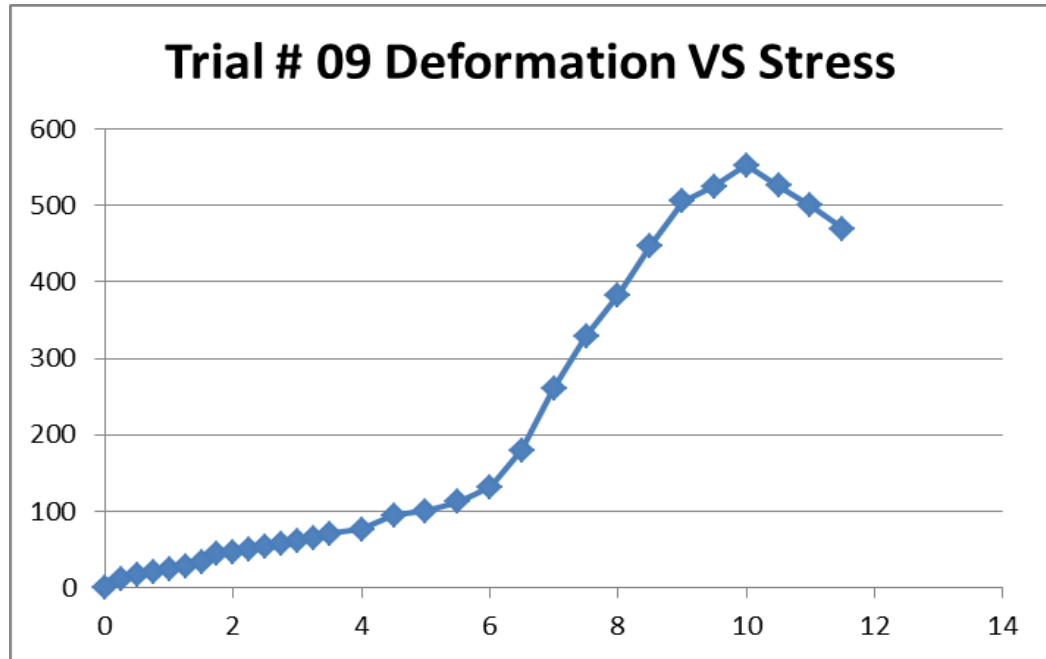**Fig 81: Plot of Stress VS Deformation (Trial 5)**

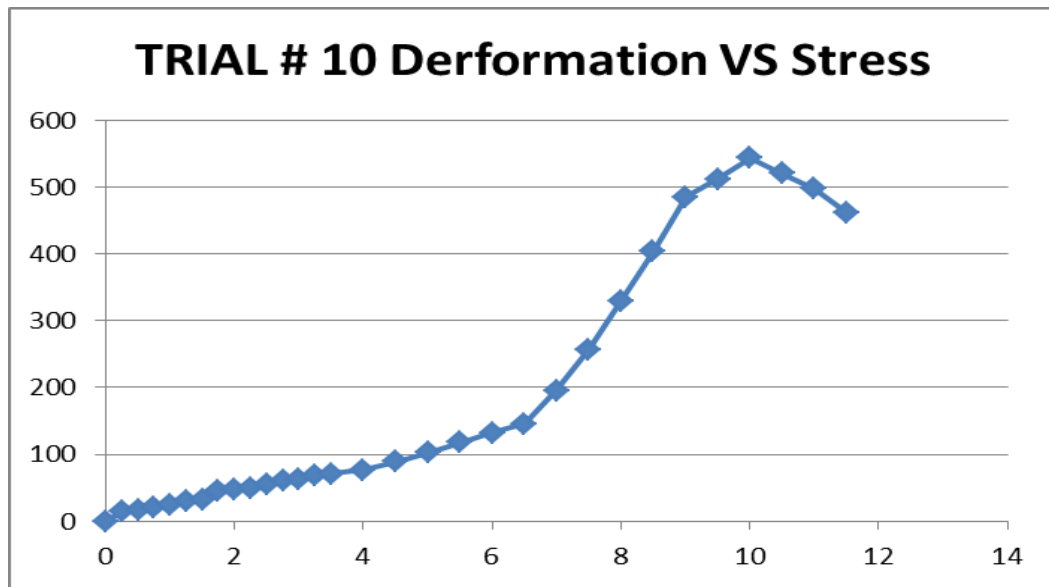**Fig 82: Plot of Stress VS Deformation (Trial 6)**

Fig 83: Plot of Stress VS Deformation (Trial 7)

Fig 84: Plot of Stress VS Deformation (Trial 8)

**Fig 85: Plot of Stress VS Deformation (Trial 9)**

Fig 86: Plot of Stress VS Deformation (Trial 10)

CHAPTER 8

DISCUSSION ON RESULTS

We carried out the testing on NUST clay and Jhelum sand sample. We compared the results obtained using our centrifuge machine with those of the triaxial testing machine and those from the Direct shear test machine.

We have obtained the results in the form of Cohesion coefficient and plotted a graphical comparison of the **C** values obtained from all these testing procedures. Following figure shows the comparison graph of the values obtained from all these tests.
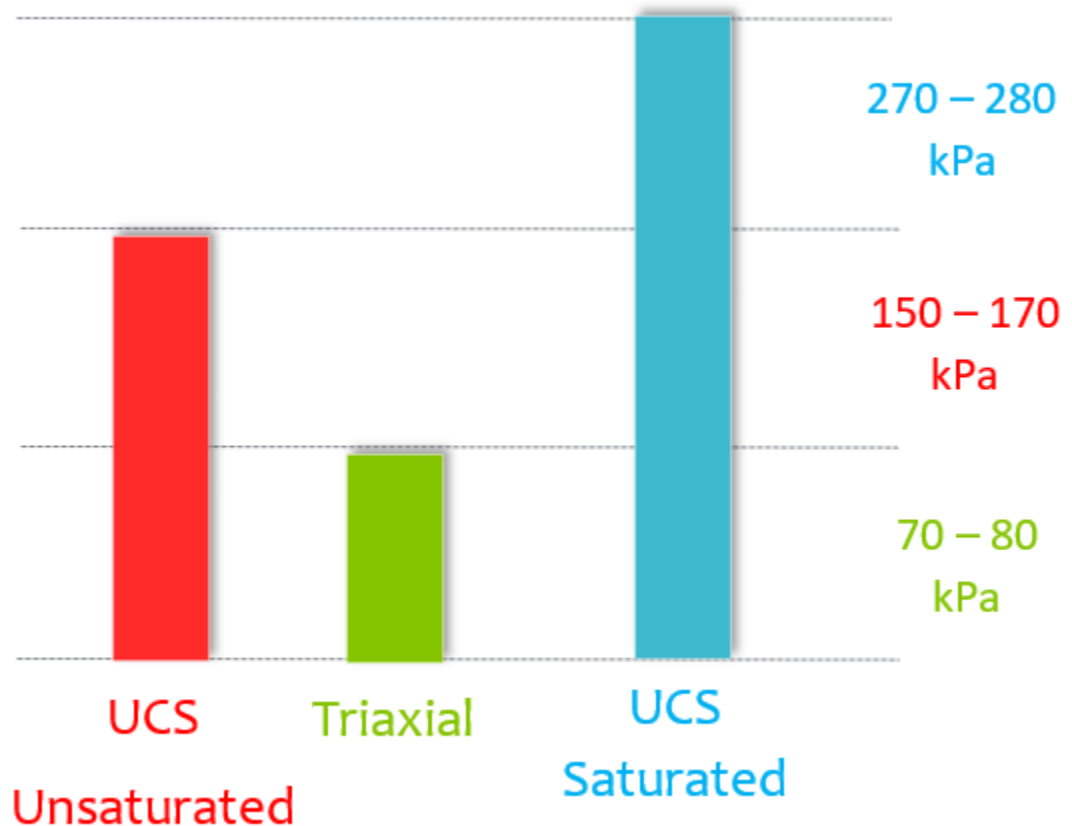
In the above graph we have developed the ranges for the **C** values on the basis of the areas of the cluster formation by the values obtained by doing multiple trials of testing. Neglecting the anomalous values, we have plotted this graph.

Now the difference between the **C** values obtained from all these tests show quite a difference. The main reason for the difference between these values is the presence of variable testing conditions in all these tests, difference in the testing mechanisms, degrees of saturation of the samples, densities of the samples and certain other parameters.

CONCLUSIONS & RECOMMENDATIONS

9.1 Conclusions

1. **ELIMINATION OF ECCENTRICITY**

   Eccentricity was eliminated by aligning the center of rotation that is the motor that provides the rotational force with the center of gravity of mass that is the cylinder that is being rotated by the motor and that carries the soil sample in it.

2. **MACHINE STABILITY STUDY**

   Machine stability study was carried out using the principles of Structural Dynamics and it showed that the foundation is sufficient for the stable operation and no damping system is required.

3. **DESIRED SAMPLES**

   Geotechnical Centrifuge can be used to acquire the soil samples of desired densities by varying the RPM's of the machine thus simulation of any field conditions has been made quite easily possible in the machine.

4. **TIME EFFICIENCY**

   Observing the saturation process that we have carried out in the centrifuge and the time that it has taken we can clearly state that the centrifuge has enabled time efficient saturation and has made it quite easy to saturate the sample in very less time that takes a lot of time in the triaxial testing apparatus.

5. **FAILURE IDENTIFICATION**

   We had devised an efficient loading mechanism in accordance with our centrifuge that had enabled us to change the loading conditions even during the fast-rotational motion of the machine but due to the unavailability of any failure identification mechanism we shifted the shearing stage of the centrifuge to the Direct Shear Test.

9.2 Recommendations

- The most important variable parameter in our centrifuge is the rotations of the motor that is the rotational force of our centrifuge. We can variate the RPMs of the motor to achieve more accurate results in terms of the density of the soil sample.

- Since we shifted to Direct Shear test to carry out the shearing phase of the centrifuge testing because of the absence of any failure identification method. Thus, working on a failure identification mechanism will enhance the capability of our centrifuge.

- To cope with the errors and uncertainties in the obtained results due to the presence of any vibrations, moisture content, saturation etc. correction factors must be worked out to make the results more accurate and eventually make the machine more accurate.

- Liquefaction potential of sand could also be modelled on this custom Centrifuge apparatus since the rotational motion provided by this machine is quite enough to produce earth quake like effects thus liquefaction potential of sand could easily be simulated on this machine.

APPENDIX

NOTATIONS

C' Drained Cohesion of Sand

Φ Angle of Friction of Soil

S_u Undrained Cohesion of Sand

q_u Unconfined Compressive Strength of Soil

k Hydraulic Conductivity of Soil

e Void Ratio

n Porosity

γ Unit Weight of Soil

G_s Specific Gravity

REFERENCES

Kimura, T., 1998. Development of geotechnical centrifuge in Japan. Proc. Centrifuge, Tokyo, Pre-print Volume, p.23-32

C. Ng, 'The state-of-the-art centrifuge modelling of geotechnical problems at HKUST', Journal of Zhejiang University SCIENCE A, vol. 15, no. 1, pp. 1-21, 2014

D. Kim, N. Kim, Y. Choo and G. Cho, 'A newly developed state-of- the-art geotechnical centrifuge in Korea', KSCE Journal of Civil Engineering, vol. 17, no. 1, pp. 77-84, 2012

13th World Conference on Earthquake Engineering Vancouver, B.C., Canada August 1-6, 2004 Paper No. 2497

T. Kimura, Geotechnical centrifuge model testing. Japanese Society of Soil Mechanics and Foundation Engineering,1984

Ko, H.Y., 1988. Summary of the state-of-the-art in centrifuge model testing. Centrifuge in Soil Mechanics, p.11-28

Jung Joo Kim, 2017. Prediction of settlement trough due to TBM tunnelling with an emphasis on groundwater depression based on centrifuge model tests and numerical analysis